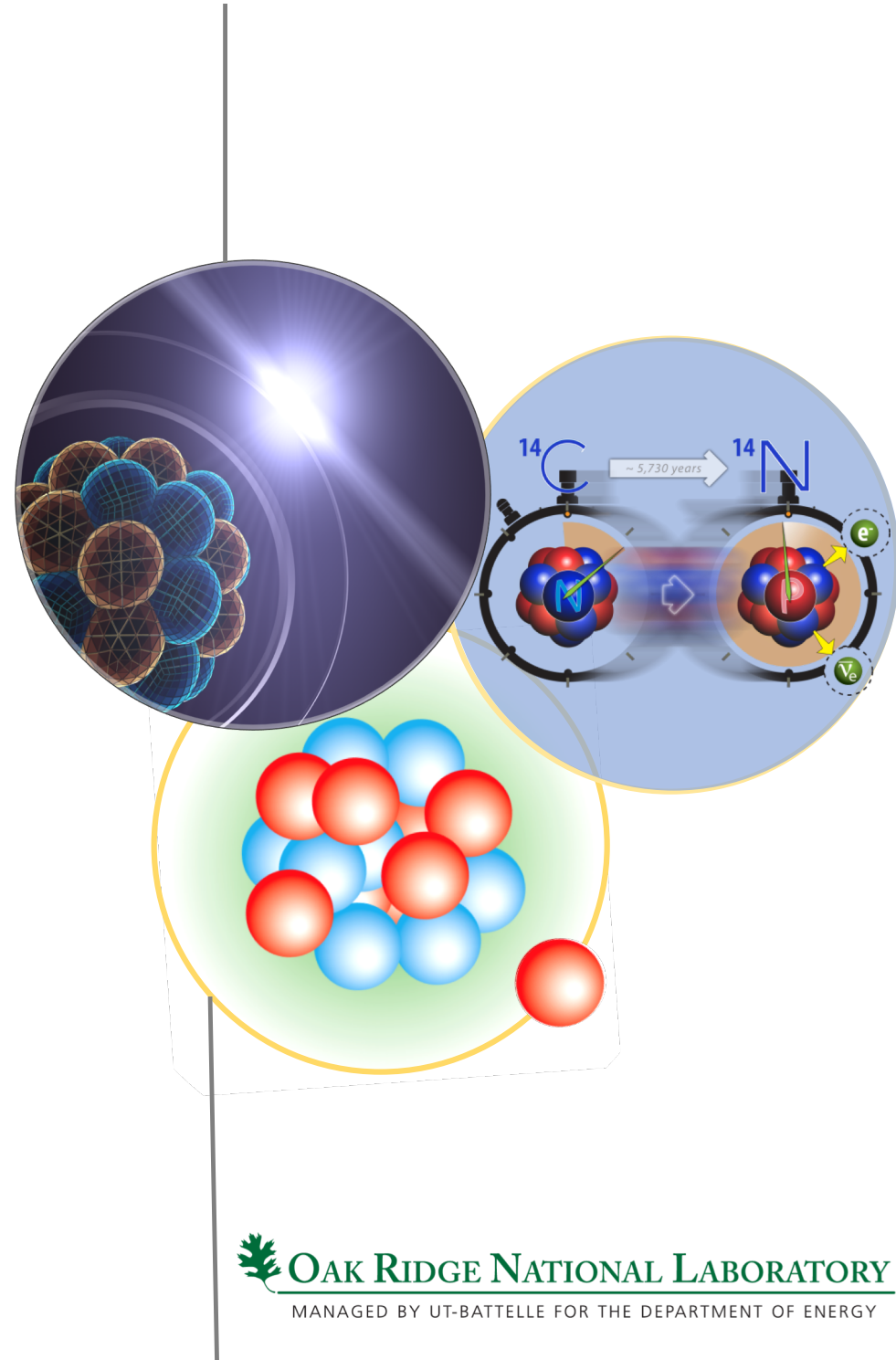


Coupled cluster computations of radii and neutron skins

Gaute Hagen
Oak Ridge National Laboratory

Intersection of nuclear structure and
high-energy nuclear collisions

INT workshop, February 16th, 2023



Collaborators



**B. Acharya, B. Hu, G. R. Jansen,
Z. H. Sun, T. Papenbrock**



S. R. Stroberg



**JOHANNES GUTENBERG
UNIVERSITÄT MAINZ**



I. vernon



**S. Bacca, F. Bonaiti, W. G. Jiang,
J. E. Sobczyk**

A. Ekström, C. Forssén



J. Holt, P. Navratil



**S. Gandolfi, S. Novario,
D. Lonardoni**



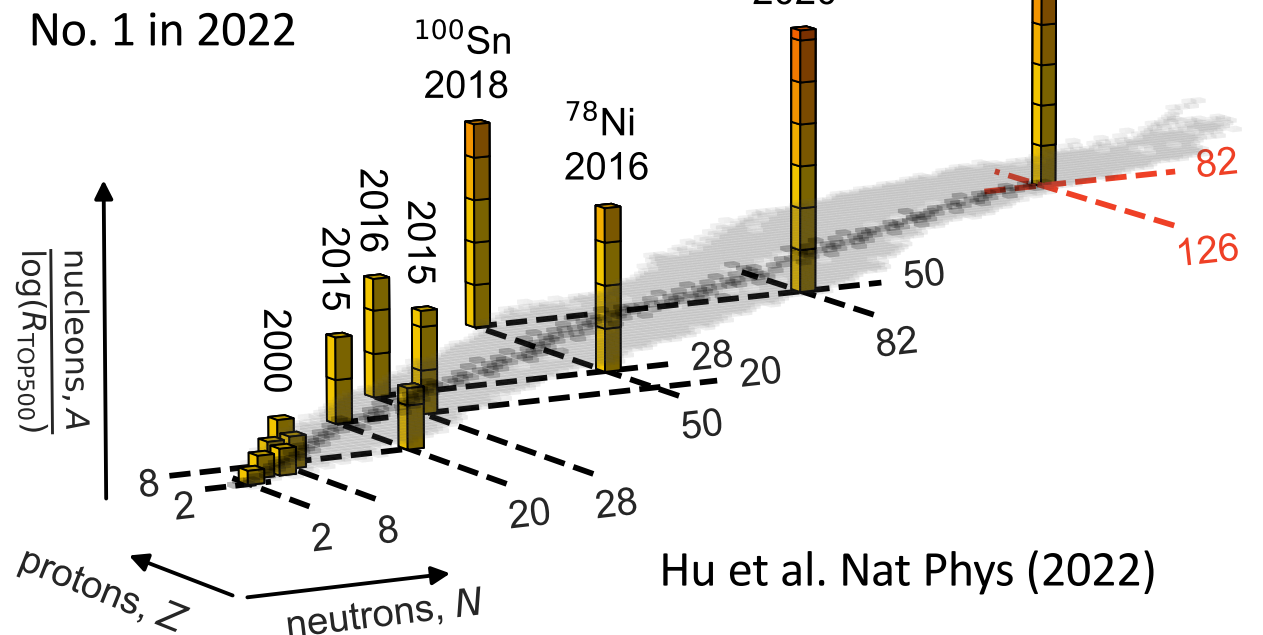
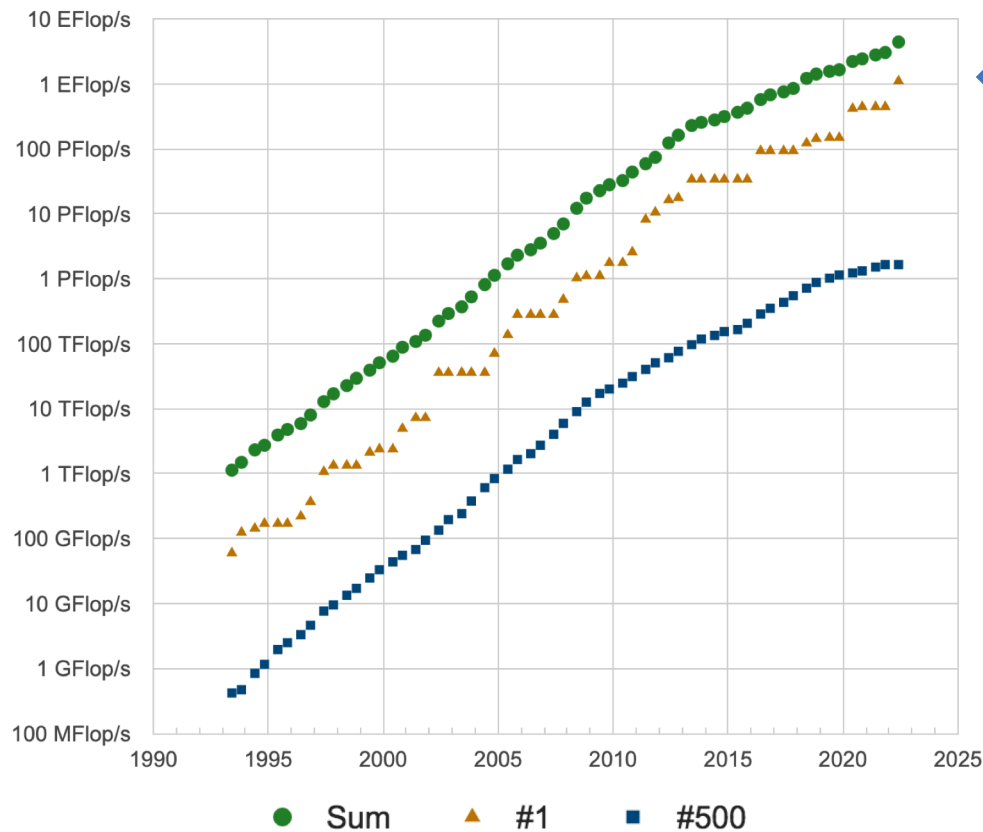
**TECHNISCHE
UNIVERSITÄT
DARMSTADT**

T. Miyagi

Trend in realistic ab-initio calculations

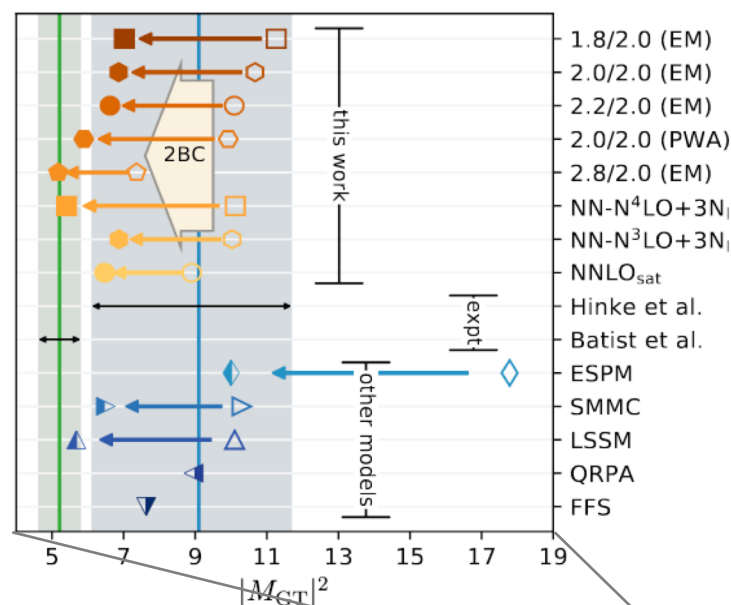
- Tremendous progress in recent years because of ideas from EFT and the renormalization group
- Computational methods with polynomial cost (coupled clusters 😊 quantum computing 🤔)
- Ever-increasing computer power?

Development with time (top500.org)

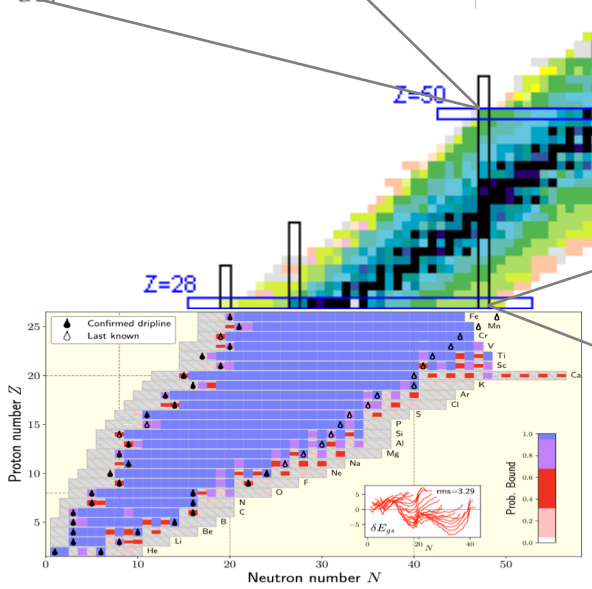


The Hamiltonian knows best

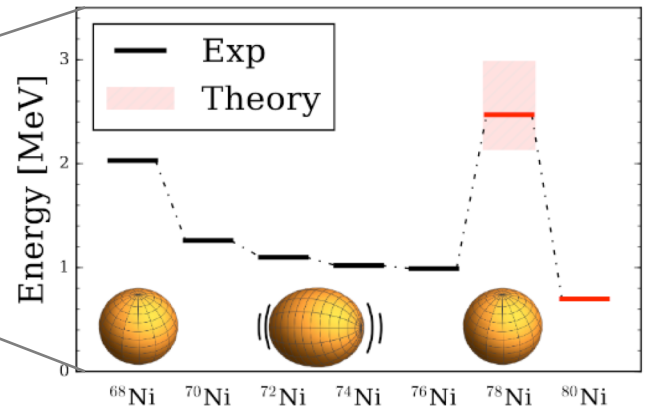
Gysbers et al, Nat Phys (2019)



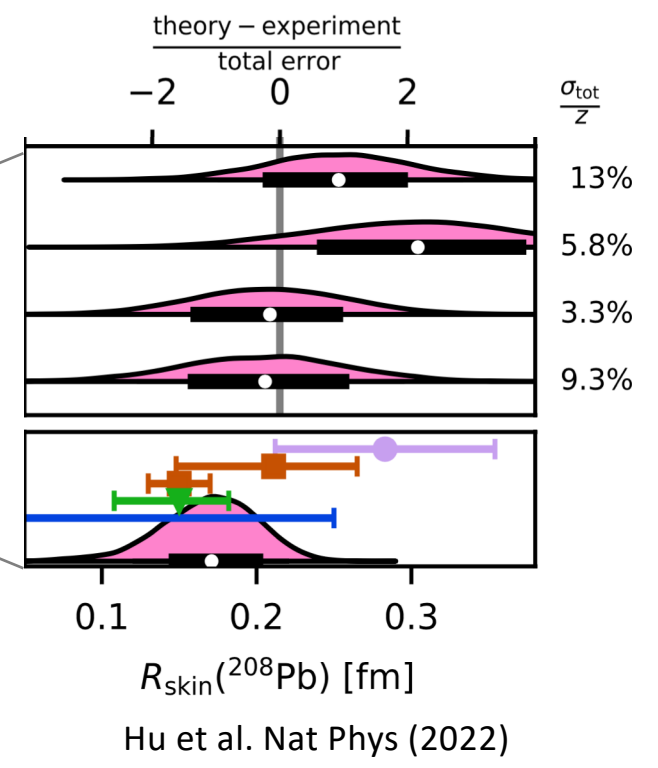
An "ab-initio revolution" is changing the way we compute nuclei



Stroberg et al, Phys Rev Lett (2021)

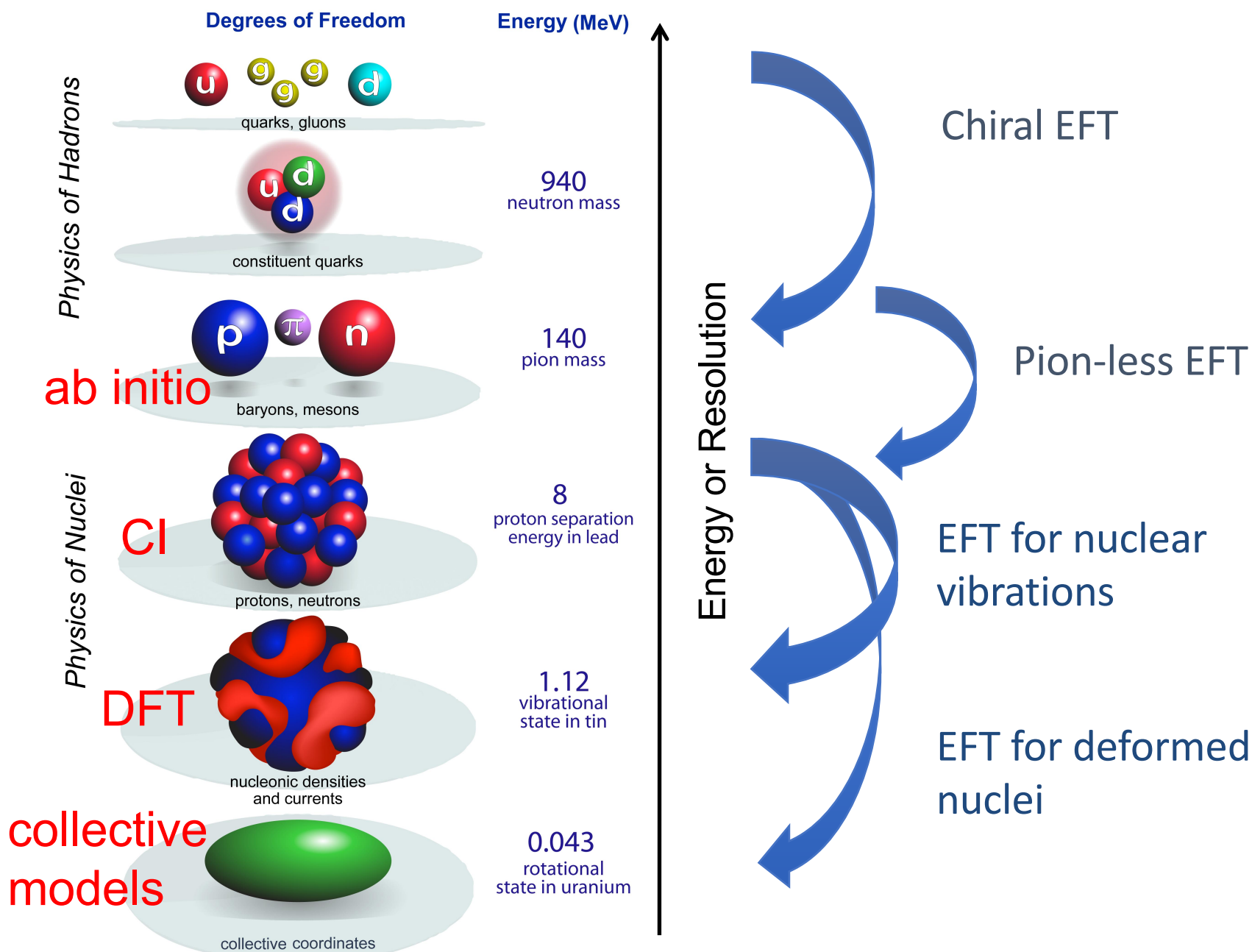


Hagen, Jansen, Papenbrock, Phys Rev Lett (2016)



Hu et al. Nat Phys (2022)

Energy scales and effective field theories



“we interpret the ab initio method to be a systematically improvable approach for quantitatively describing nuclei using the finest resolution scale possible while maximizing its predictive capabilities”

What is *ab initio* in nuclear theory?
 A. Ekström et al, arXiv:2212.11064 (2022)

Fig.: Bertsch, Dean, Nazarewicz, SciDAC review (2007)

Energy scales and effective field theories

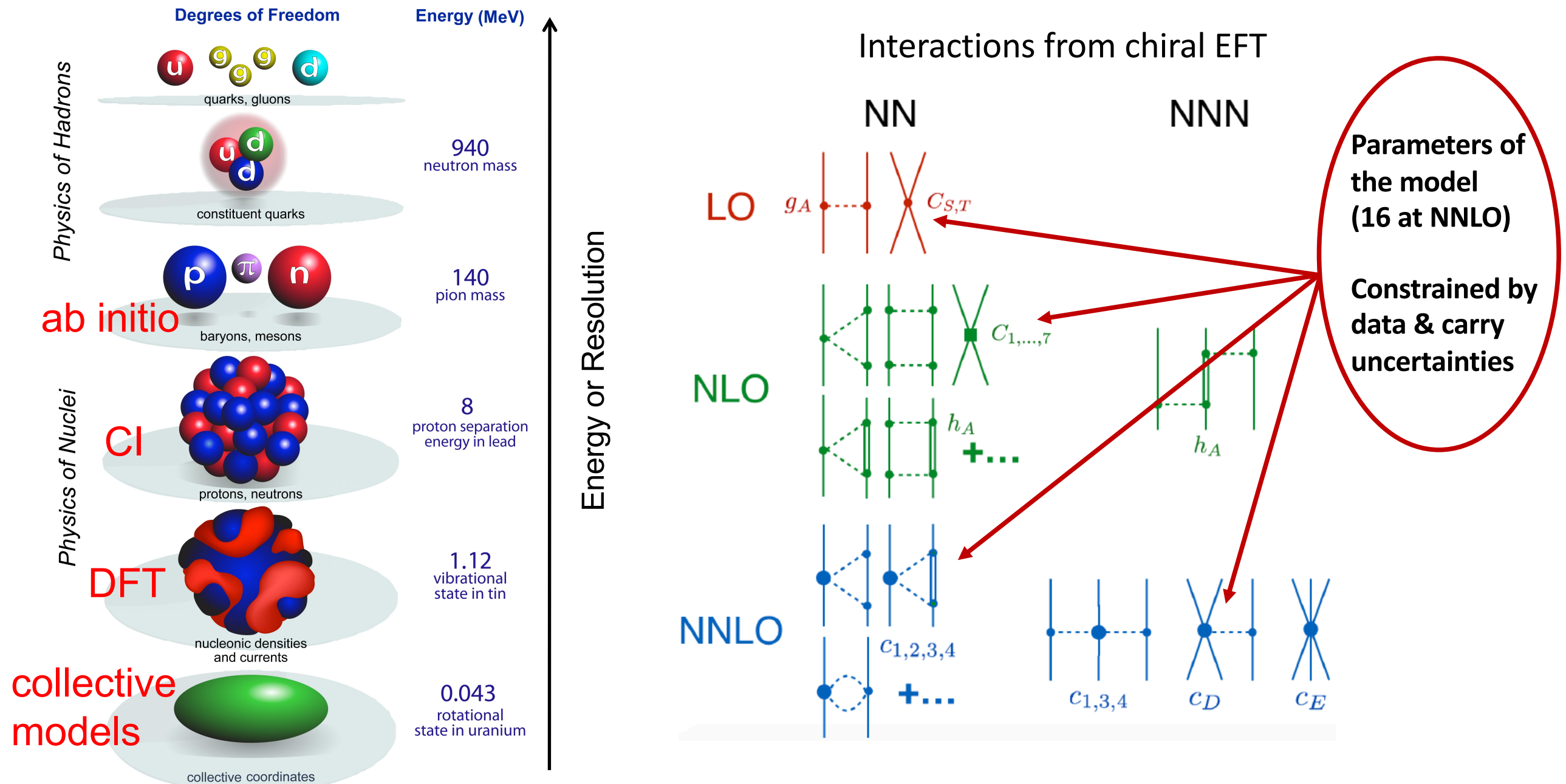
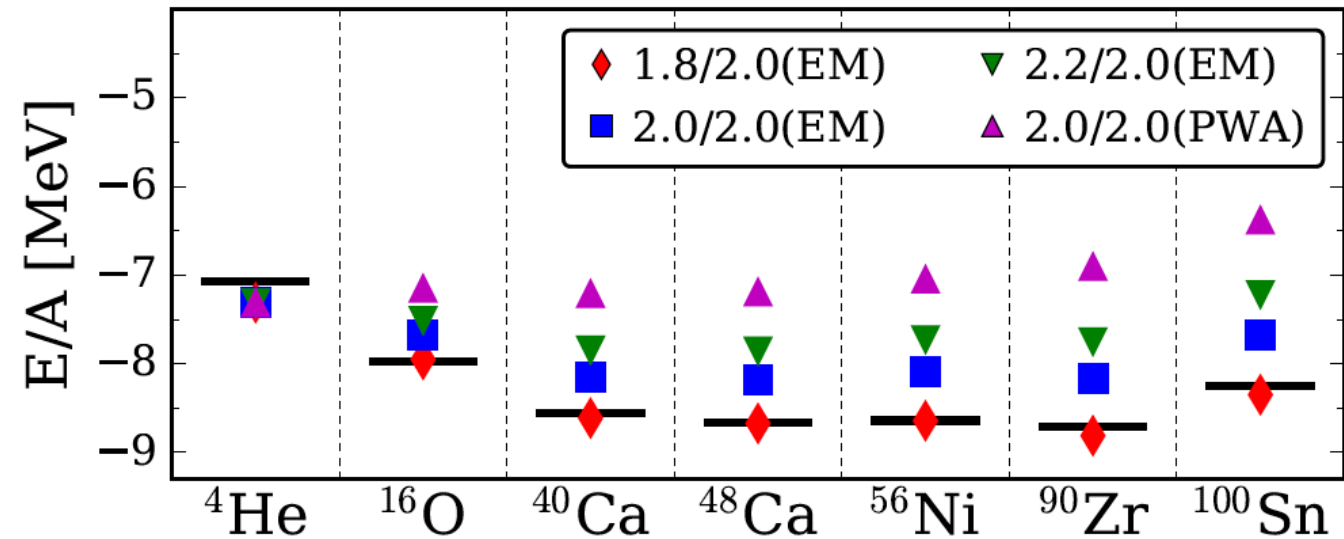
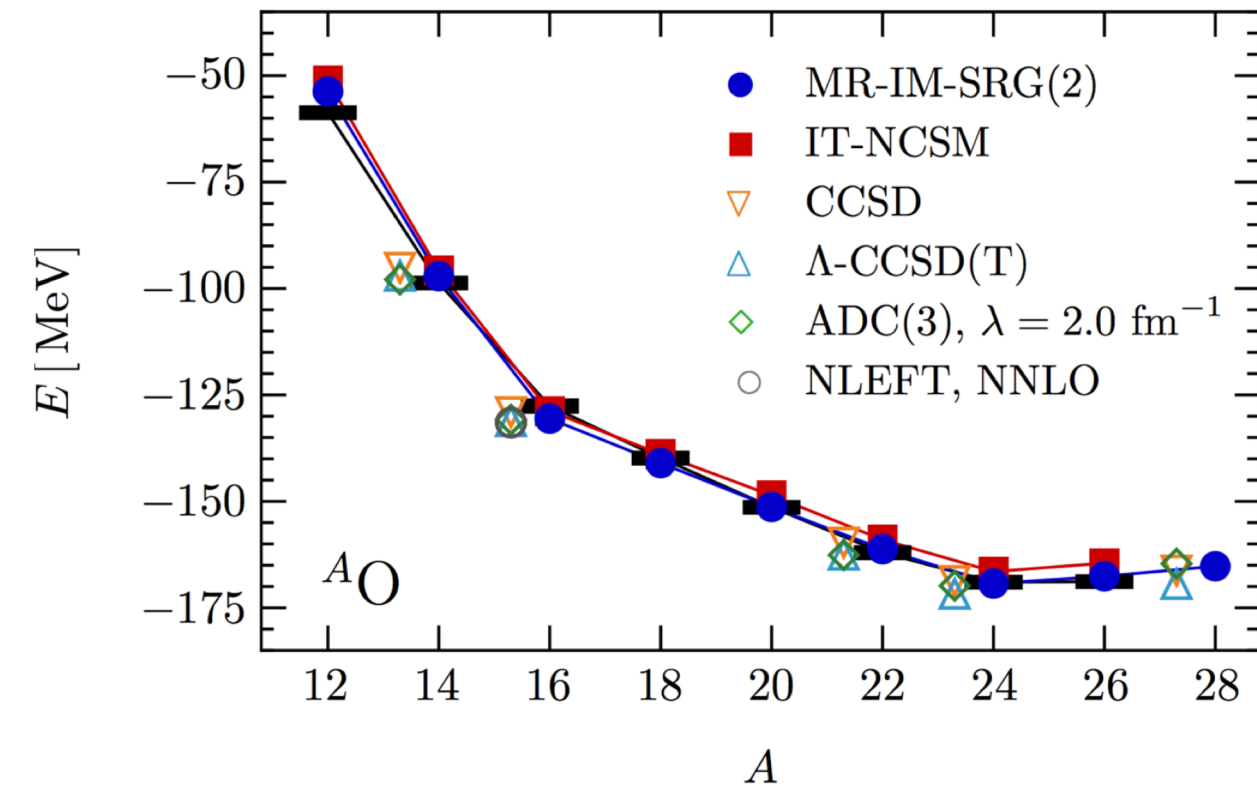


Fig.: Bertsch, Dean, Nazarewicz, SciDAC review (2007)

What precision/accuracy can we aim for in ab-initio calculations of nuclei?

Different many-body approaches (CC, IMSRG, SCGF,...) agree with each for binding energies and radii (challenges exist for transitions, isotope shifts, and deformed shapes)

Some chiral potentials (models) work better than others



H. Hergert Phys. Scripta 92, 023002 (2017)

K. Hebeler *et al* PRC (2011).
T. Morris *et al*, PRL (2018).

Solving the quantum many-nucleon problem

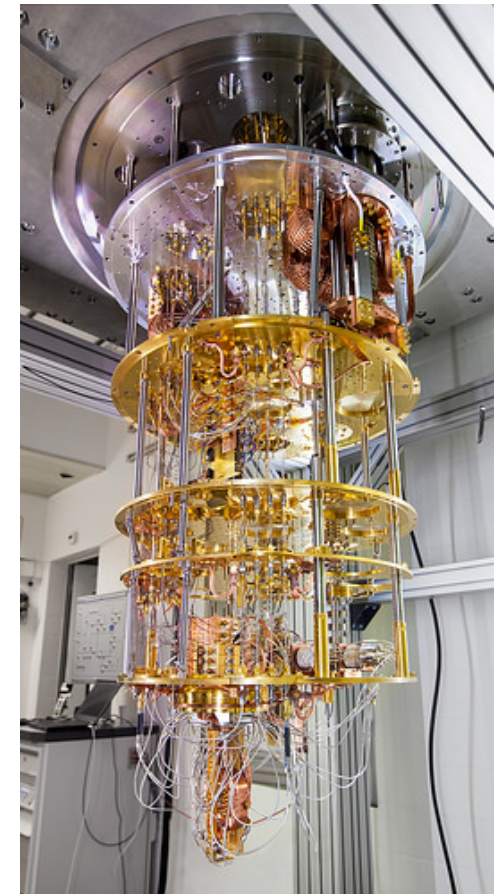
An exponentially hard problem to solve!

$$H|\Psi\rangle = E|\Psi\rangle$$

Polynomial scaling

Systematically improvable approaches
with controlled approximations:
Coupled-cluster, IMSRG, Gorkov, SCGF,...

IBM Q Experience

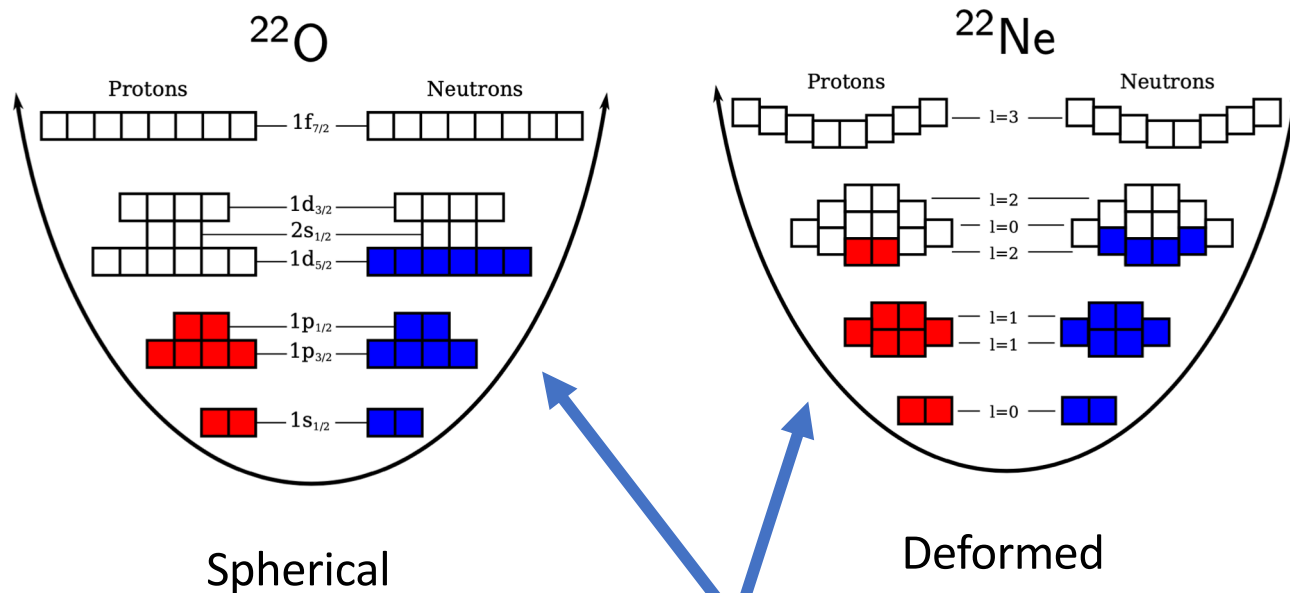


Fault tolerant quantum computing?

Solving the quantum many-nucleon problem

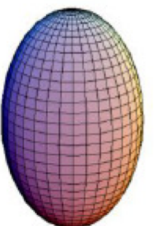
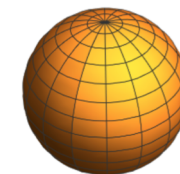
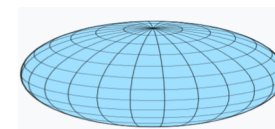
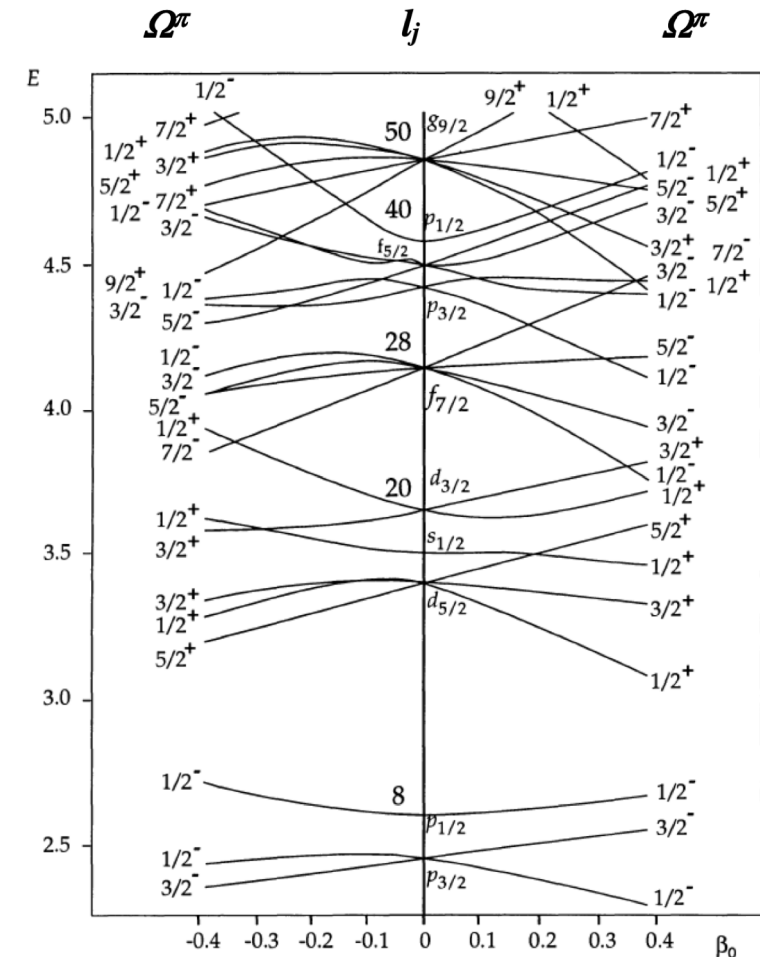
The key lies in choosing the correct starting point

Wave-function based methods starts from a mean-field reference state



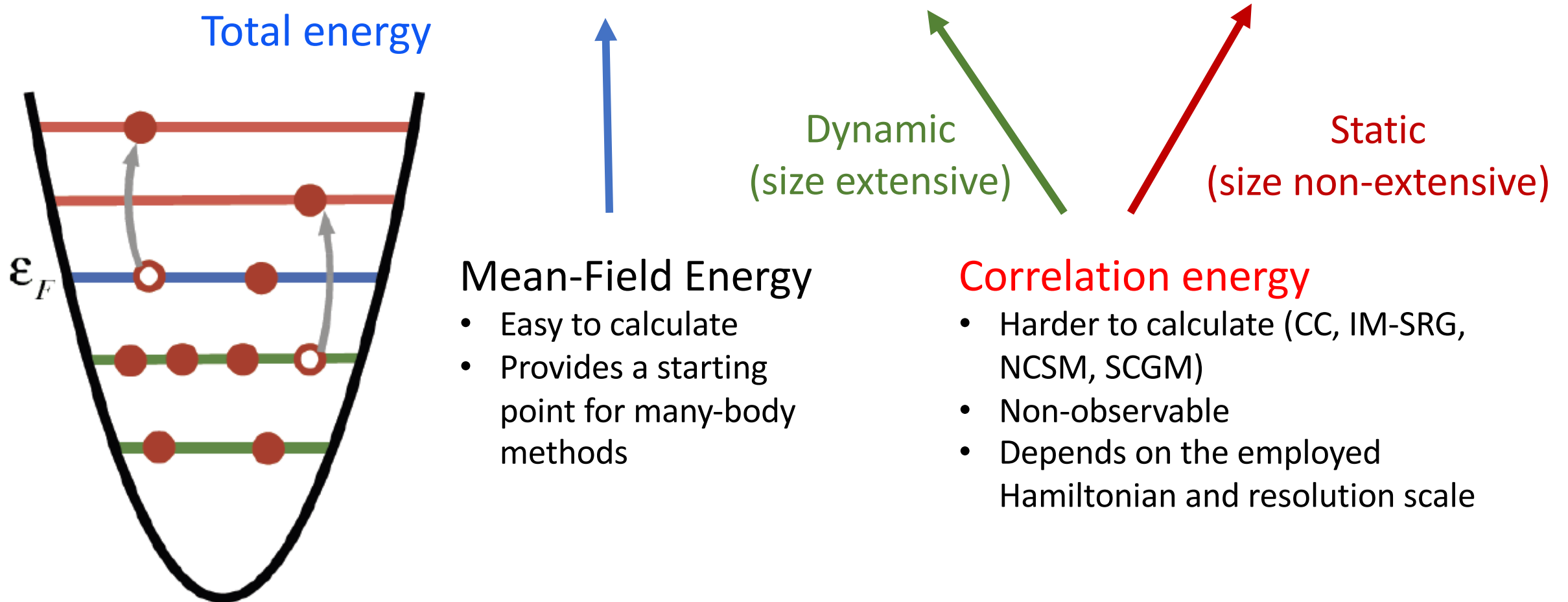
$$|\Psi\rangle = \Omega |\Phi\rangle$$

Wave-operator (includes many-body correlations)



Correlation energy in wave-function based methods

$$E = E_{\text{ref}} + \Delta E_{\text{CC}} + \delta E$$



Coupled-cluster method

$$\Psi = e^T |\Phi\rangle$$

$$T = T_1 + T_2 + \dots$$

$$T_1 = \sum_{ia} t_i^a a_a^\dagger a_i \quad T_2 = \frac{1}{4} \sum_{ijab} t_{ij}^{ab} a_a^\dagger a_b^\dagger a_j a_i$$

$$\bar{H}_{\text{CCSD}} = \begin{pmatrix} \text{0p0h} & \text{1p1h} & \text{2p2h} \\ E_{\text{CCSD}} & \bar{H}_{0S} & \bar{H}_{0D} \\ 0 & \bar{H}_{SS} & \bar{H}_{SD} \\ 0 & \bar{H}_{DS} & \bar{H}_{DD} \end{pmatrix} \begin{matrix} \text{0p0h} \\ \text{1p1h} \\ \text{2p2h} \end{matrix}$$

$$E = \langle \Phi | \bar{H} | \Phi \rangle$$

$$0 = \langle \Phi_i^a | \bar{H} | \Phi \rangle$$

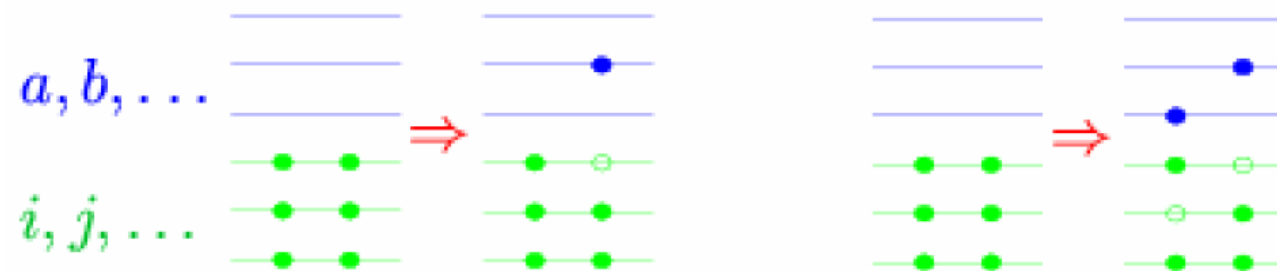
$$0 = \langle \Phi_{ij}^{ab} | \bar{H} | \Phi \rangle$$

$$\bar{H} \equiv e^{-T} H e^T = (H e^T)_c = \left(H + H T_1 + H T_2 + \frac{1}{2} H T_1^2 + \dots \right)_c$$

- ☺ Scales gently (polynomial) with increasing system size
- ☺ Truncation is only approximation
- ☺ A lot of freedom in the choice of reference state (spherical, deformed, pairing,...)

CCSD generates similarity transformed Hamiltonian with no 1p-1h and no 2p-2h excitations

Correlations are *exponentiated* 1p-1h and 2p-2h excitations. Part of Ap-Ah excitations included!



Comparing coupled-cluster with exact CI

$$C_1 = T_1, \quad \text{CCSD } (N^6)$$

$$C_2 = T_2 + \frac{1}{2}T_1^2, \quad \text{CCSDT } (N^8)$$

$$C_3 = T_3 + T_1T_2 + \frac{T_1^3}{3!},$$

$$C_4 = T_4 + \frac{T_2^2}{2} + T_1T_3 + \frac{T_1^2T_2}{2} + \frac{T_1^4}{4!},$$

CCSDTQ (N^{10})

Exact CI:

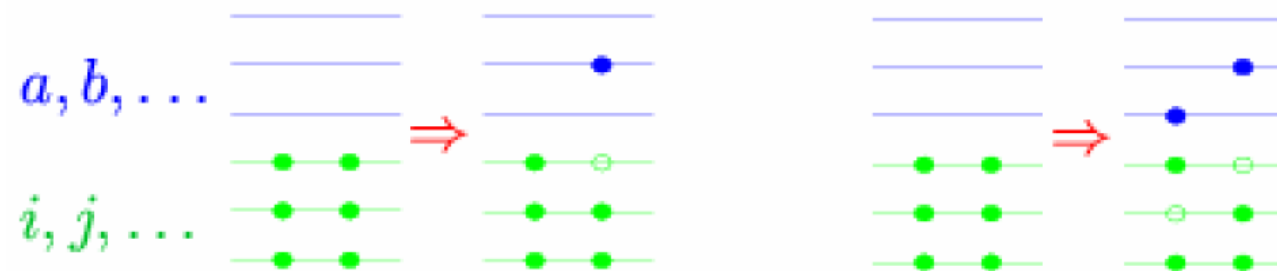
$$|\Psi\rangle = \Omega|\Phi\rangle = \left(1 + \sum_{i=1}^A C_i\right)|\Phi\rangle$$

- CCSD captures most of the 3p3h and 4p4h excitations (scales as $n_o^2 n_u^4$)
- In order to describe α -cluster states need to include full quadruples (CCSDTQ) (scales $n_o^4 n_u^6$)

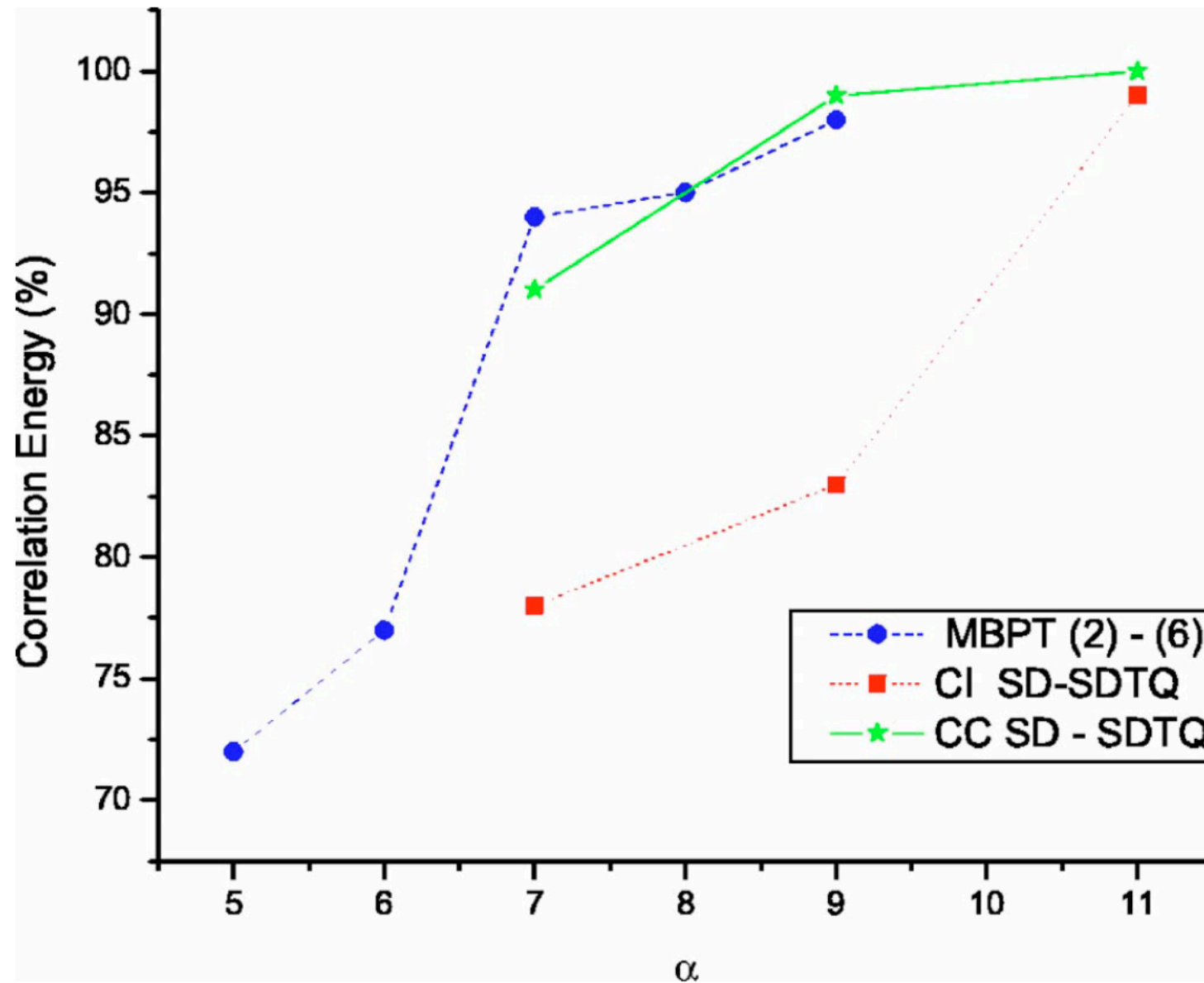


C_A

Correlations are *exponentiated* 1p-1h and 2p-2h excitations. Part of Ap-Ah excitations included!



Convergence of coupled-cluster method

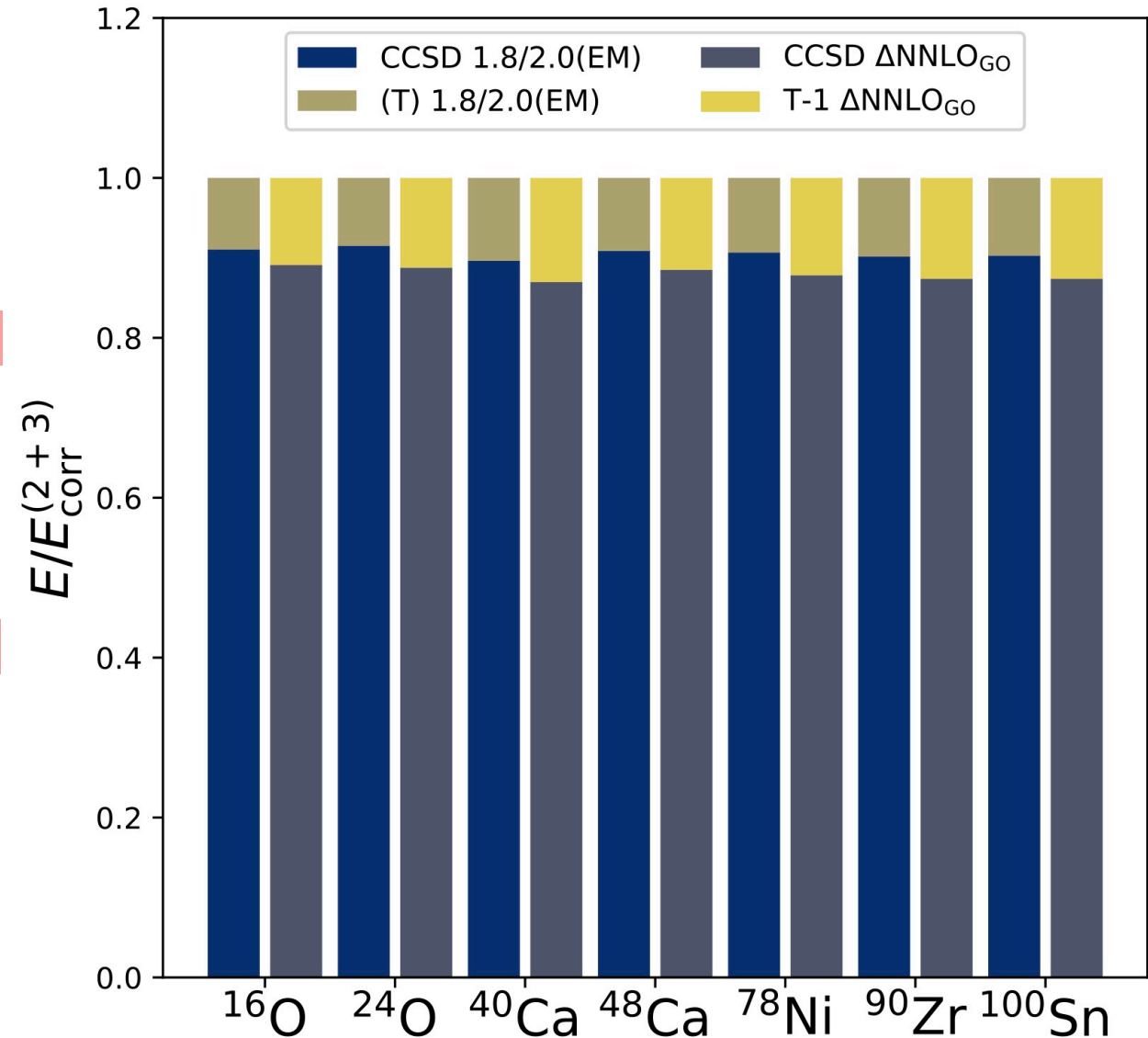


Convergence of coupled-cluster method

Energies	^{16}O	^{22}O	^{24}O	^{28}O
$(\Lambda_\chi = 500 \text{ MeV})$				
E_0	25.946	46.52	50.74	63.85
ΔE_{CCSD}	-133.53	-171.31	-185.17	-200.63
ΔE_3	-13.31	-19.61	-19.91	-20.23
E	-120.89	-144.40	-154.34	-157.01
$(\Lambda_\chi = 600 \text{ MeV})$				
E_0	22.08	46.33	52.94	68.57
ΔE_{CCSD}	-119.04	-156.51	-168.49	-182.42
ΔE_3	-14.95	-20.71	-22.49	-22.86
E	-111.91	-130.89	-138.04	-136.71
Experiment	-127.62	-162.03	-168.38	

G. Hagen, et al, Phys. Rev. C 80, 021306 (2009)

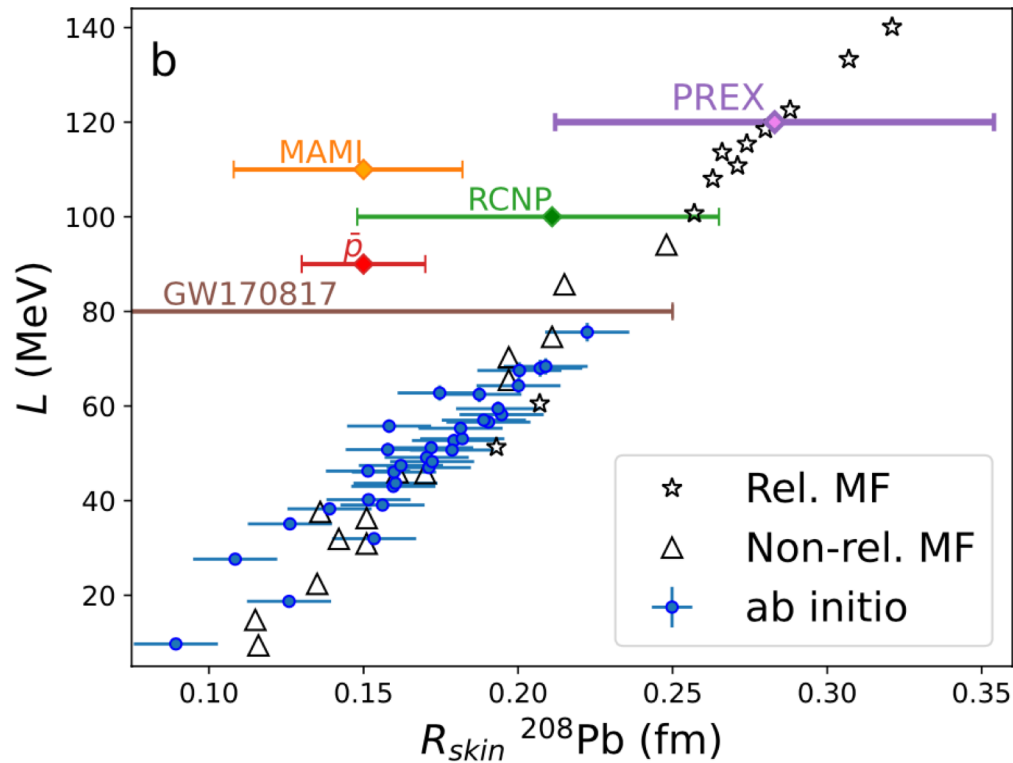
$\Delta E_3 \sim 10 - 13\%$



A. Ekström, et al, arXiv:2212.11064 (2022)

What is the size of atomic nuclei?

Hu et al, Nature Physics (2023)



- Different models predict correlations between neutron skin and the slope of the symmetry parameter
- Radii (charge/matter) also informs us about shell structure, pairing and superfluidity, and density distributions in nuclei



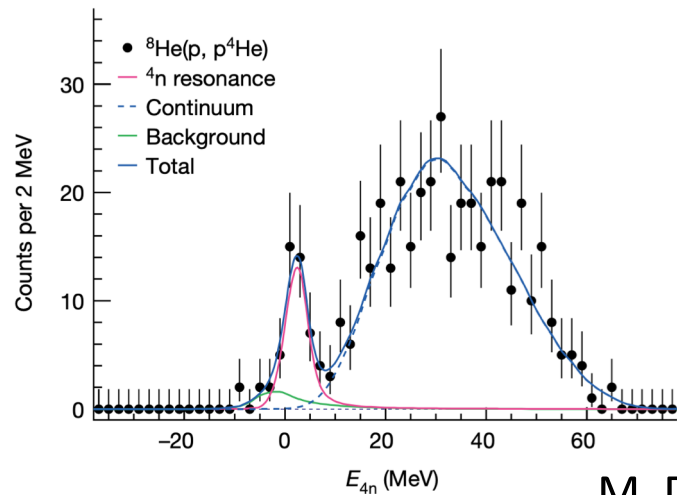
"Illustration: JingChen | Chalmers University of Technology | Yen Strandqvist"

Neutron skin = Difference between radii of neutron and proton distributions

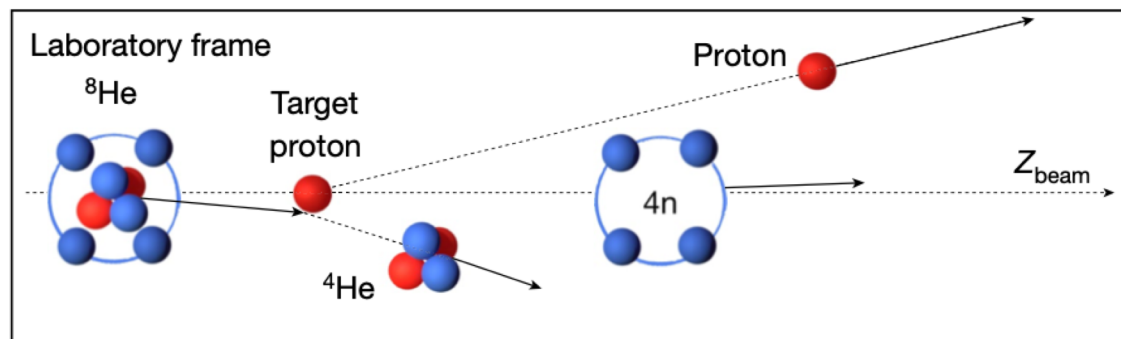
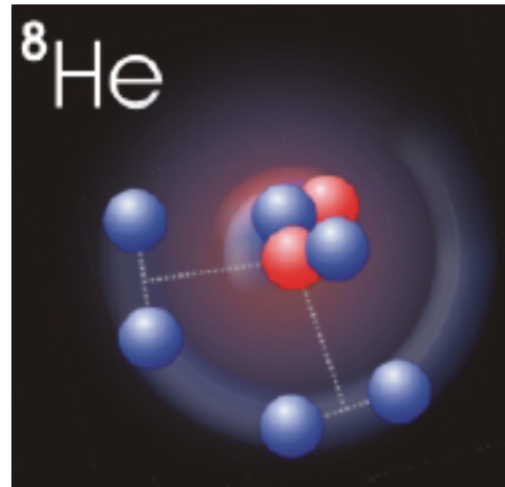
Relates atomic nuclei to neutron stars via neutron EOS

Structure of ^8He and $4n$ correlations

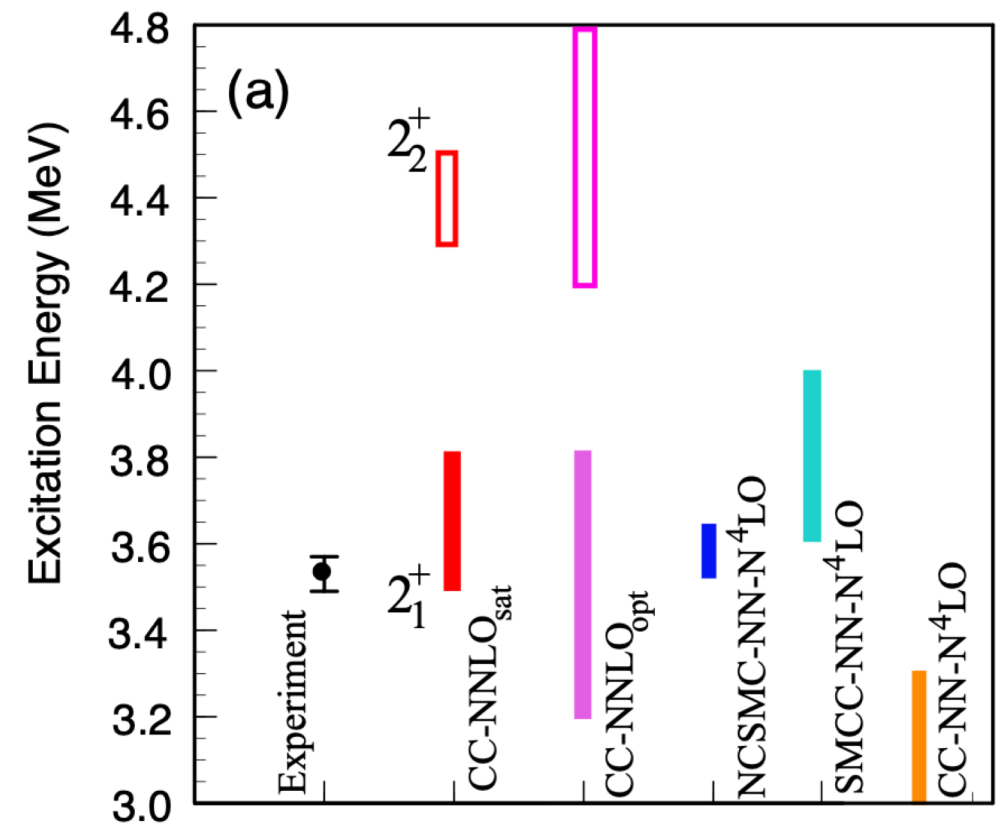
- Largest known N/Z ratio
- Doubly magic in the naive shell model
- Low lying 2^+ state indicates softness towards being deformed in the ground-state
- Tetra-neutron correlations



M. Duer et al, Nature (2022)



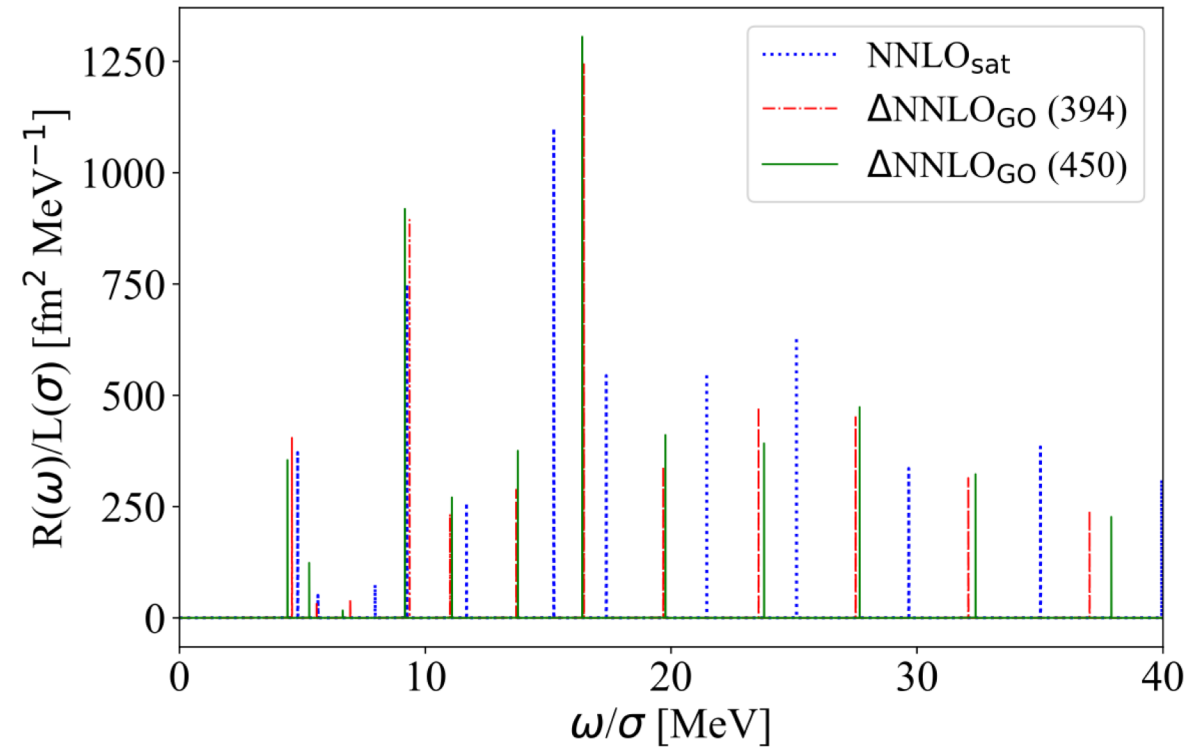
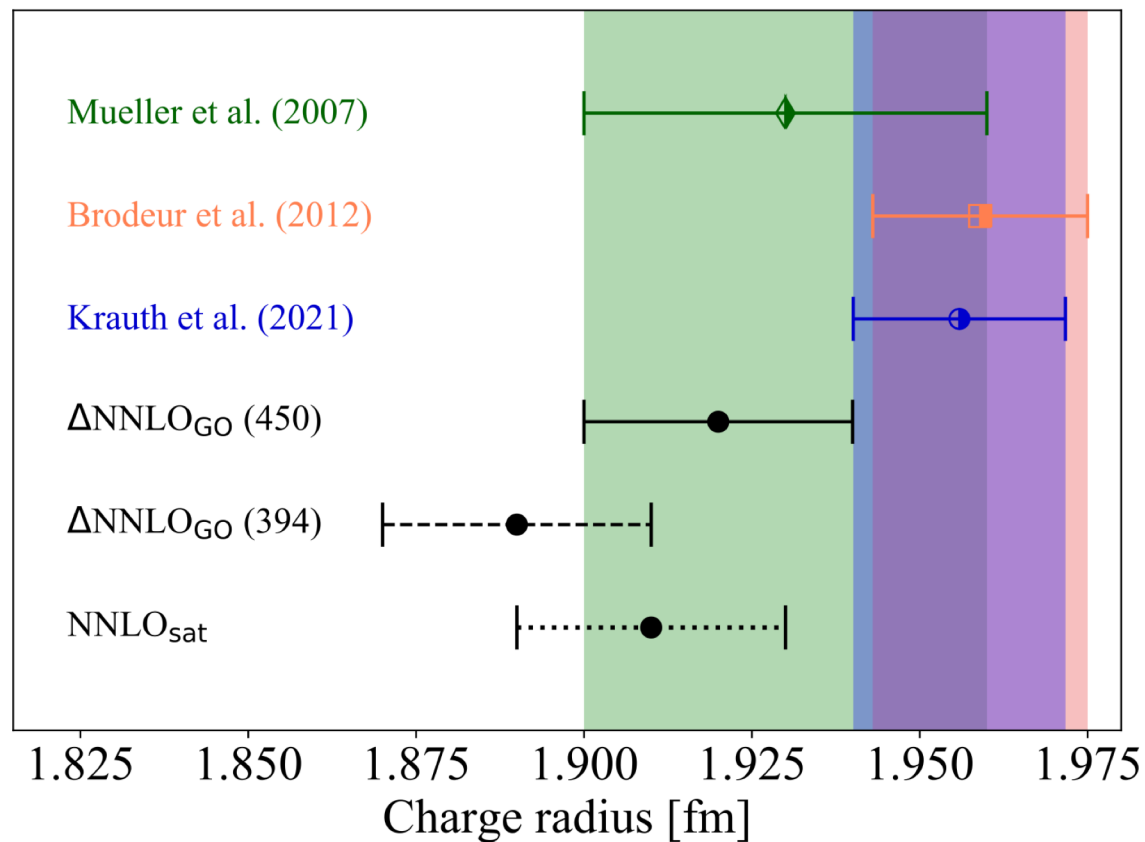
M. Holl, R. Kanungo, et al, Phys. Lett. B 822, 136710 (2021)



Charge radius and dipole polarizability of ${}^8\text{He}$

- Dipole polarizability more than five times larger than that of ${}^4\text{He}$
- Indicates existence of low lying dipole strength
- Charge radii slightly smaller compared to new data

F. Bonaiti, et al Phys. Rev. C 105, 034313 (2022)



Interaction

α_D (fm^3)

NNLO_{sat}

0.37(3)

$\Delta\text{NNLO}_{\text{GO}}(450)$

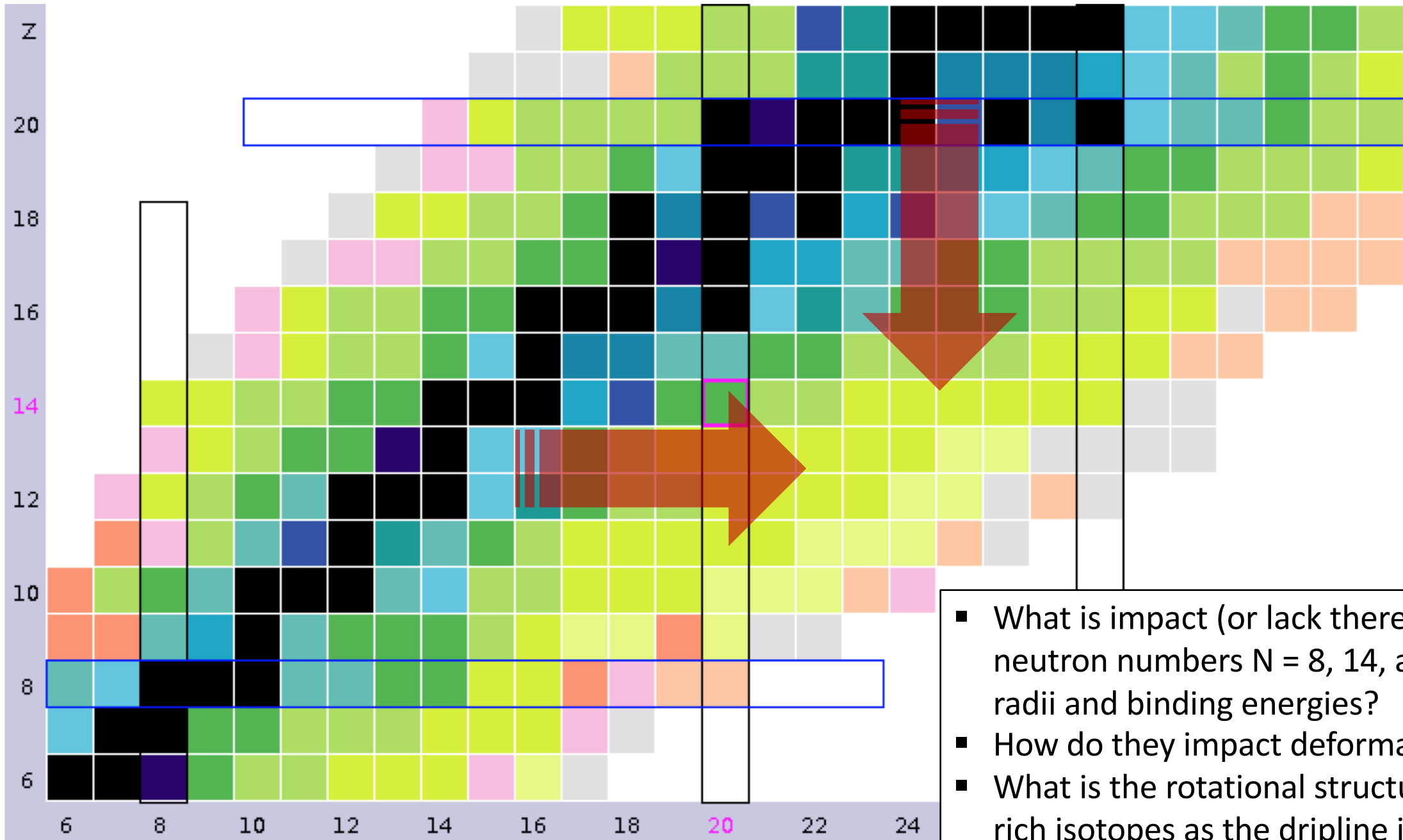
0.42(3)

$\Delta\text{NNLO}_{\text{GO}}(394)$

0.39(2)

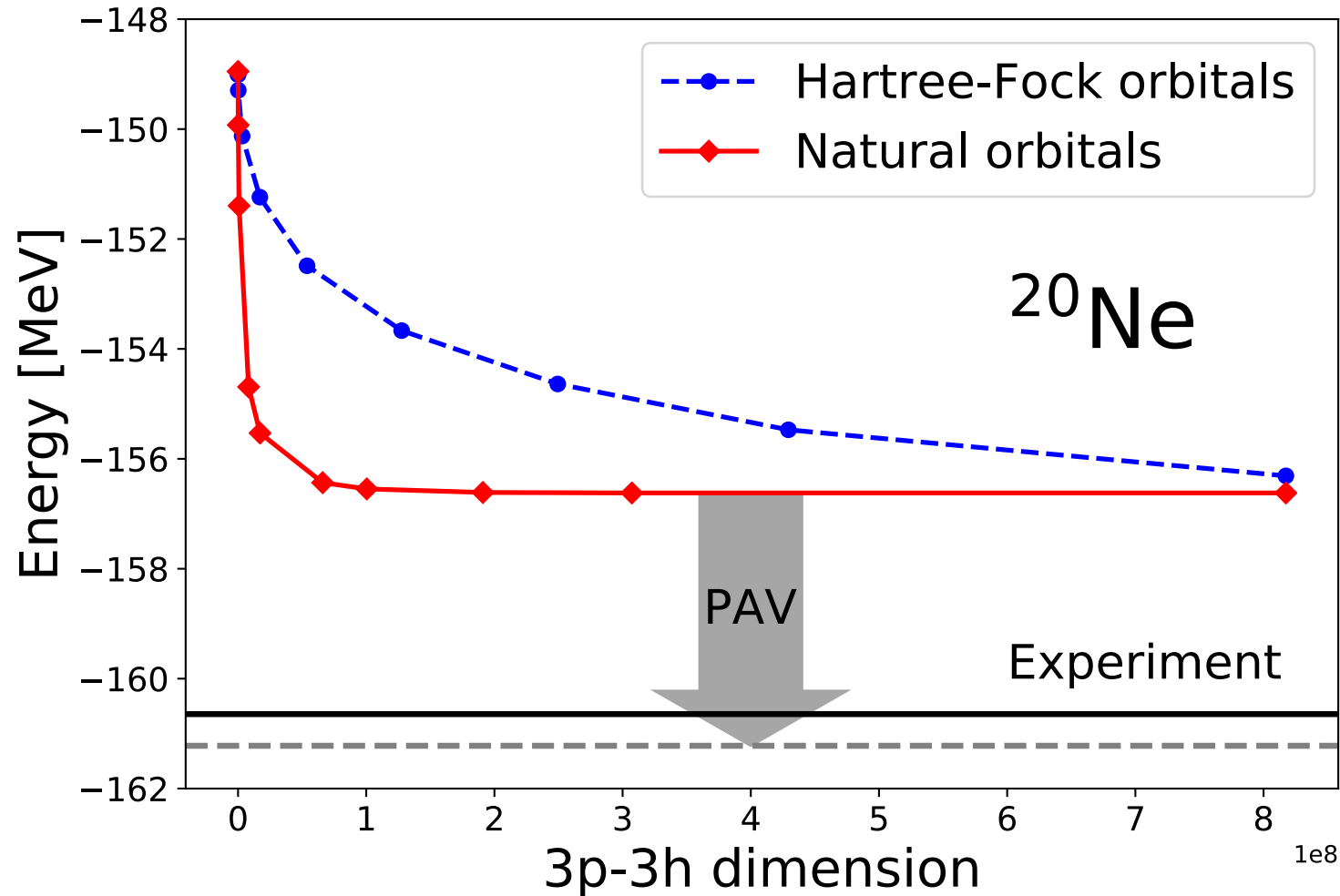
$$\alpha_D = 2\alpha \int d\omega \frac{R(\omega)}{\omega}$$

Towards island of inversion with ab initio methods



- What is impact (or lack thereof) of the “magic” neutron numbers $N = 8, 14,$ and 20 on charge radii and binding energies?
- How do they impact deformation past $N = 20$?
- What is the rotational structure of neutron-rich isotopes as the dripline is approached?

Coupled-cluster computations of deformed nuclei – natural orbitals

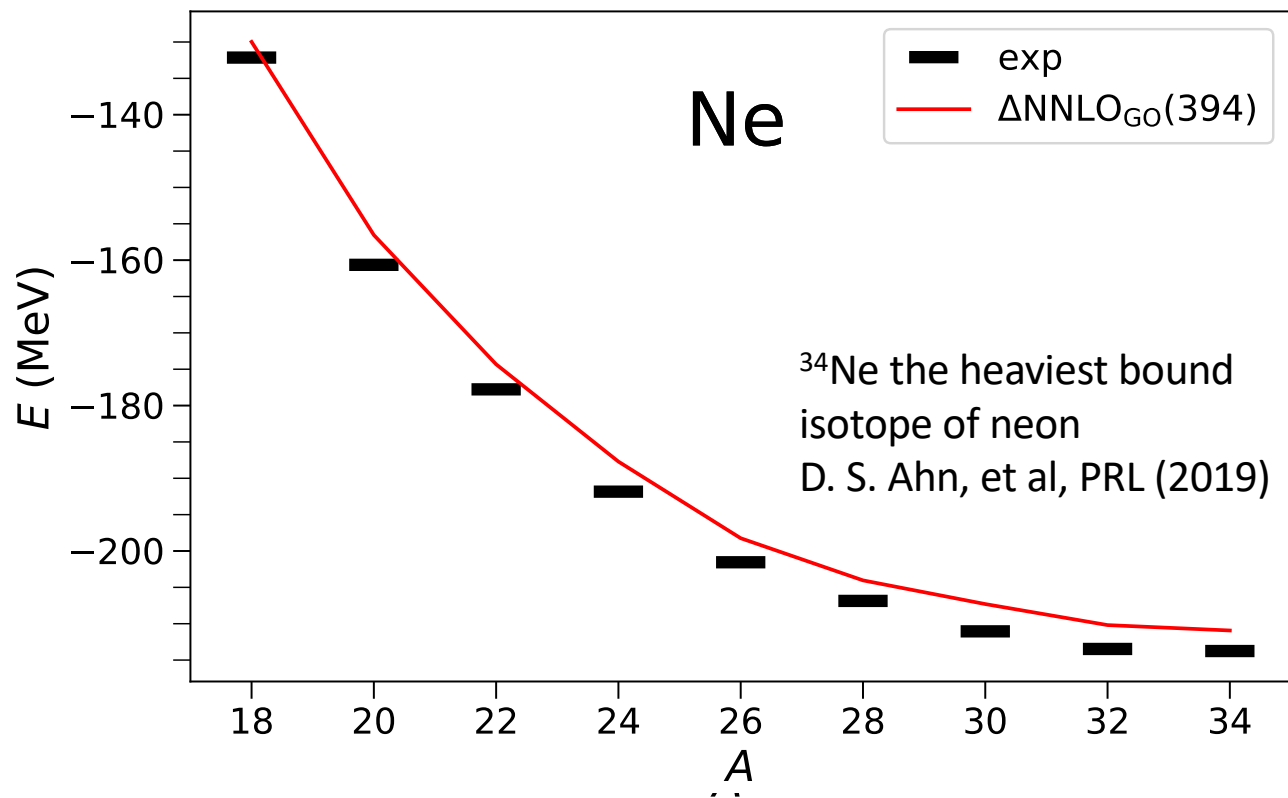


- Coupled-cluster calculations from axially symmetric reference states
- Natural orbitals from many-body perturbation theory [A. Tichai, et al PRC (2019)] yields rapid convergence with respect 3p3h excitations in CCSDT-1
- Hartree-Fock with projection after variation (PAV) gives upper bound on the energy gain from symmetry restoration

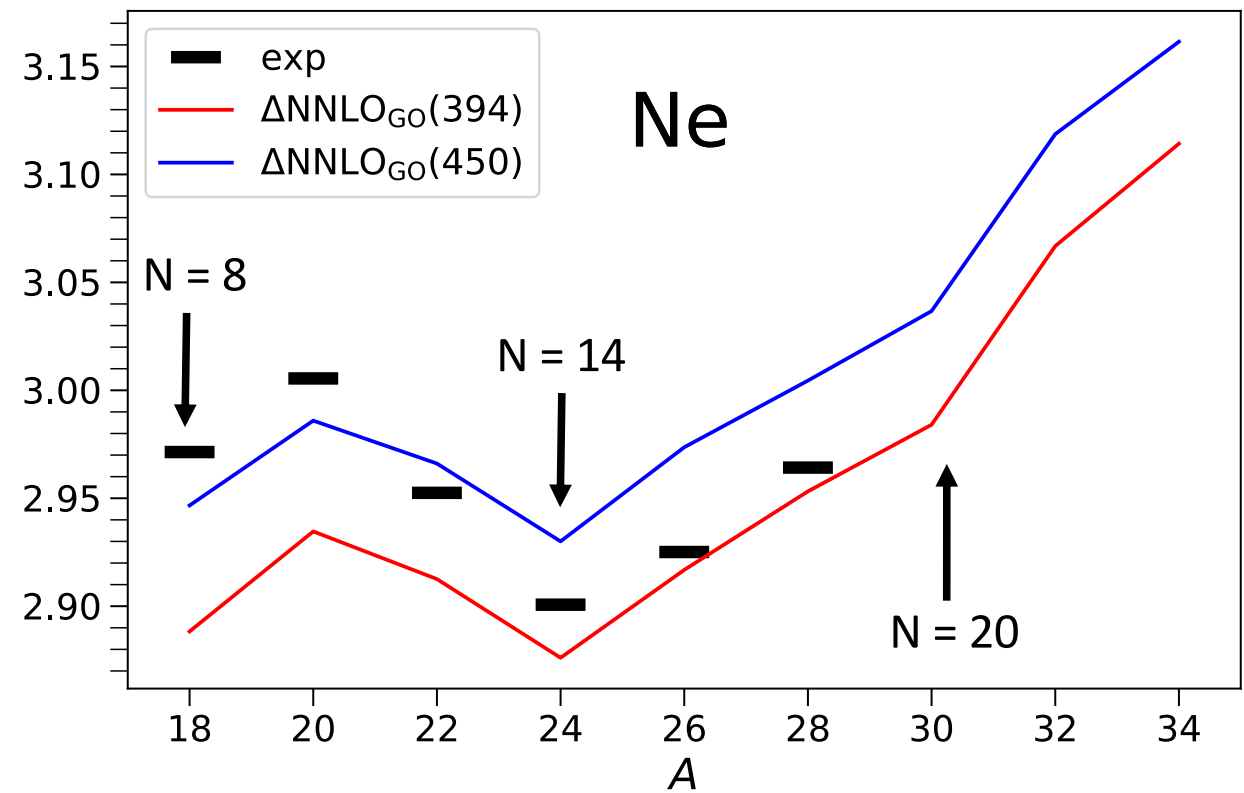
Computations of neon isotopes

- Dripline correctly predicted at ^{34}Ne
- Charge radii predicts shell closures at $N = 8$, $N = 14$, and at $N = 20$

$N = 12$, $hw = 16\text{MeV}$

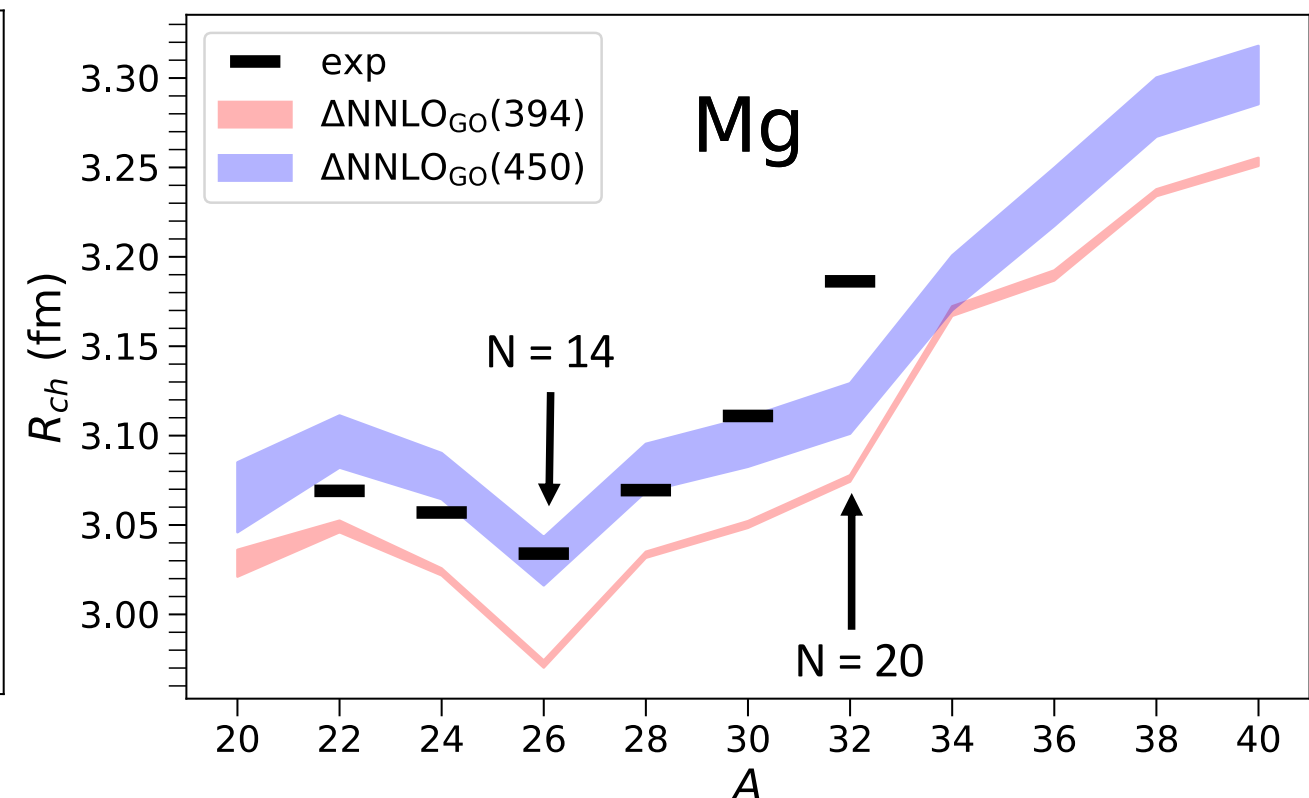
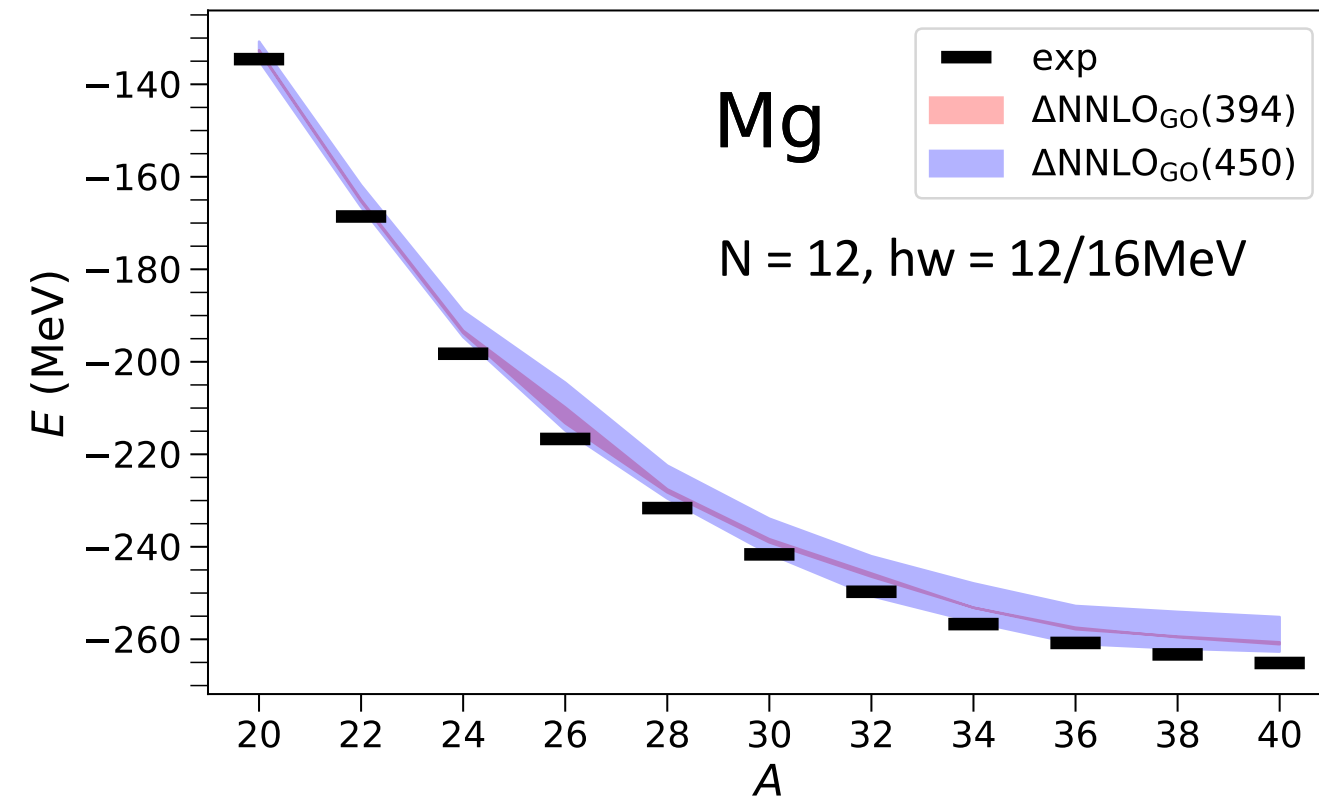


$N = 12$, $hw = 16\text{MeV}$

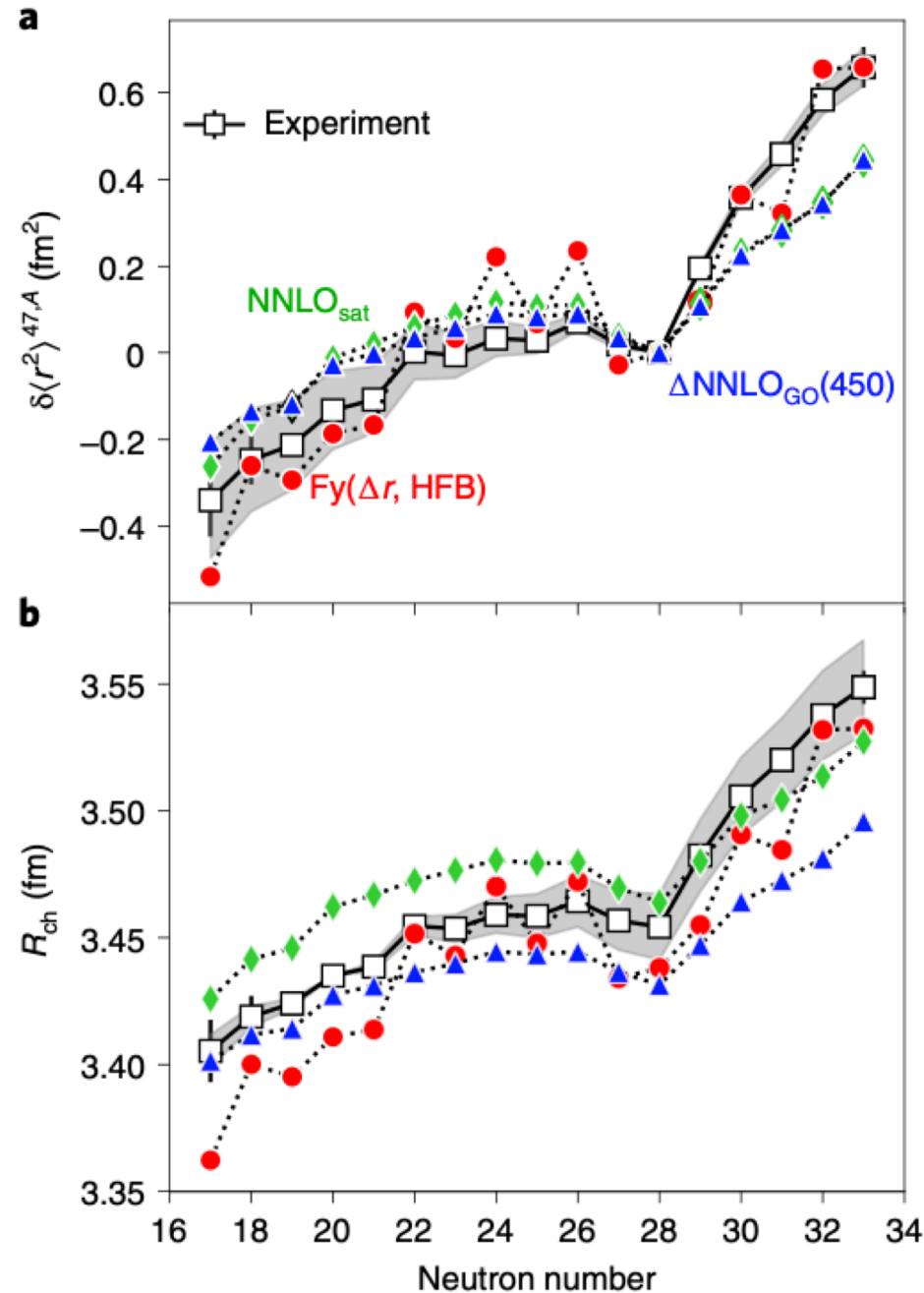


Computations of magnesium isotopes

- Dripline predicted at ^{40}Mg – continuum may impact the location of the dripline
- Charge radii predicts shell closures at $N = 8$, $N = 14$, and at $N = 20$
- The bands indicate uncertainties from model-space truncations



Charge radii of neutron-rich potassium isotopes



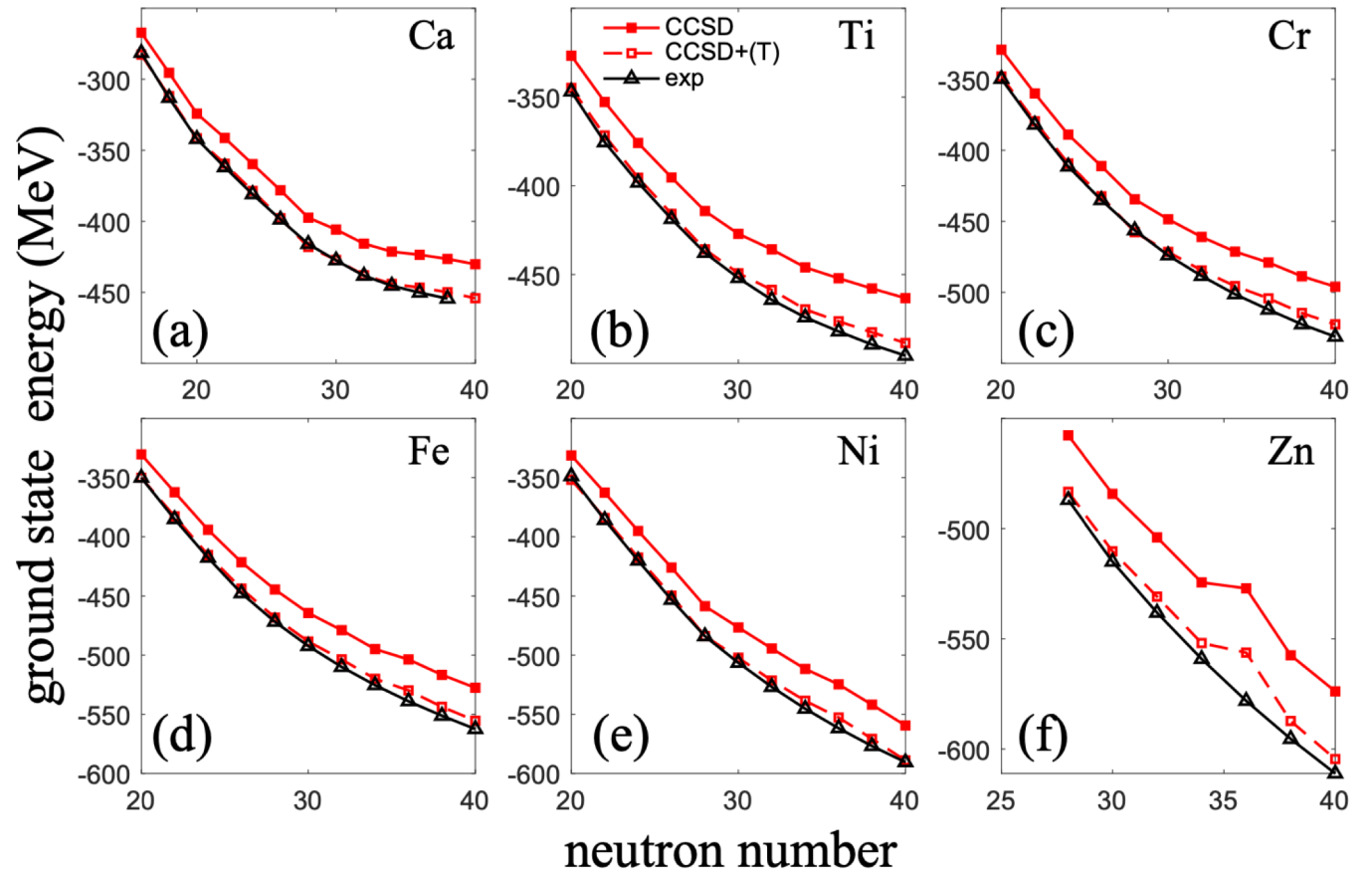
- First high precision measurement of ^{52}K charge radius by CRIS @ ISOLDE/CERN
- Steep increase in charge radii beyond $N = 28$ challenges theory
- No signature of $N = 32$ shell closure
- Isotope shifts not sensitive to details of NNLO chiral Hamiltonians

A. Koszorus, et al, Nature Physics, Open Access (2021)

Coupled-cluster computations of even-even Ca-Zn nuclei

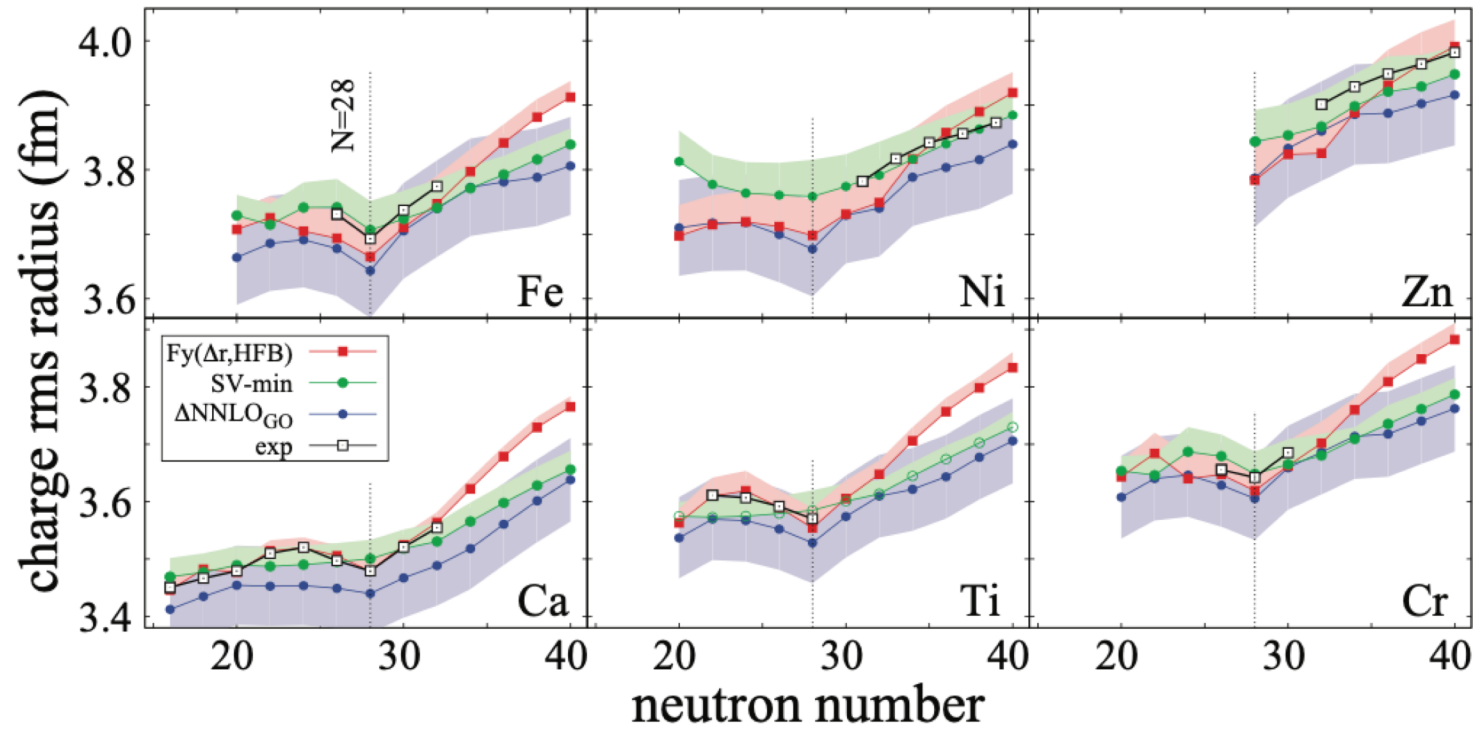
- We construct natural orbitals from a Hartree-Fock calculation using $N_{\text{max}} = 14$.
- The normal-ordered Hamiltonian in natural orbitals is truncated to a smaller model-space (See J. Hoppe et al. Phys. Rev. C 103, 014321 (2021))
- We achieve rapid convergence for energies and radii

$N_{\text{max}}^{\text{nat}}$	$\hbar\omega=12$ MeV		$\hbar\omega=16$ MeV	
	E (MeV)	R_{ch} (fm)	E (MeV)	R_{ch} (fm)
6	-473.731	3.857	-474.445	3.848
8	-513.502	3.882	-515.685	3.869
10	-520.787	3.896	-523.355	3.882
12	-521.746	3.900	-524.384	3.886



CCSD ground-state energies with estimated triples (12% of CCSD correlation energy)

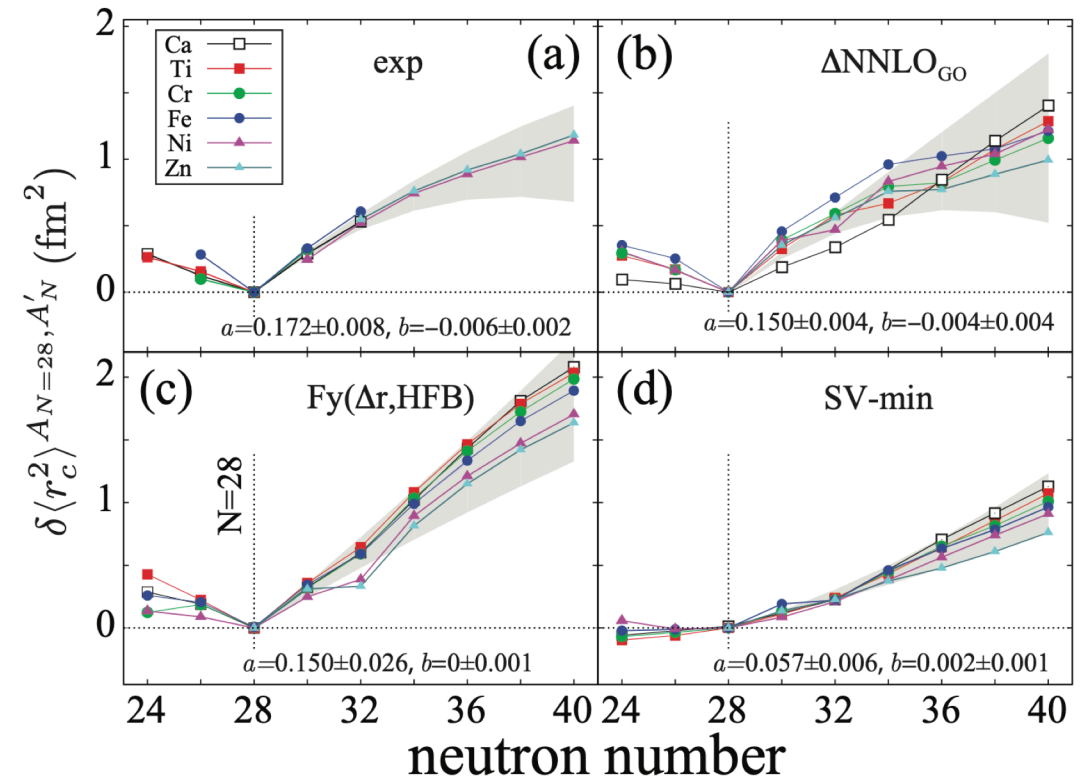
Coupled-cluster computations of even-even Ca-Zn nuclei



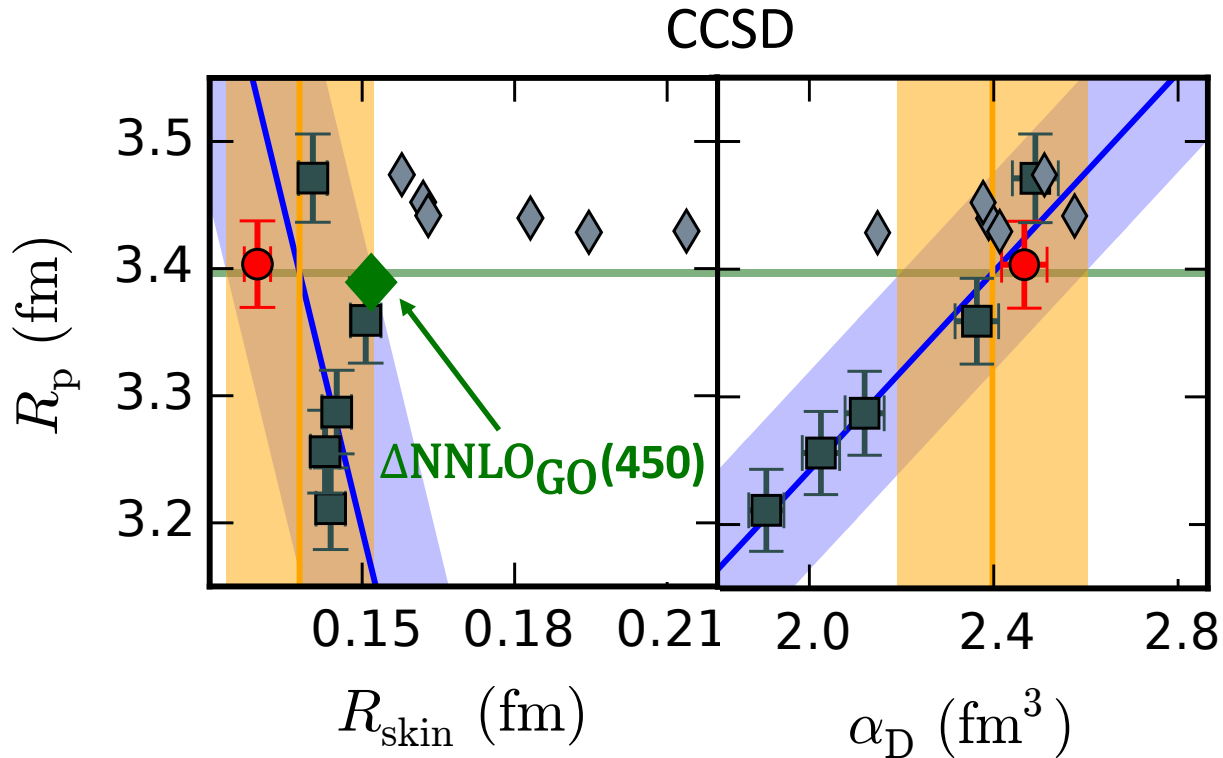
M. Kortelainen, Z. H. Sun, G. Hagen, W. Nazarewicz, T. Papenbrock, P-G. Reinhard, Phys. Rev. C 105, L021303 (2022)

Element independent increase in radii beyond $N = 28$ for Ca-Zn isotopes
 The trend is explained by fitting the Z averaged isotope shift to a parabolic expression from generalized seniority picture

$$\delta\langle r_c^2 \rangle^{A_m, A_m+n} = an + bn^2$$



Neutron skin and dipole polarizability of ^{48}Ca



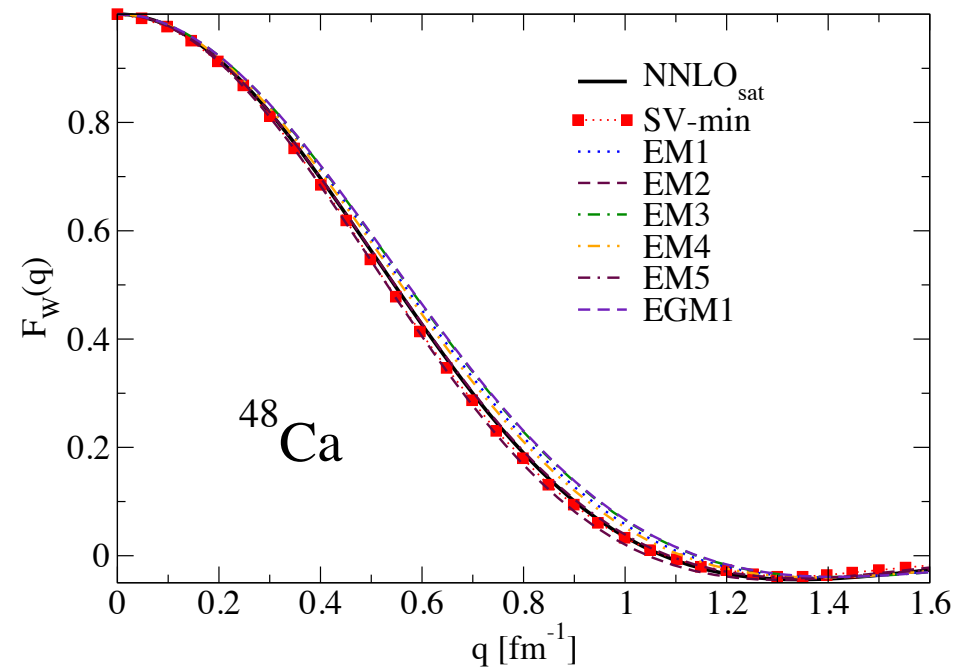
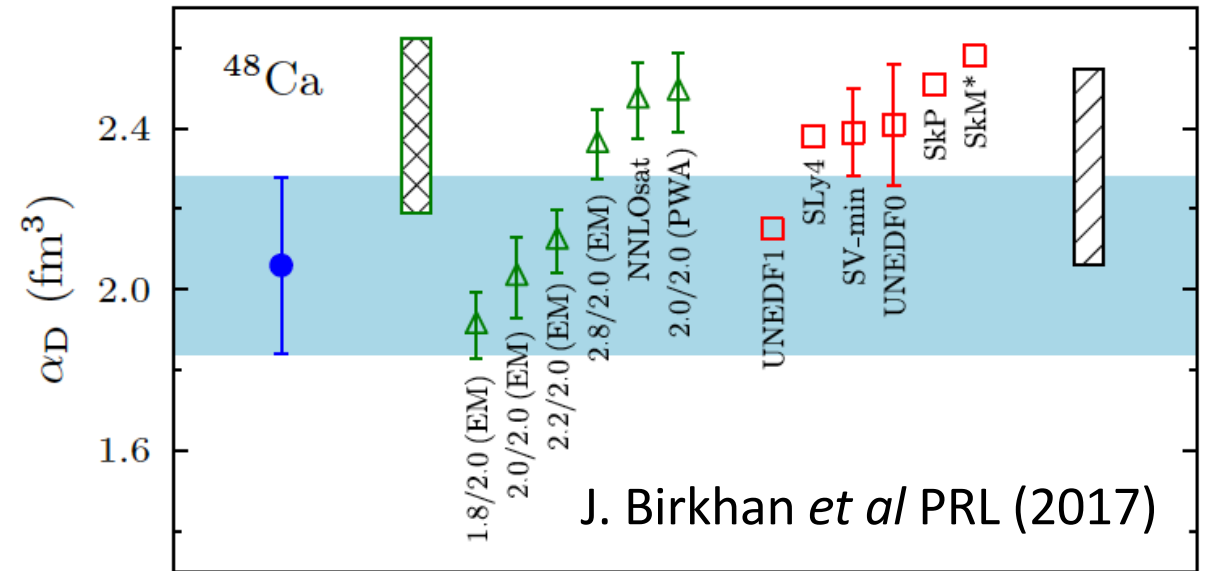
G. Hagen *et al*, Nature Physics **12**, 186–190 (2016)

- Neutron skin significantly smaller than in DFT
- Results for ^{48}Ca agrees with CREX

$$R_{\text{skin}} = 0.121 \pm 0.035 \text{ fm}$$

$$\text{CREX: } F_w(q = 0.873 \text{ fm}^{-1}) = 0.1304 \pm 0.0052$$

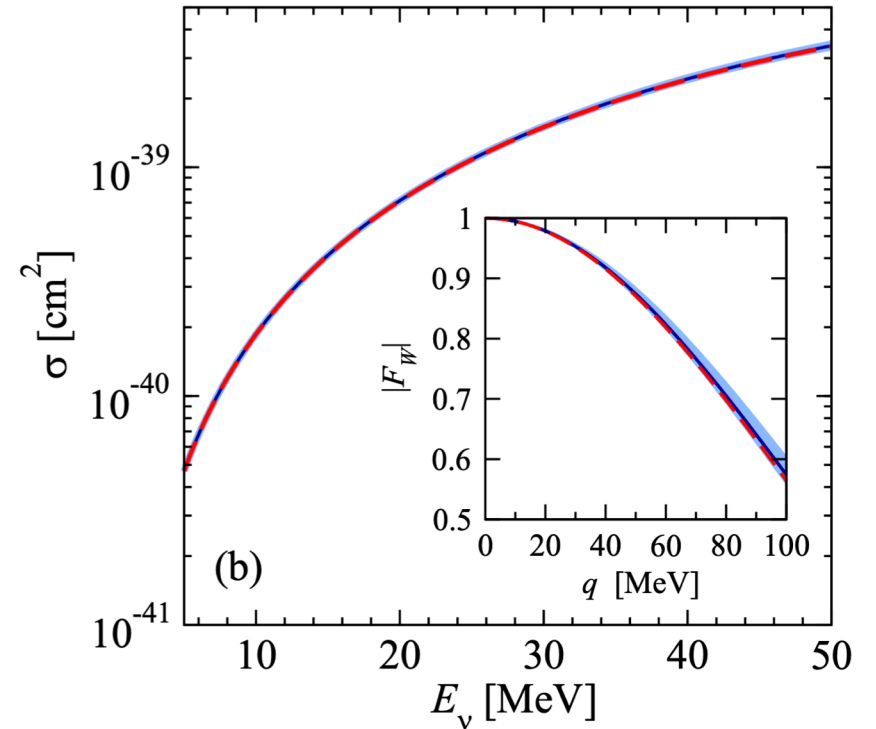
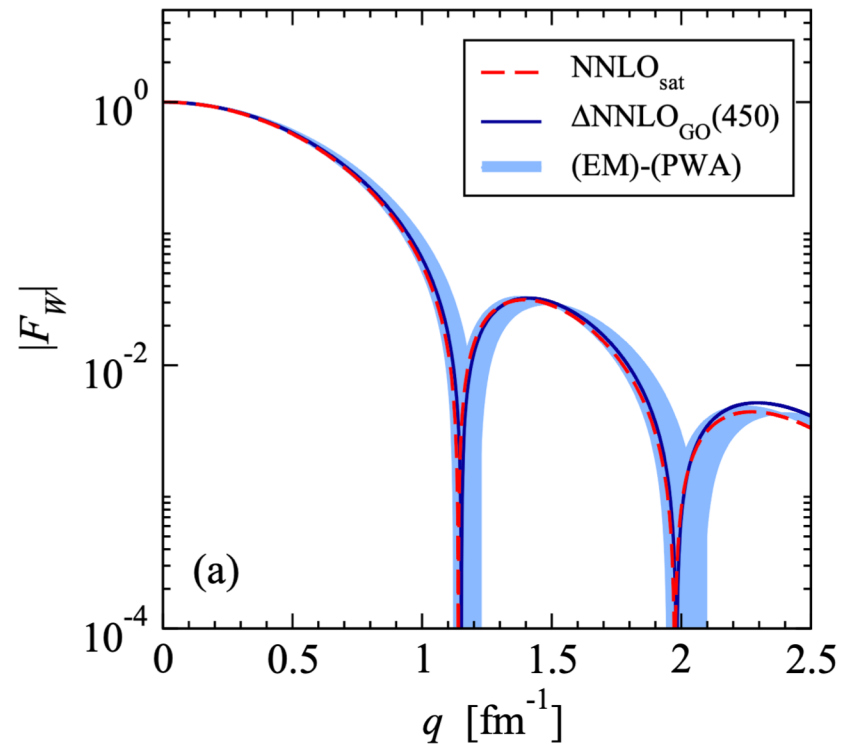
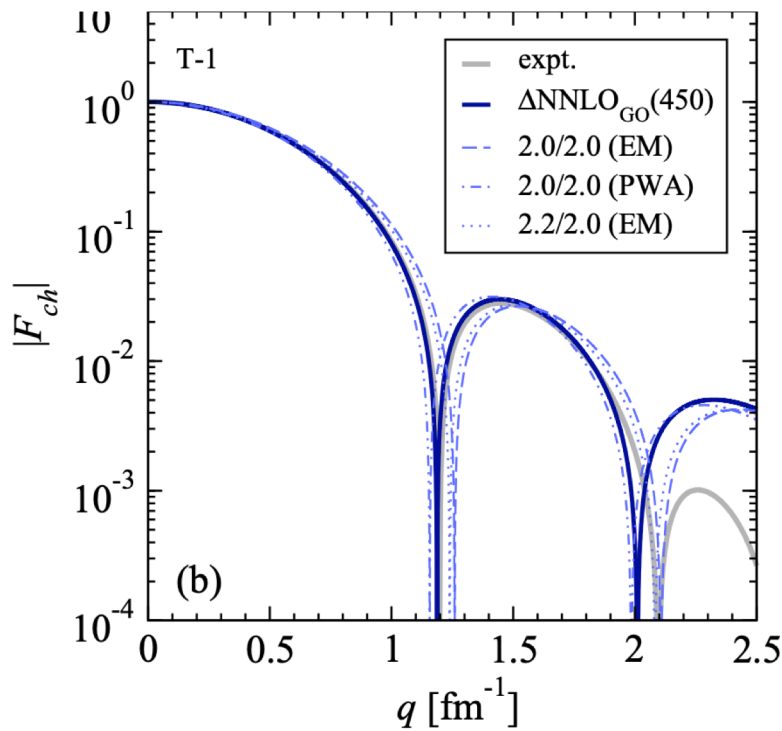
$$\text{Coupled-Cluster: } 0.102 \leq F_w(q = 0.873 \text{ fm}^{-1}) \leq 0.161$$



Coherent elastic neutrino scattering (CE ν NS) on ^{40}Ar

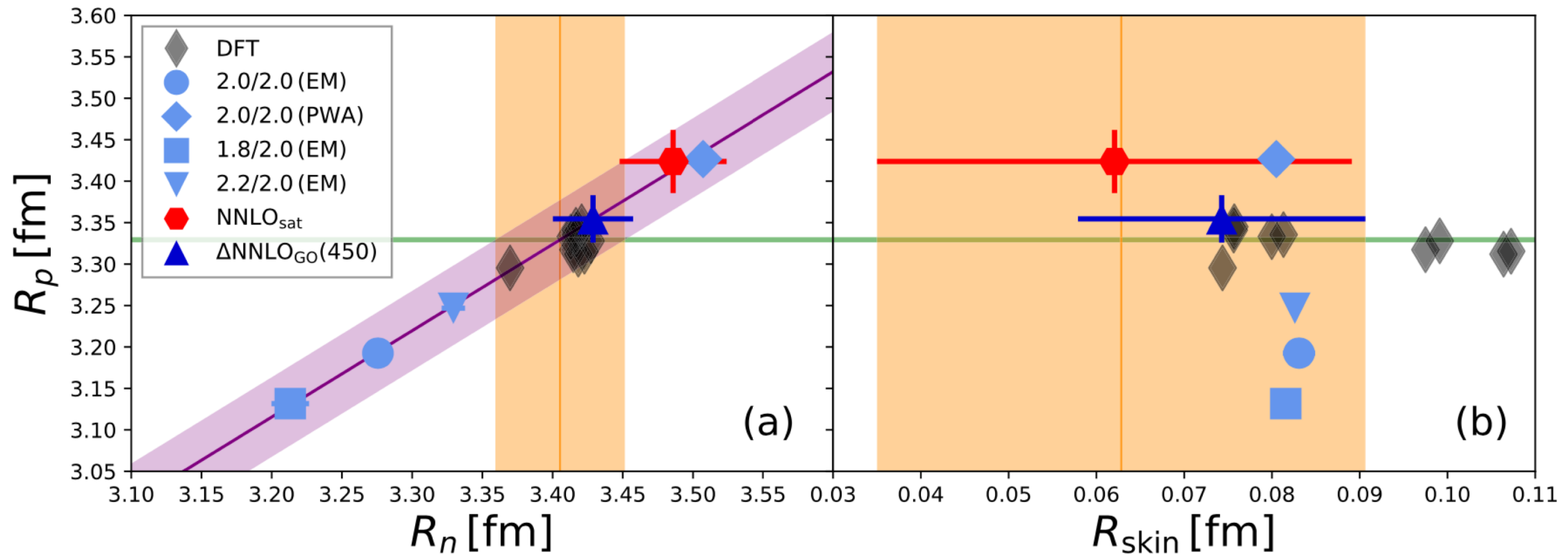
Coherent cross section $\frac{d\sigma}{dT}(E_\nu, T) \simeq \frac{G_F^2}{4\pi} M \left[1 - \frac{MT}{2E_\nu^2} \right] Q_W^2 F_W^2(q^2)$

- Good agreement with data for charge form-factor in ^{40}Ar
- Mild sensitivity to employed interaction in energy region relevant to coherent scattering
- Need higher-precision experiments in order to inform/constrain nuclear models

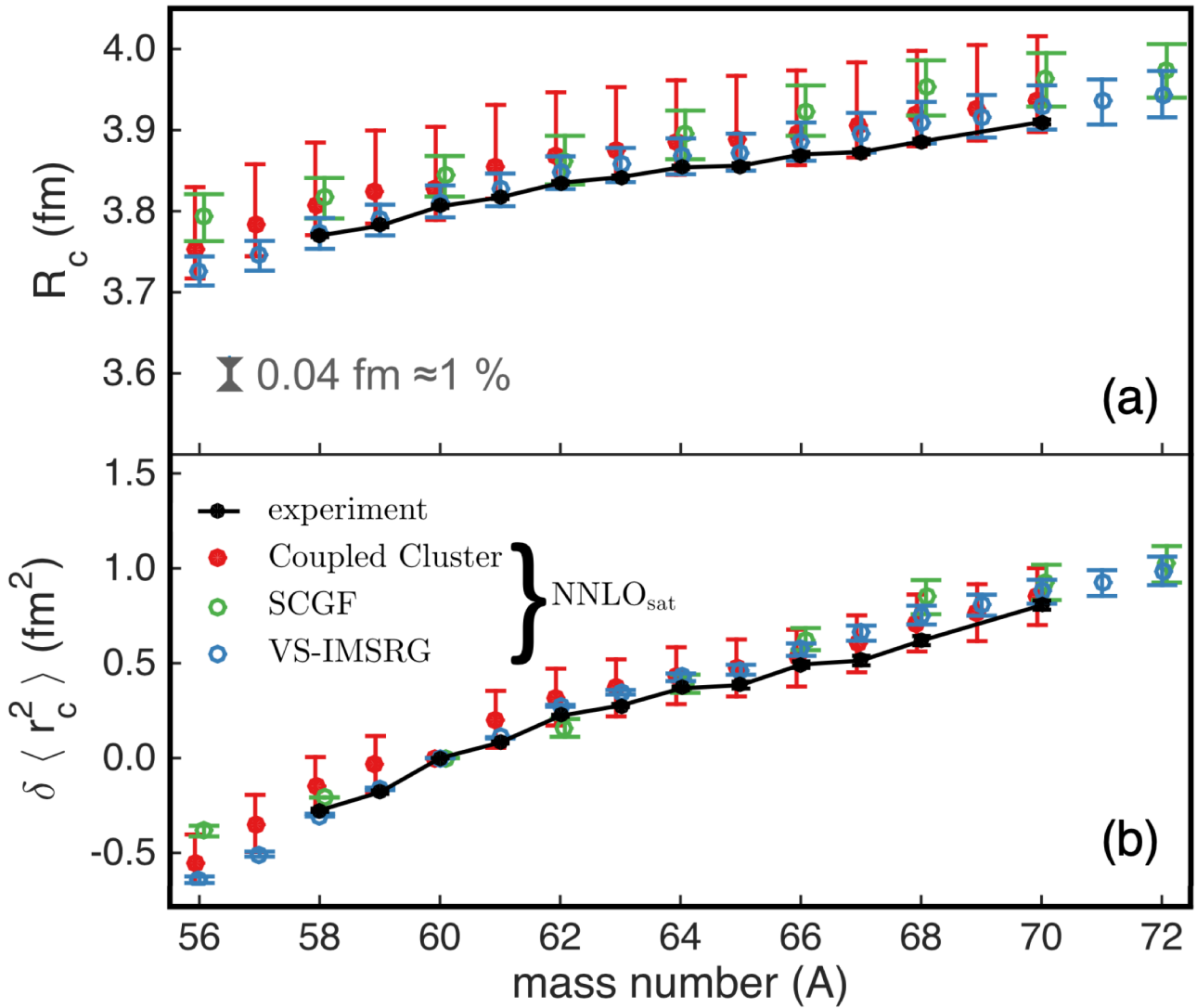


Coherent elastic neutrino scattering (CE ν NS) on ^{40}Ar

The neutron radius and skin of ^{40}Ar from coupled cluster with interactions from chiral EFTs are consistent with DFT predictions – This is contrary to the case of ^{48}Ca



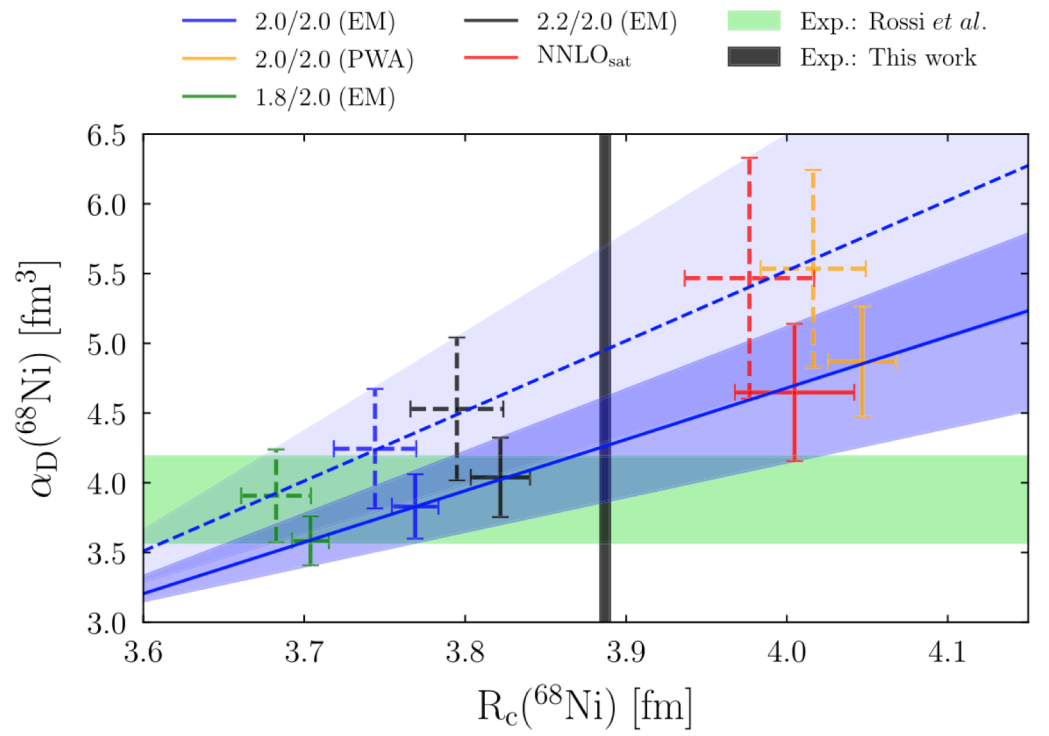
Radii, skins, and dipole polarizability of nickel isotopes



S. Malbrunot-Ettenauer, et al, Phys. Rev. Lett. 128, 022502 (2022)

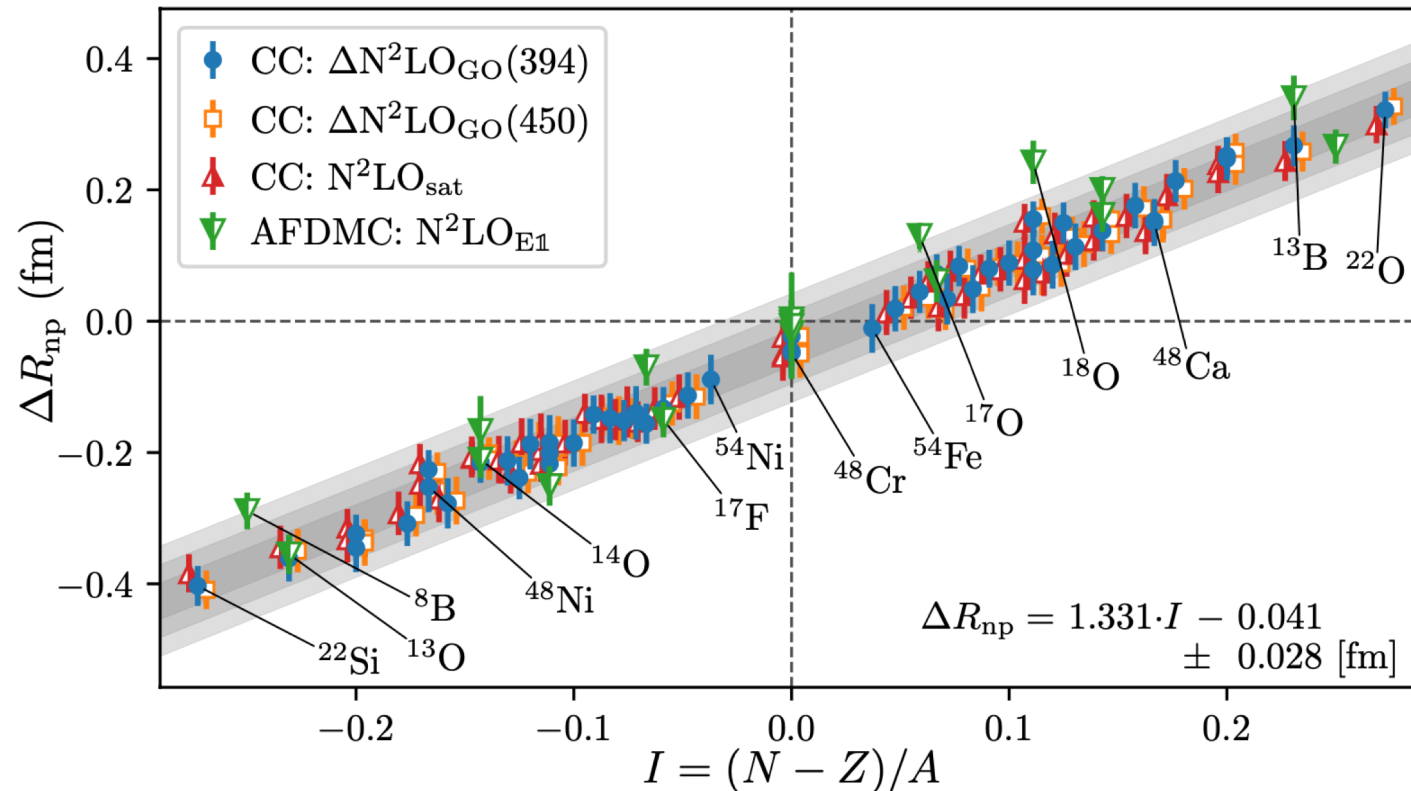
Kaufmann et al, Phys. Rev. Lett. 124, 132502 (2020)

Hamiltonian	α_D	R_p	R_n	R_{skin}	R_c
1.8/2.0 (EM)	3.58(18)	3.62(1)	3.82(1)	0.201(1)	3.70(1)
2.0/2.0 (EM)	3.83(23)	3.69(2)	3.89(2)	0.202(3)	3.77(1)
2.2/2.0 (EM)	4.04(28)	3.74(2)	3.94(2)	0.203(4)	3.82(2)
2.0/2.0 (PWA)	4.87(40)	3.97(2)	4.17(3)	0.204(8)	4.05(2)
NNLO _{sat}	4.65(49)	3.93(4)	4.11(5)	0.183(8)	4.00(4)



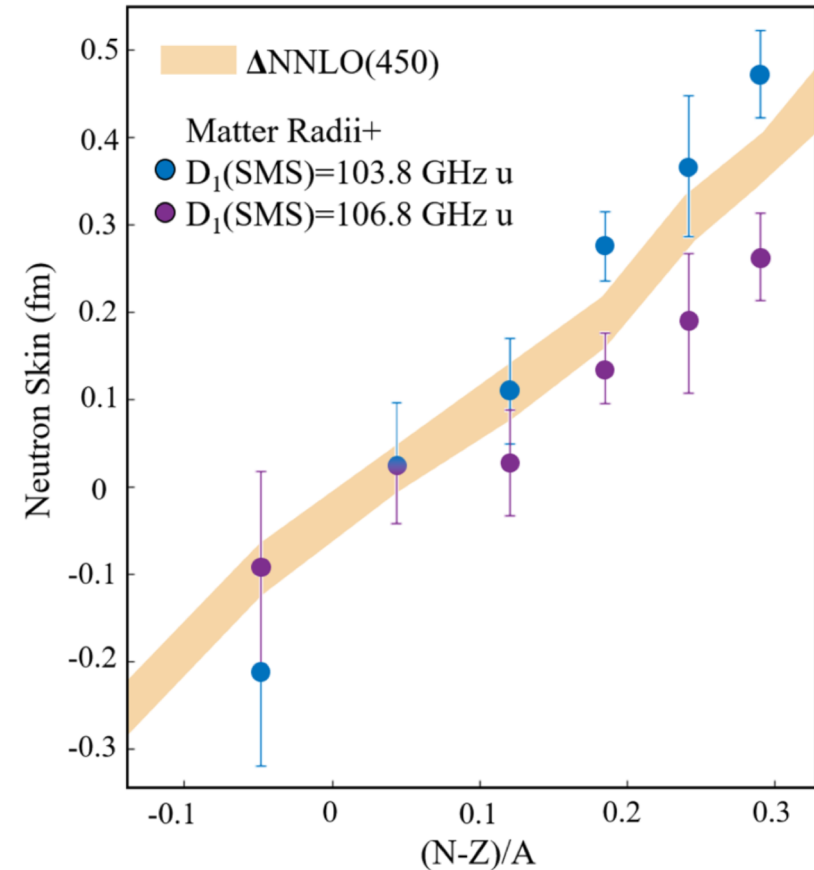
Trends of neutron skins of mirror nuclei

S. J. Novario, et al, Phys. Rev. Lett. **130**, 032501 (2023)



Simplicity from complexity

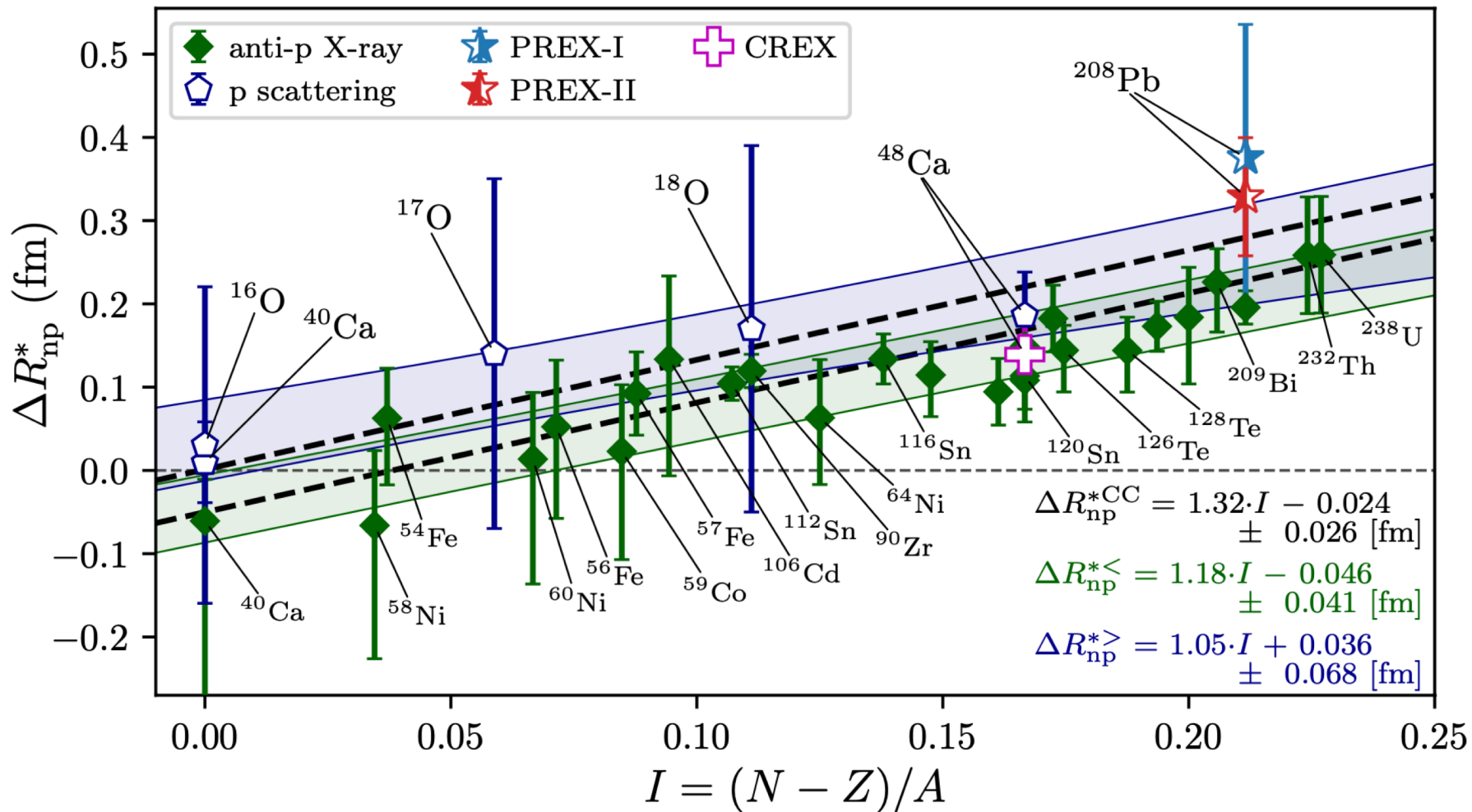
Different ab-initio methods and interactions confirm a linear relation between neutron skin and isospin asymmetry that can be derived from the liquid drop model



B. Ohayon, et al, Phys. Rev. C **105**, L031305 (2022)

Neutron skin of sodium isotopes as a function of isospin asymmetry. Data used available matter radii and charge radii from isotope shift measurements using two different values of the atomic parameter K_{SMS}

Trends of neutron skins of mirror nuclei



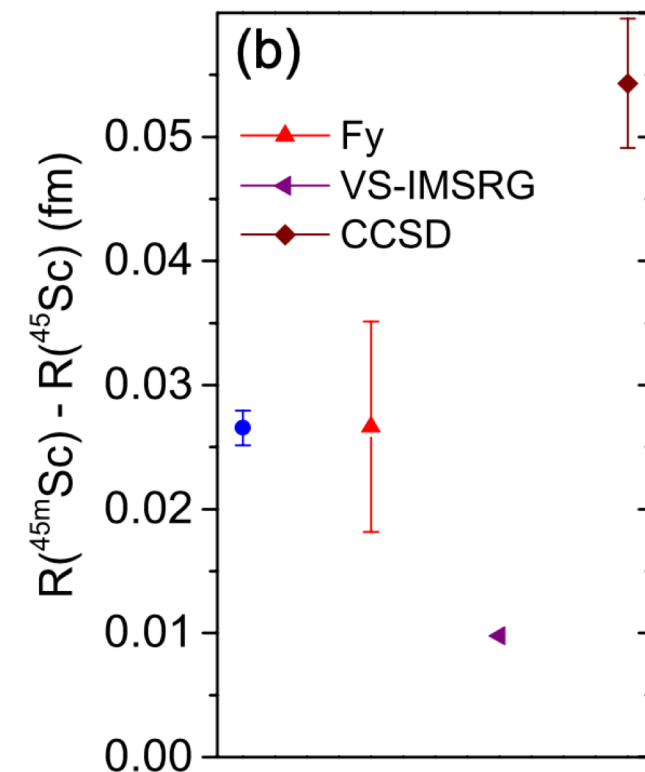
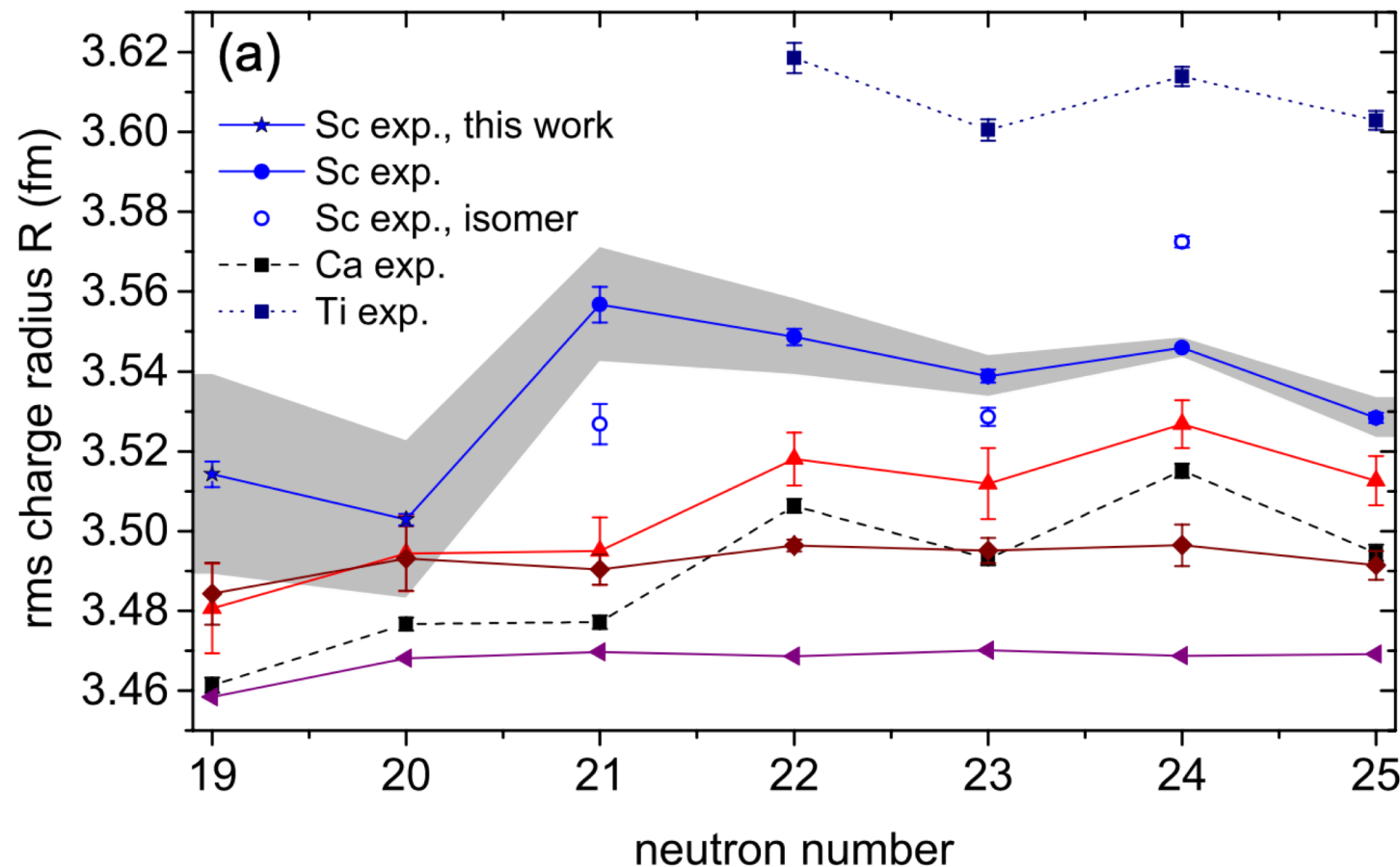
- Coulomb-subtracted neutron skin thickness plotted against the isospin asymmetry from available experimental data
- Our results overlaps with antiprotonic x-ray and proton-scattering data

S. J. Novario, D. Lonardoni, S. Gandolfi, G. Hagen, Phys. Rev. Lett. 130, 032501 (2023)

$$\Delta R_{np}^* = \Delta R_{np} + ZA^{-1/3} \times 0.0033 \text{ fm}$$

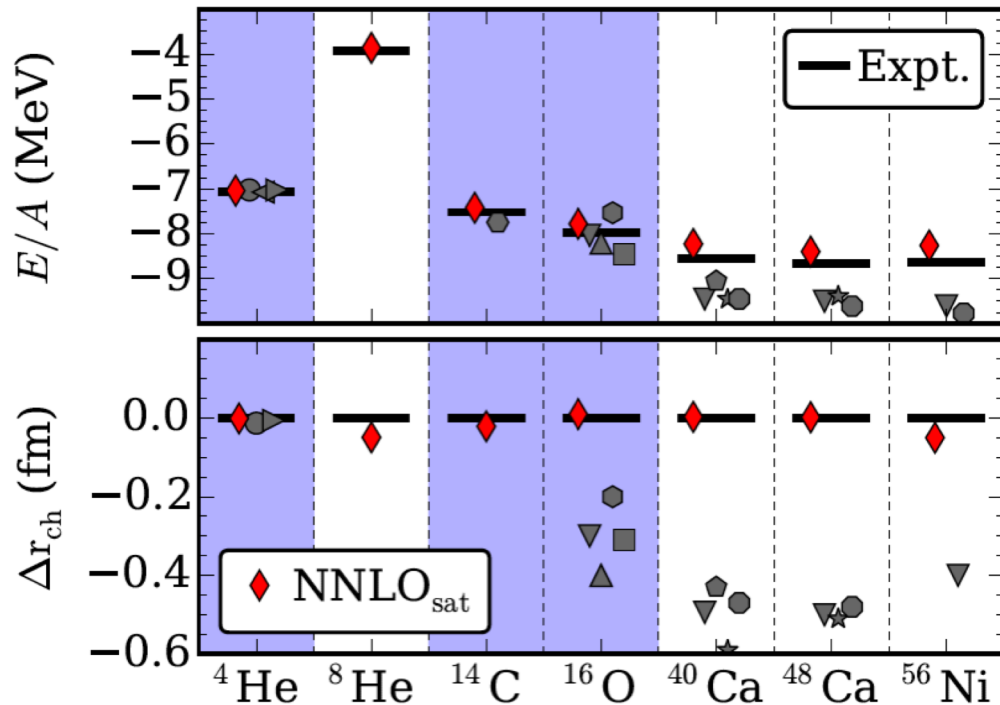
Surprising charge-radius kink in the Sc isotopes at N=20 challenge theory

- Measurement of charge radii of neutron deficient 40Sc and 41Sc nuclei at ISOLDE/CERN
- Kink seen at neutron number N = 20 which is missing in the neighboring isotopic chains
- Description of large charge radius of deformed isomer in 45Sc requires large collective spaces

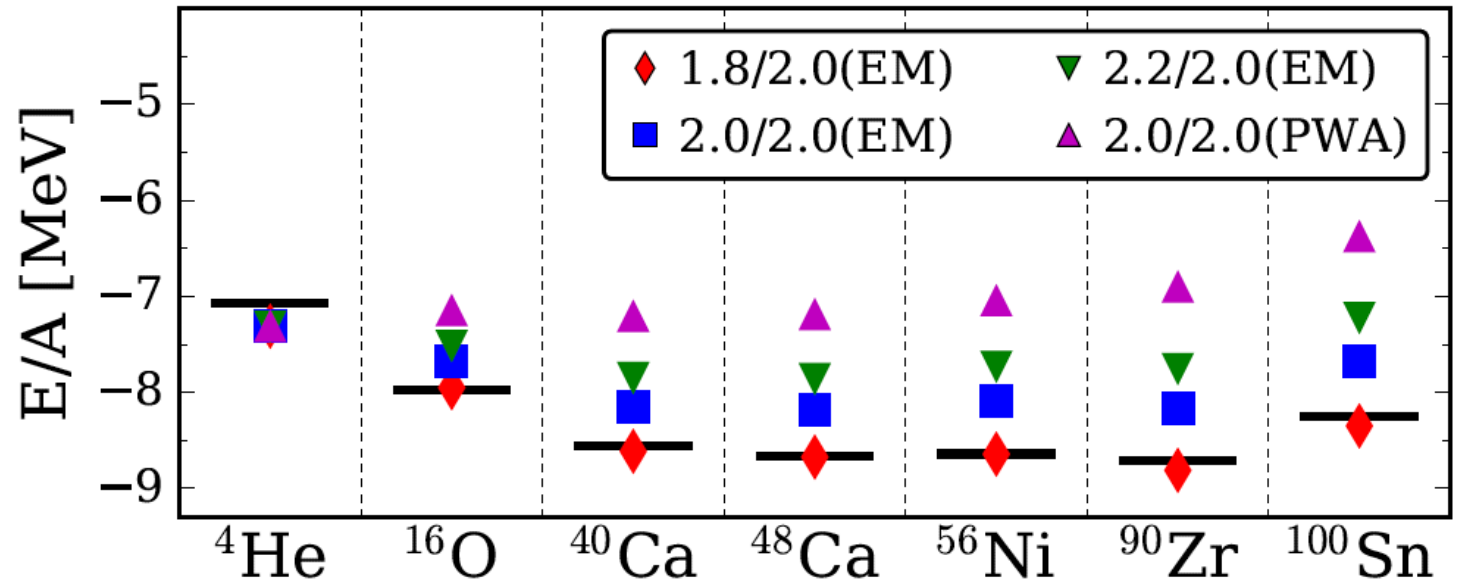


K. König et al, in preparation (2023)

Why do some interaction models work better than others?



A. Ekström *et al*, Phys. Rev. C **91**, 051301(R) (2015).



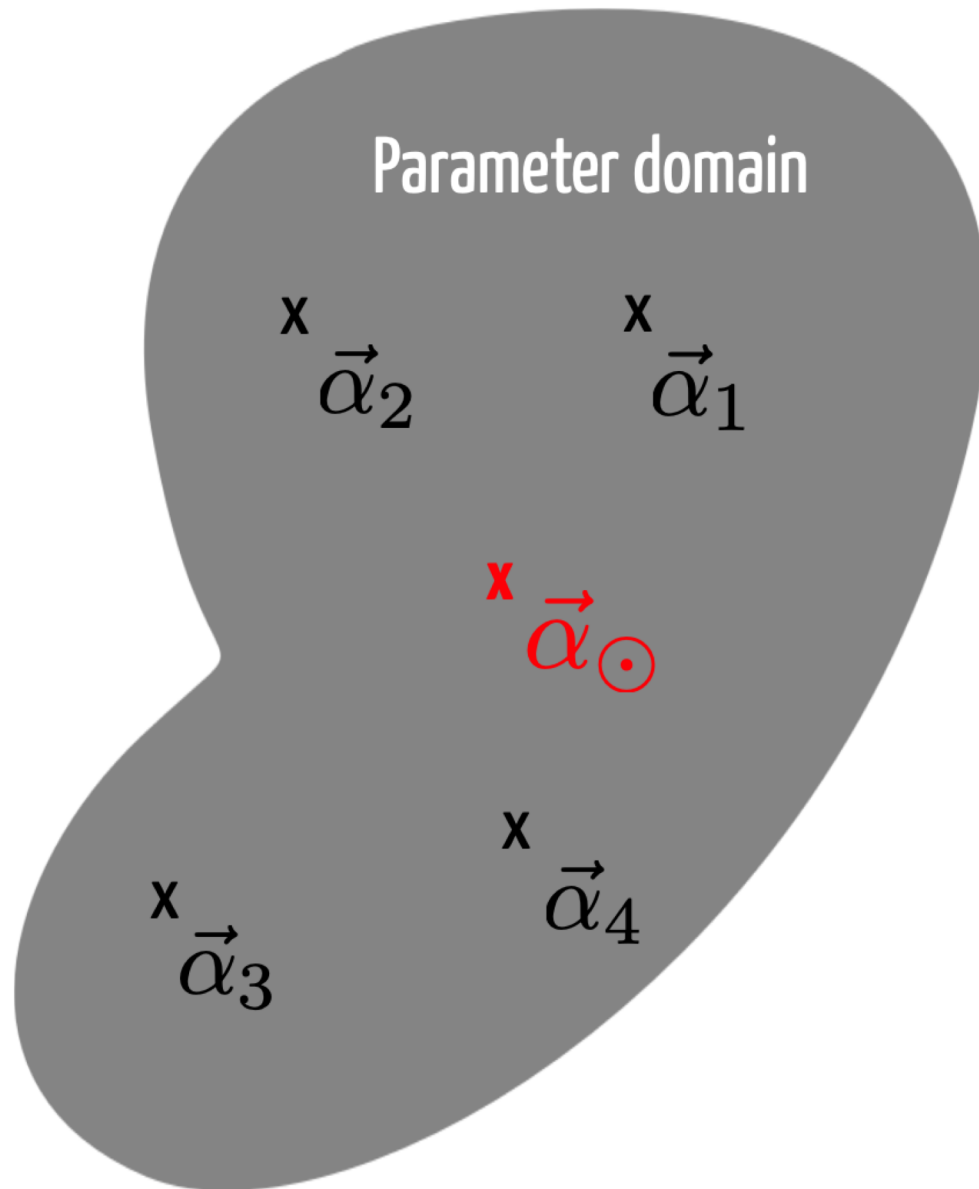
K. Hebeler *et al* PRC (2011).

T. Morris *et al*, PRL (2018).

To answer this we need predictions with rigorous **uncertainty quantification** and **sensitivity analyses** that are grounded in the description of the underlying nuclear Hamiltonian

Emulating ab-initio coupled-cluster calculations

Andreas Ekström, Gaute Hagen PRL **123**, 252501 (2019)



- Generalization of the eigenvector continuation method [Frame D. et al., Phys. Rev. Lett. 121, 032501 (2018), S. König et al Phys. Lett. B 810 (2020) 135814]
- Write the Hamiltonian in a linearized form

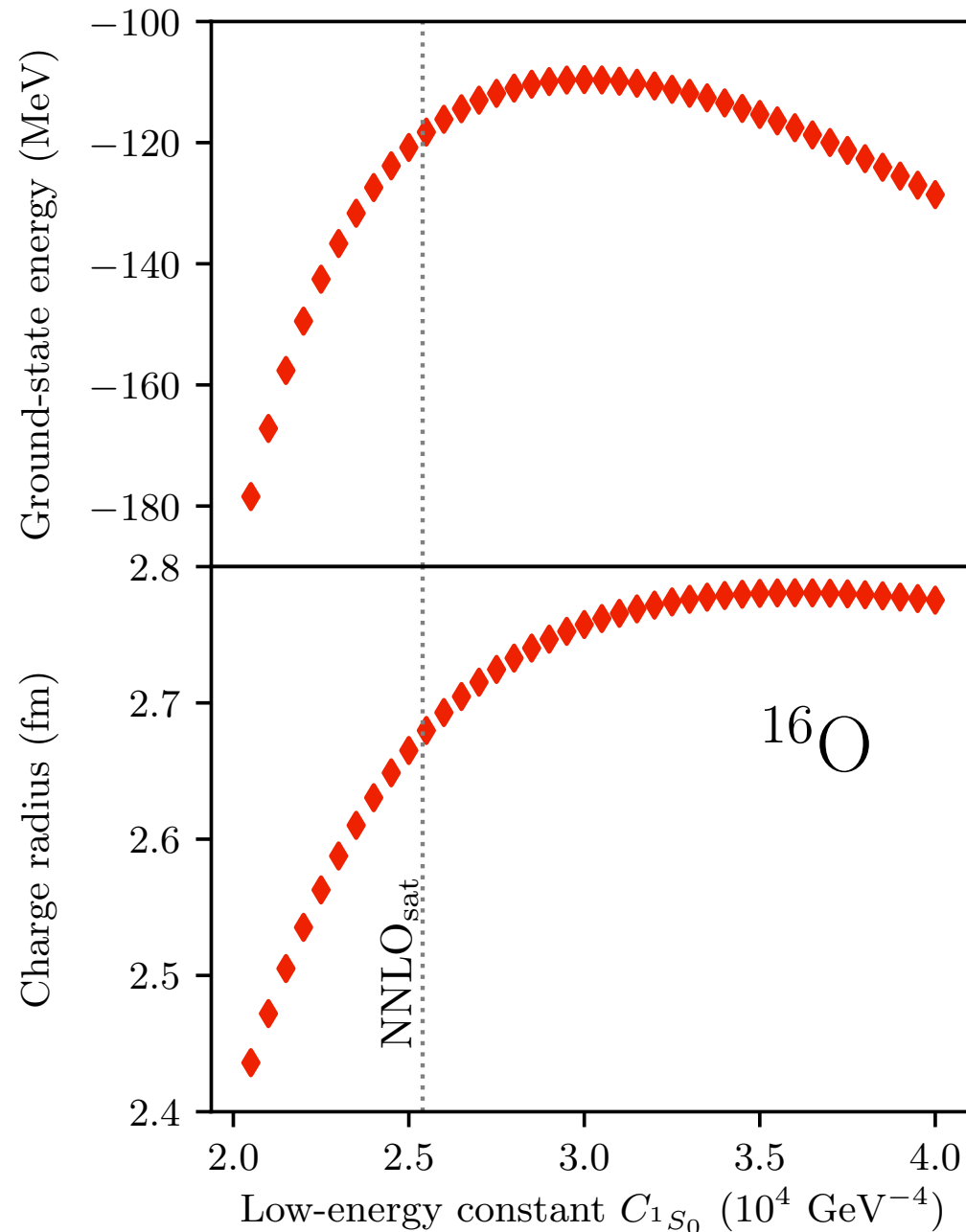
$$H(\vec{\alpha}) = \sum_{i=0}^{N_{\text{LECS}}=16} \alpha_i h_i$$

- Select “training points” where we solve exact coupled-cluster
- Project the target Hamiltonian onto sub-space of training vectors and diagonalize the generalized eigenvalue problem

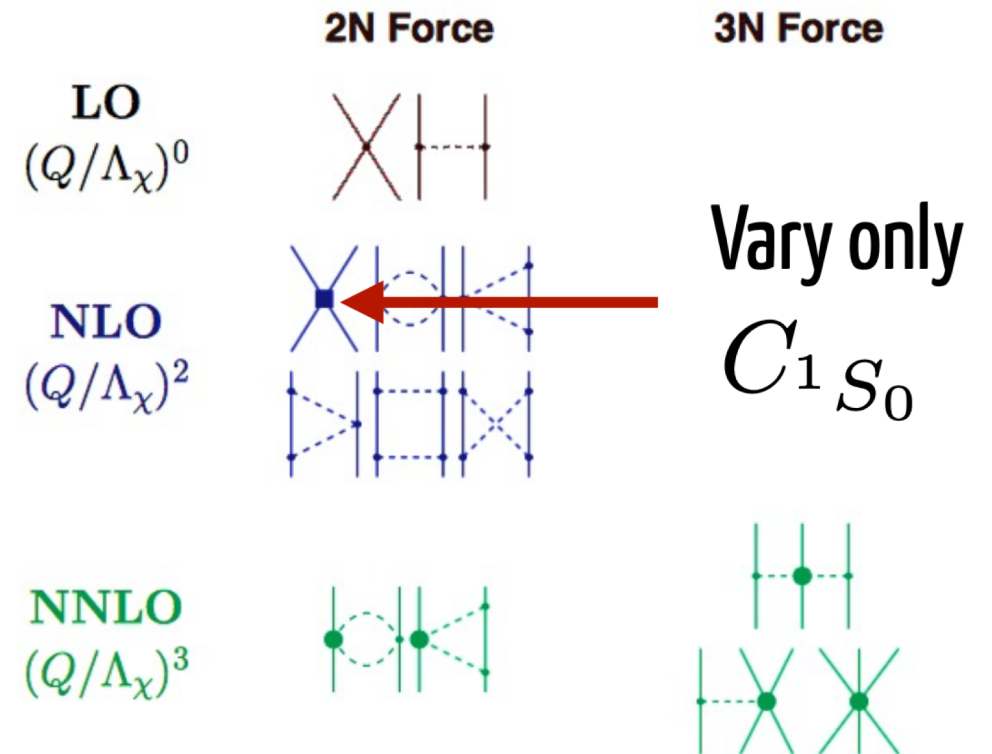
$$\mathbf{H}(\vec{\alpha}_{\odot}) \vec{c} = E(\vec{\alpha}_{\odot}) \mathbf{N} \vec{c},$$

Emulating ab-initio coupled-cluster calculations

Andreas Ekström, Gaute Hagen PRL **123**, 252501 (2019)

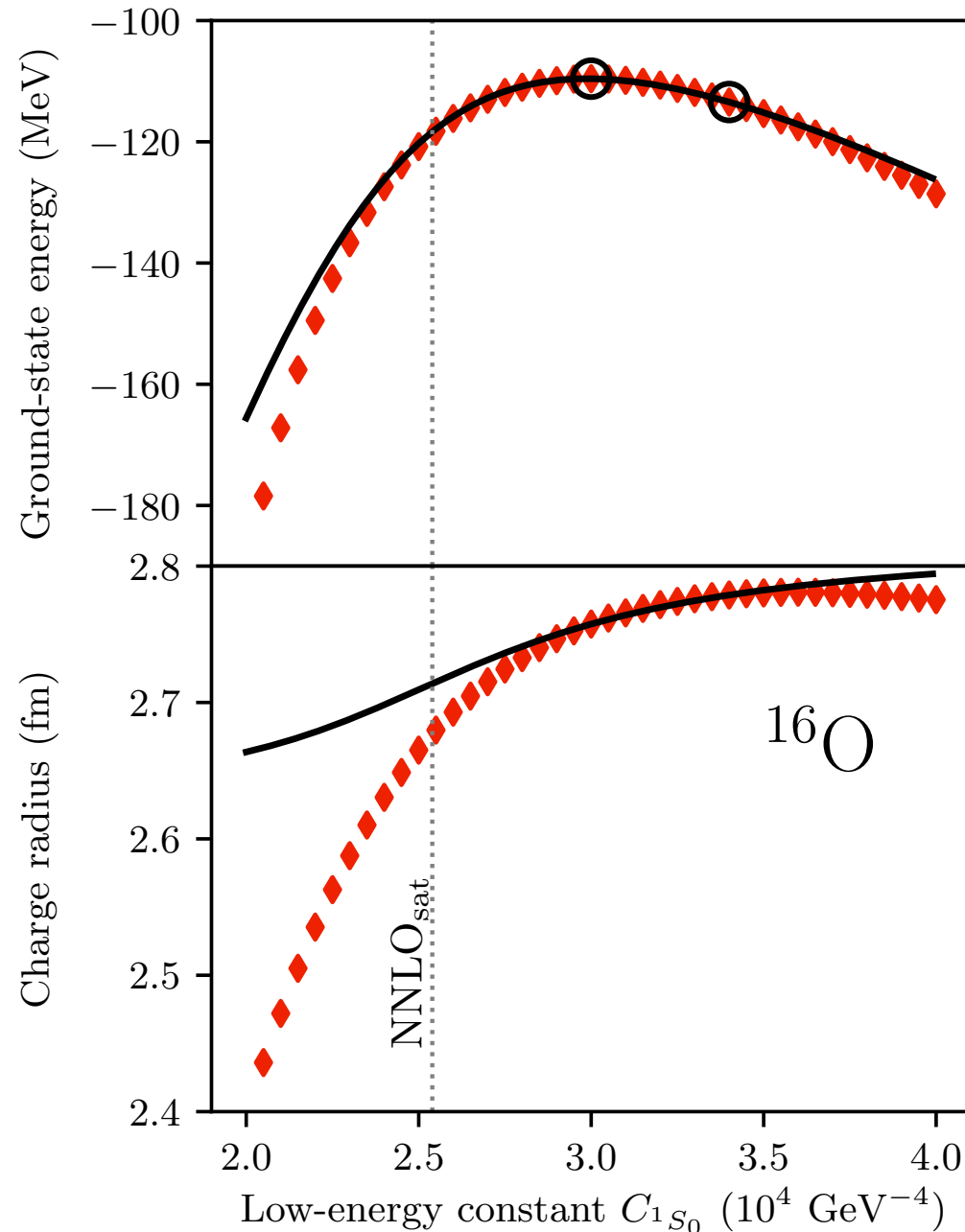


Exact coupled cluster calculations at the singles and doubles level

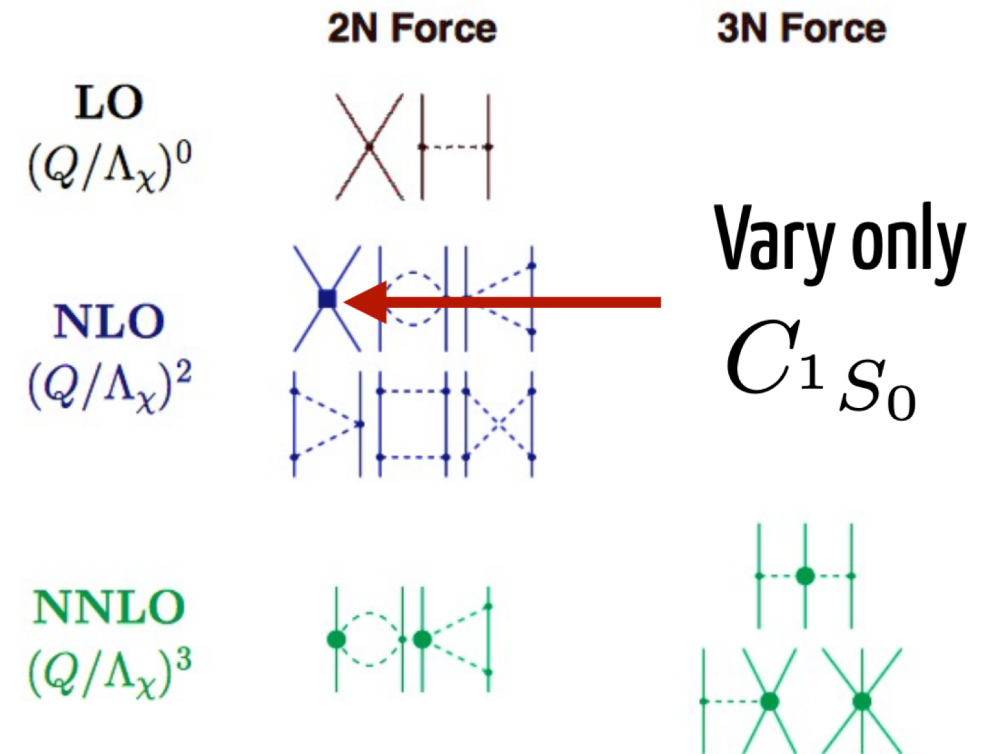


Emulating ab-initio coupled-cluster calculations

Andreas Ekström, Gaute Hagen PRL **123**, 252501 (2019)

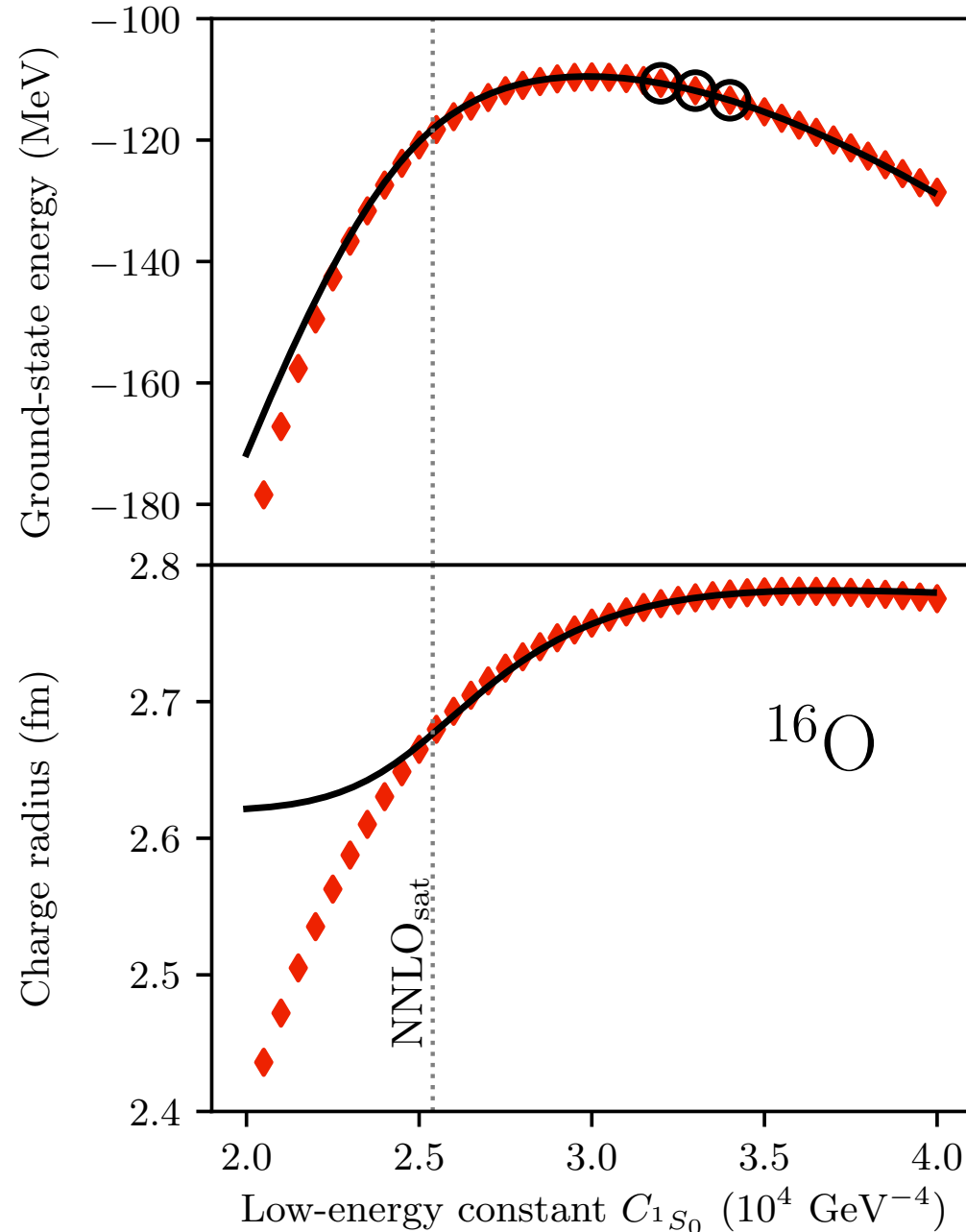


Exact coupled cluster calculations at the singles and doubles level

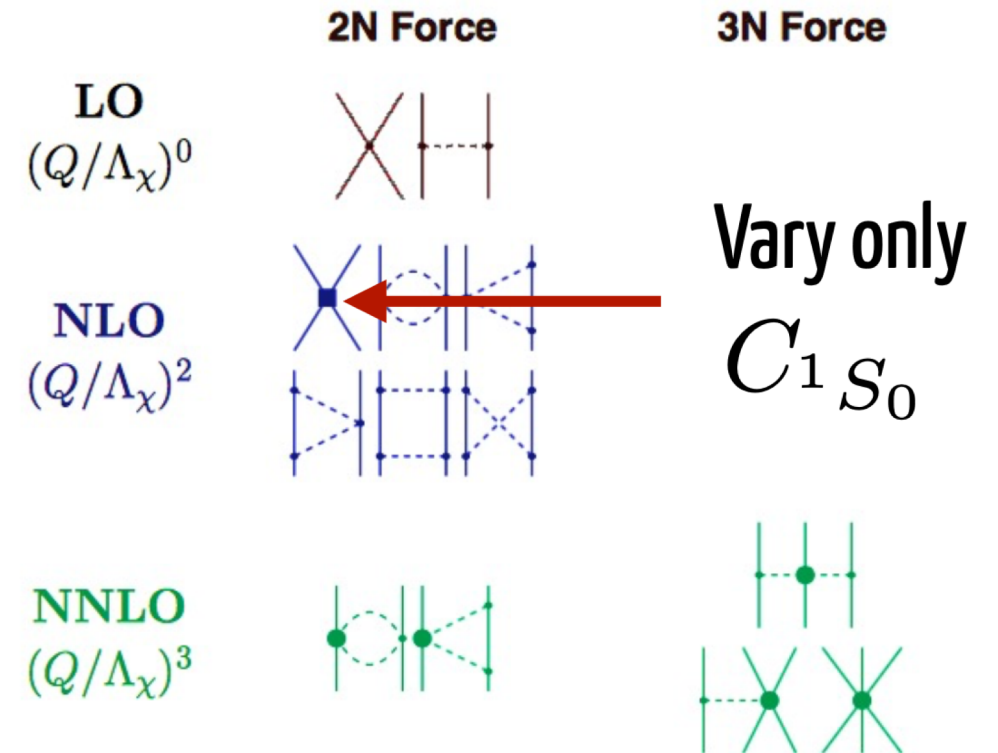


Emulating ab-initio coupled-cluster calculations

Andreas Ekström, Gaute Hagen PRL **123**, 252501 (2019)

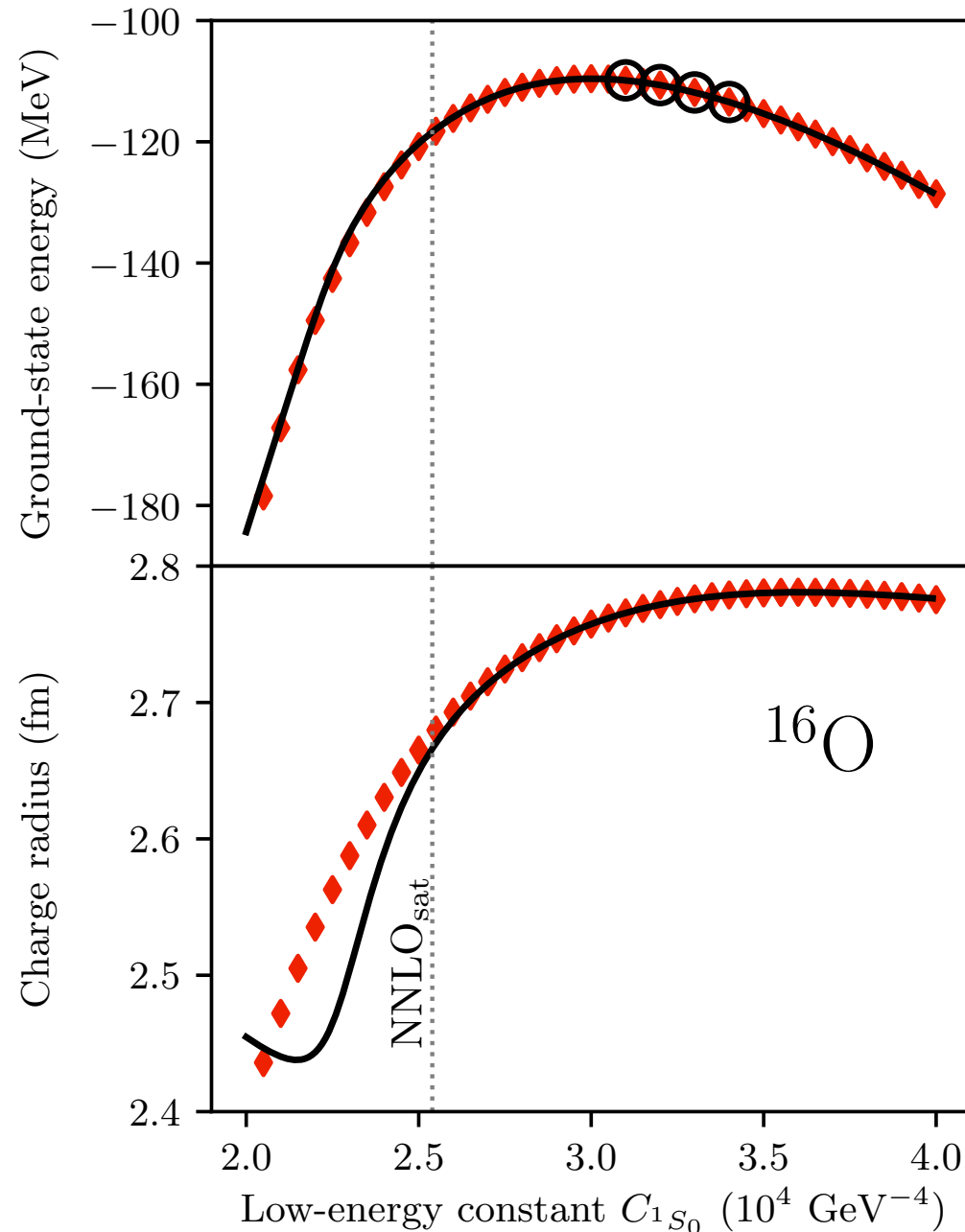


Exact coupled cluster calculations at the singles and doubles level

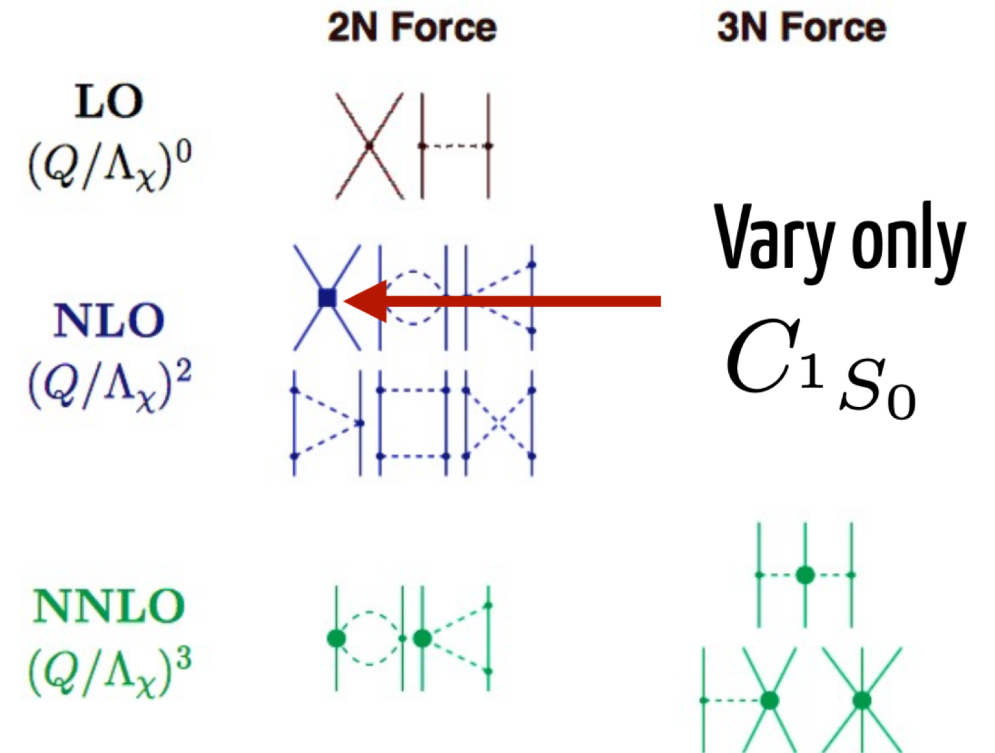


Emulating ab-initio coupled-cluster calculations

Andreas Ekström, Gaute Hagen PRL **123**, 252501 (2019)

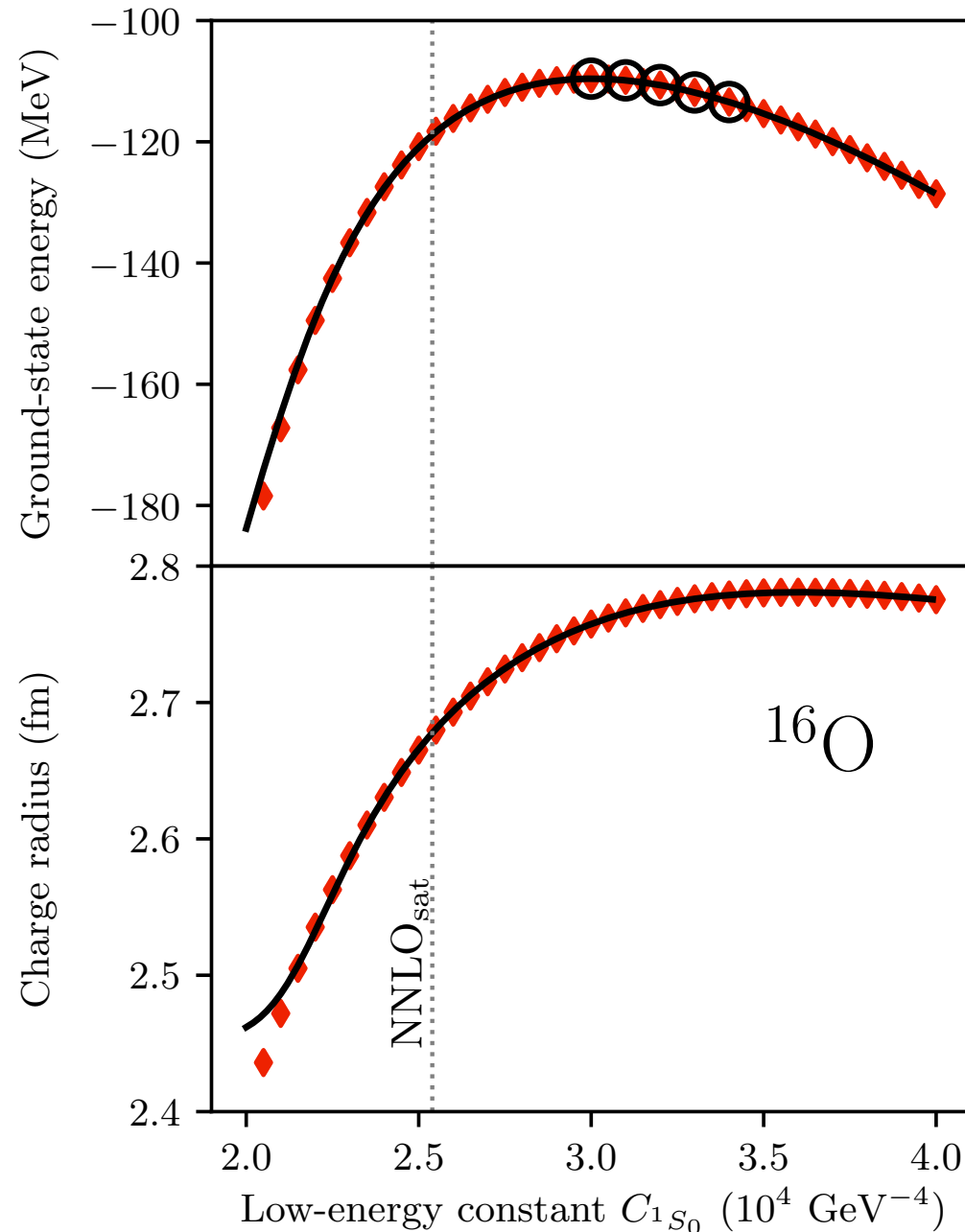


Exact coupled cluster calculations at the singles and doubles level

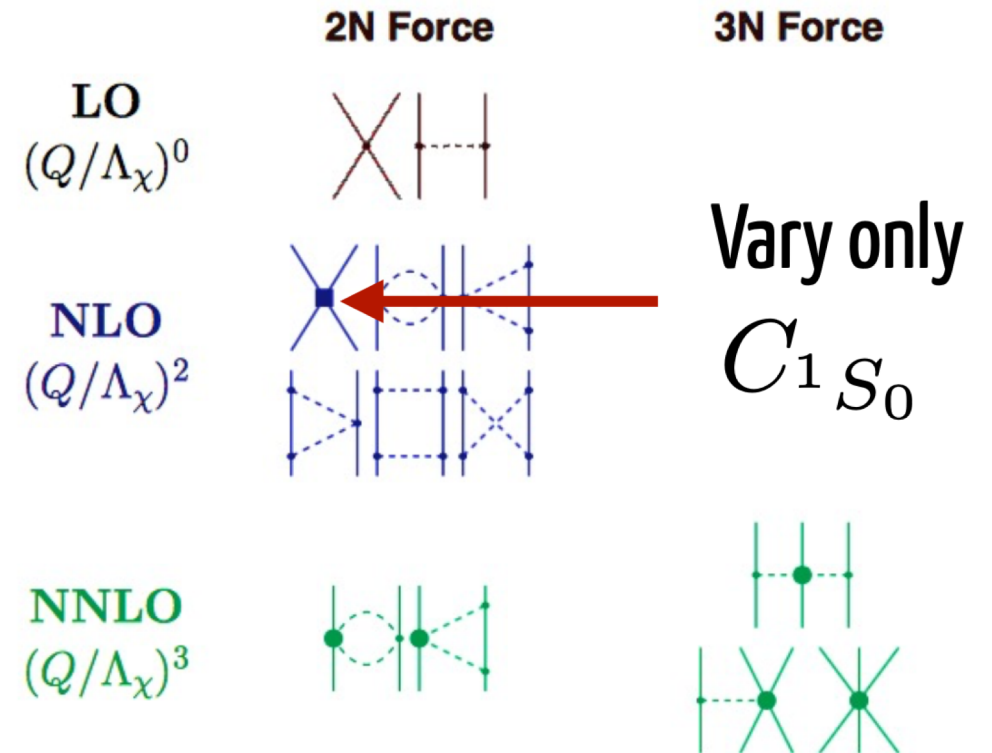


Emulating ab-initio coupled-cluster calculations

Andreas Ekström, Gaute Hagen PRL **123**, 252501 (2019)

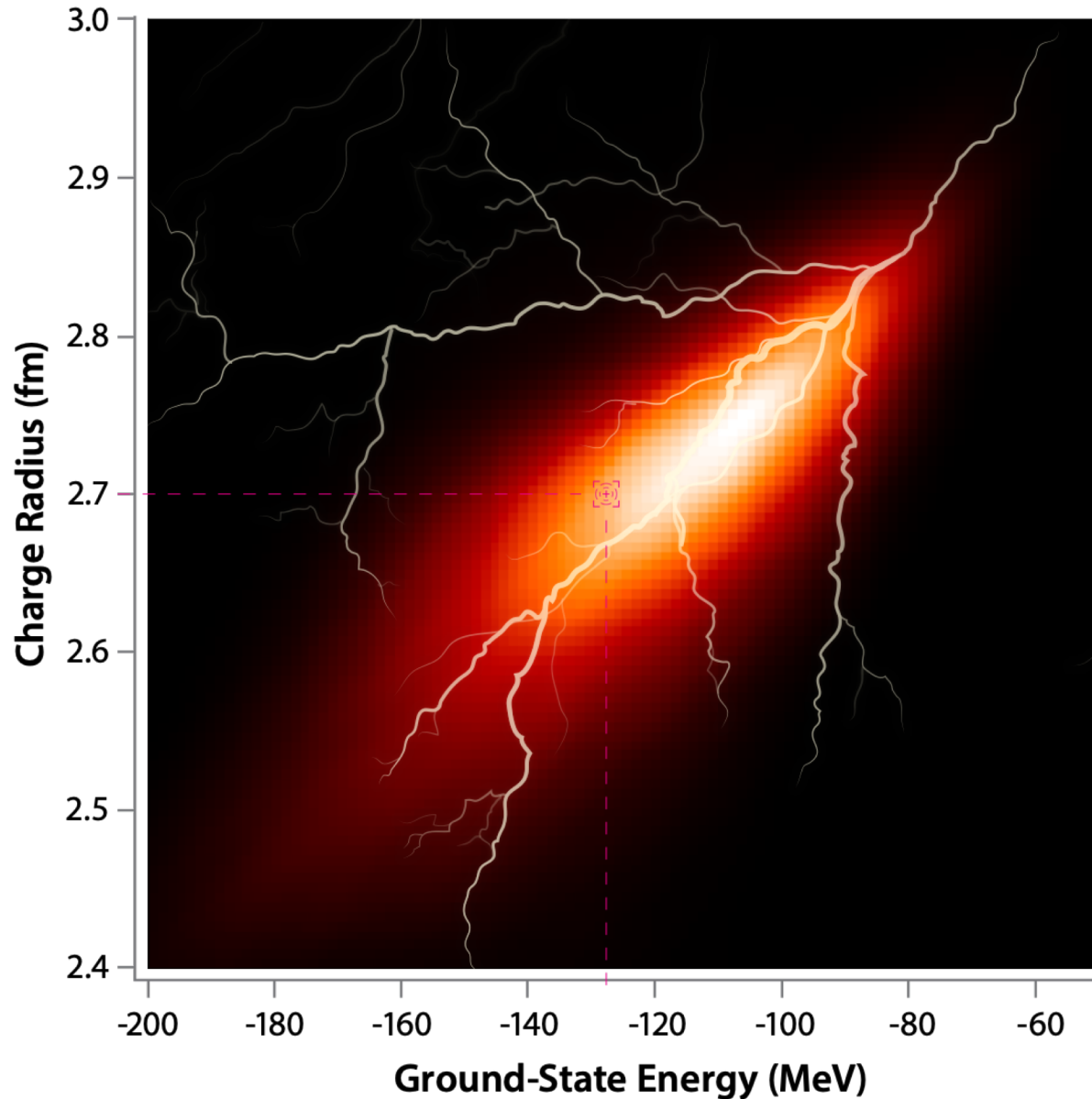


Exact coupled cluster calculations at the singles and doubles level



Computing nuclei at lightning speed

(~5 mins: ~ 10^5 energy/radius calculations of ^{16}O)



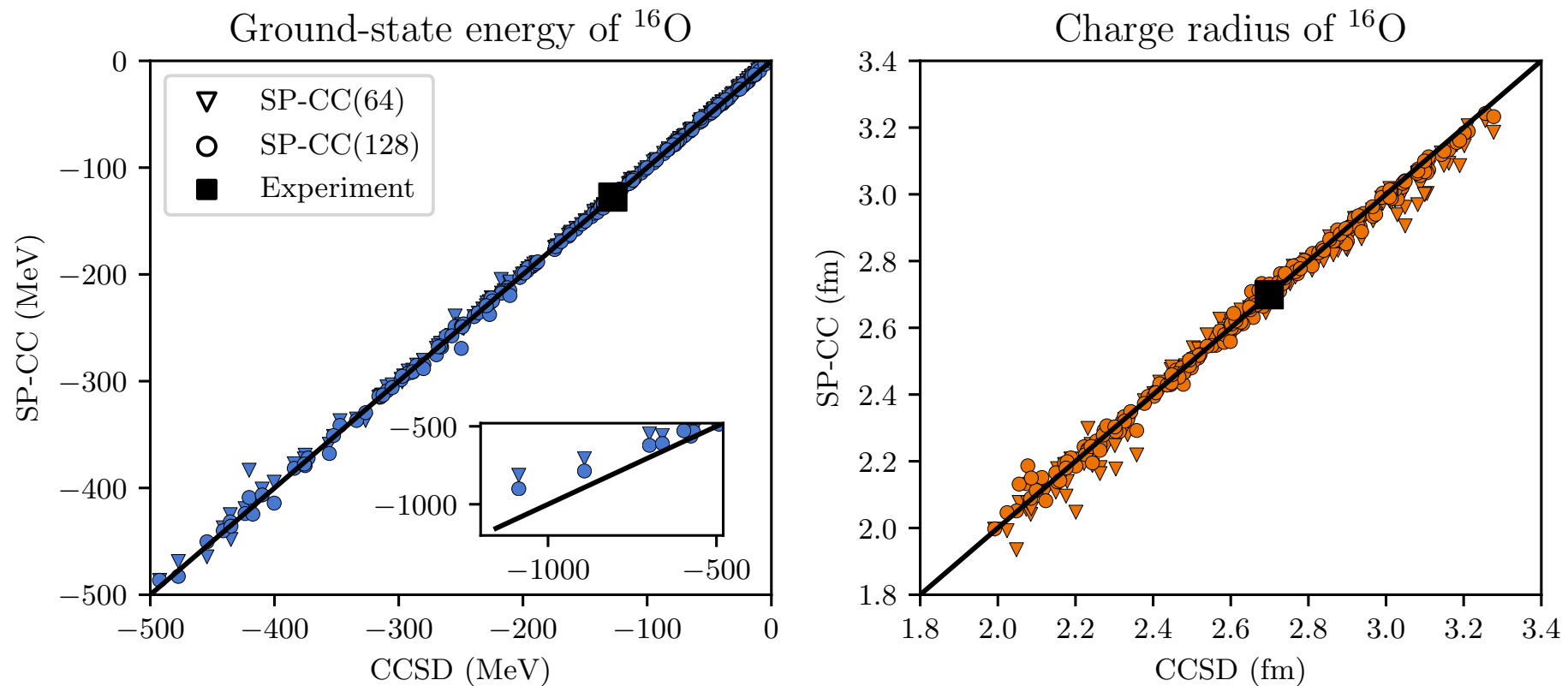
Realtime speed and accuracy of emulated ground-state energy and charge radius of ^{16}O for different values of interaction parameters

$$H(\vec{\alpha}) = \sum_{i=0}^{N_{\text{LECS}}=16} \alpha_i h_i$$

Accuracy: roughly the pixel size

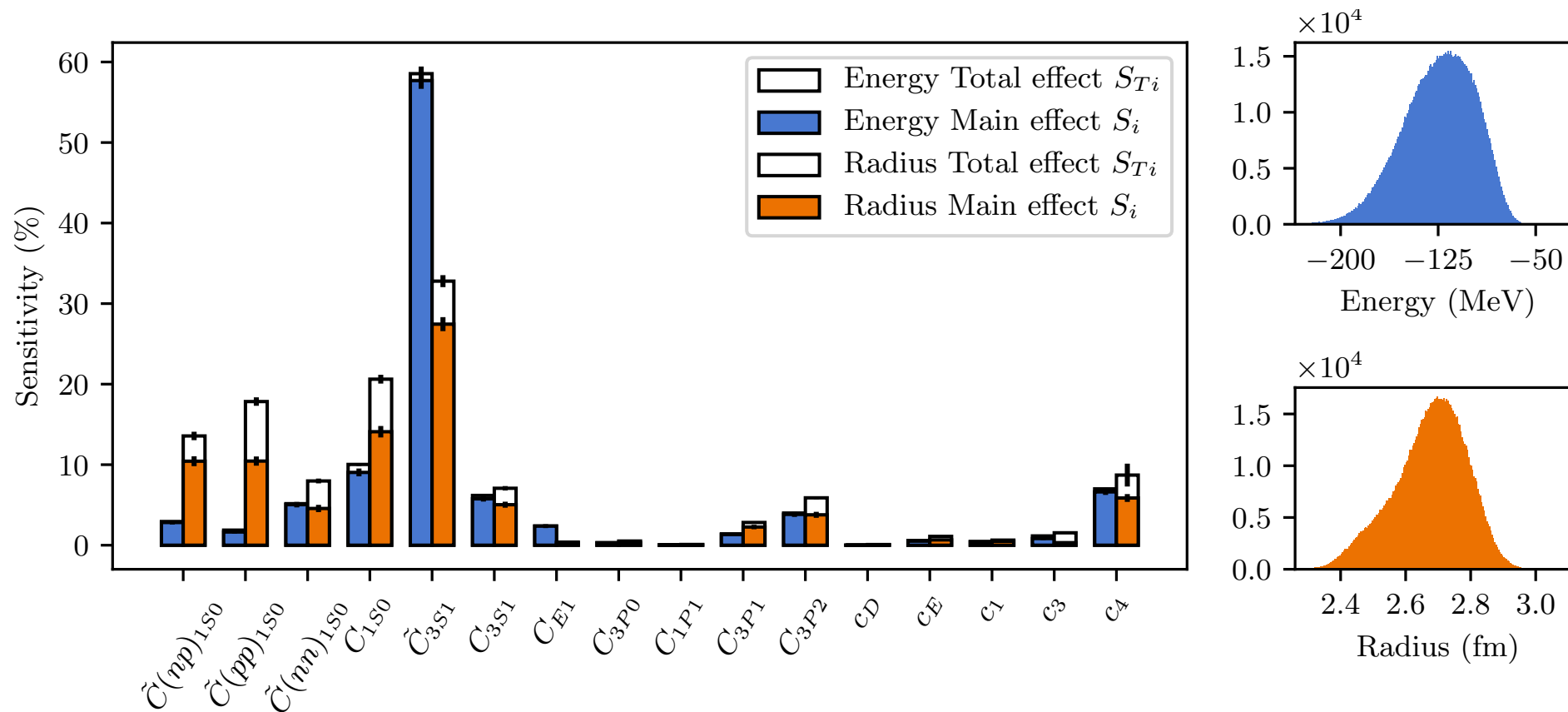
Speedup: 20 years of single node computations can be replaced by a 1 hour run on a laptop

Sub-space projected coupled-cluster – cross validation in 16 dimensions



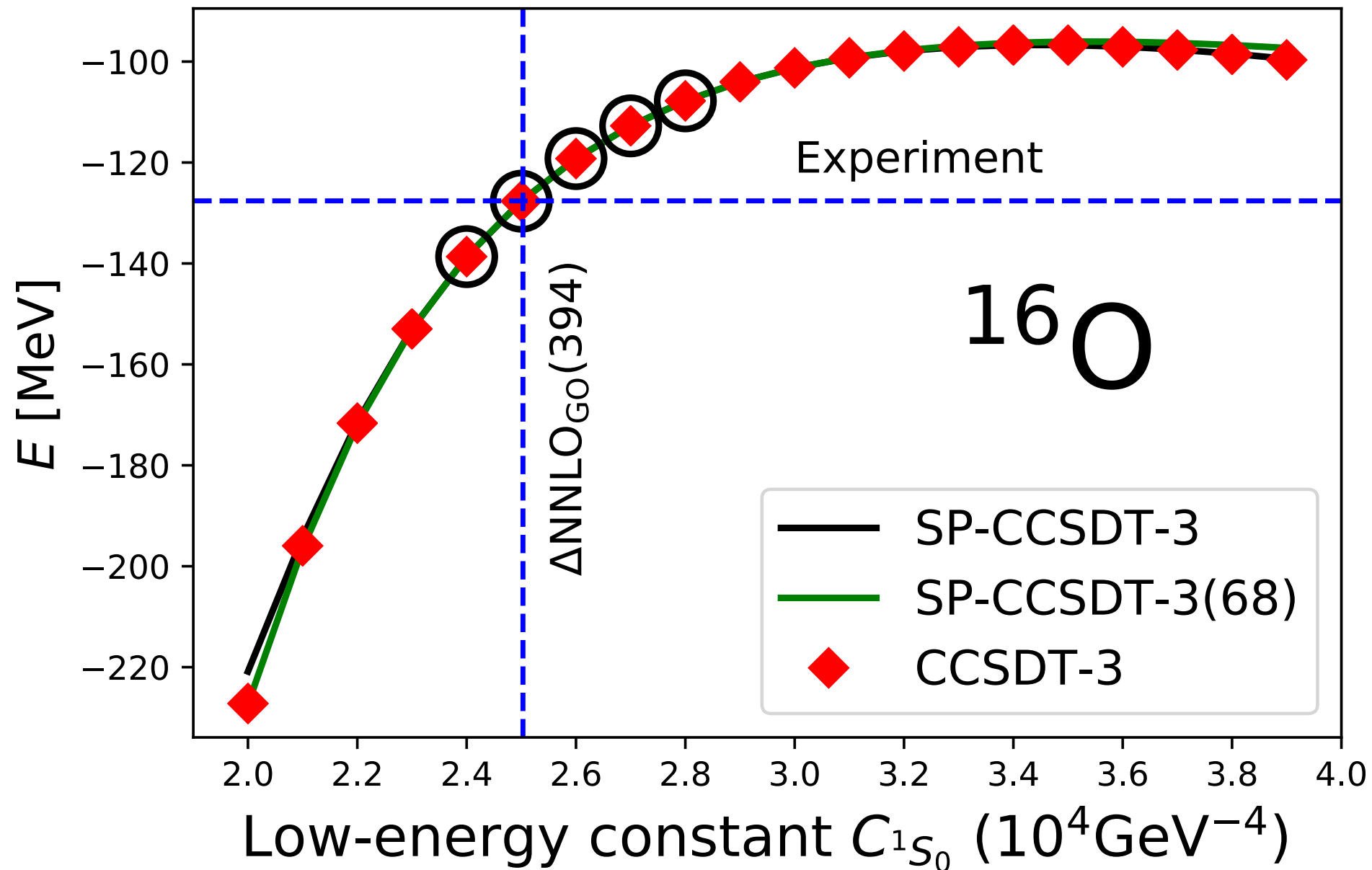
- Select 64 and 128 sub-space vectors in the 16 dimensional space of LECs using a space-filling latin hypercube design
- Select 200 randomly exact CCSD calculations in a 20% domain around NNLO_{sat}
- With 64 subspace vectors we achieve a 1% accuracy relative to exact CCSD solutions

A global sensitivity analysis of the radius and binding energy of ^{16}O

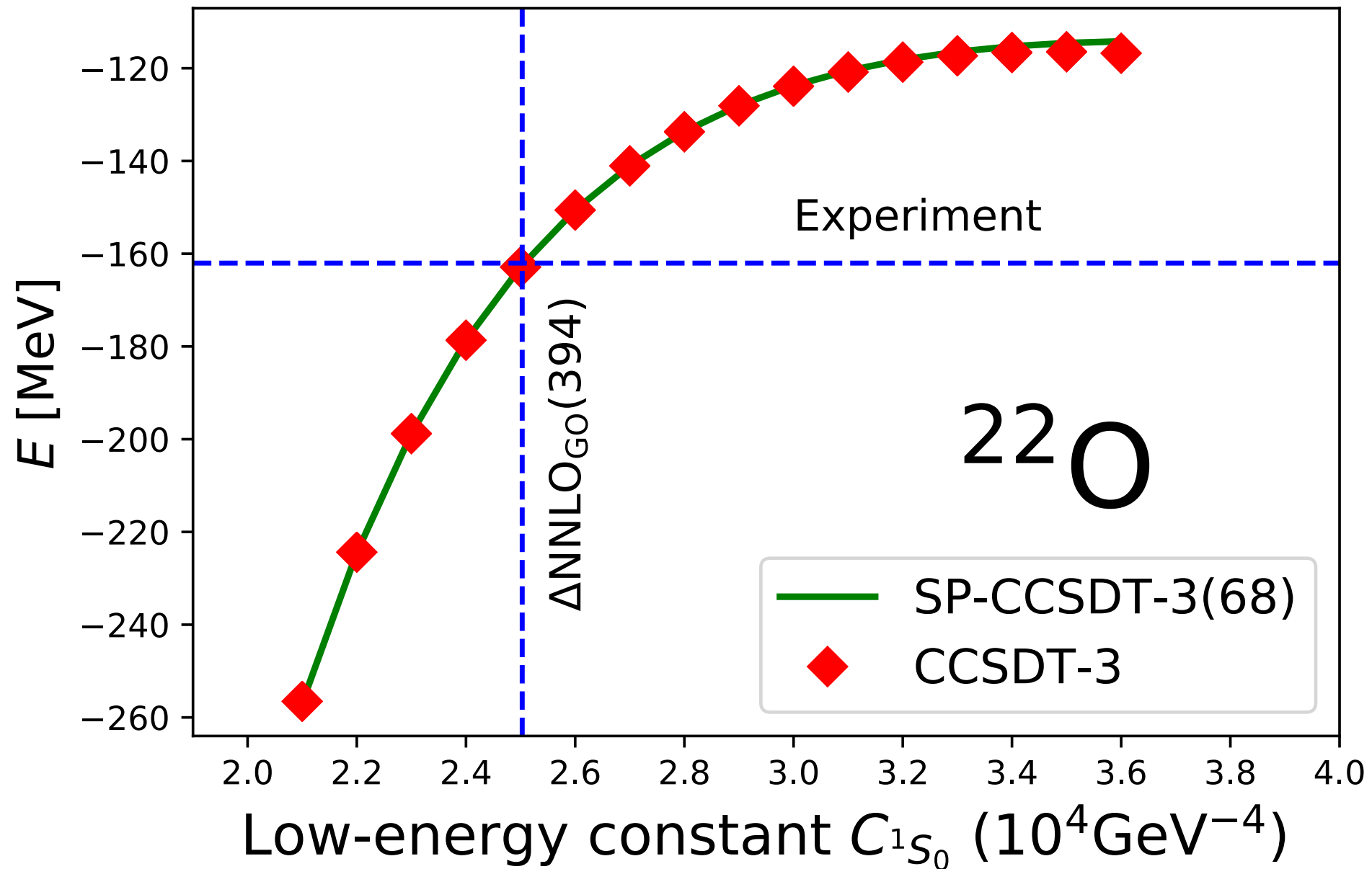


- Compute the binding energy and charge radius at one million different values of the 16 LECs in one hour on a standard laptop (would require 20 years of equivalent exact CCSD computations)
- About 60% of the variance in the energy can be attributed to the 3S1-wave, whereas the radius depends sensitively on several LECs and their higher-order correlations

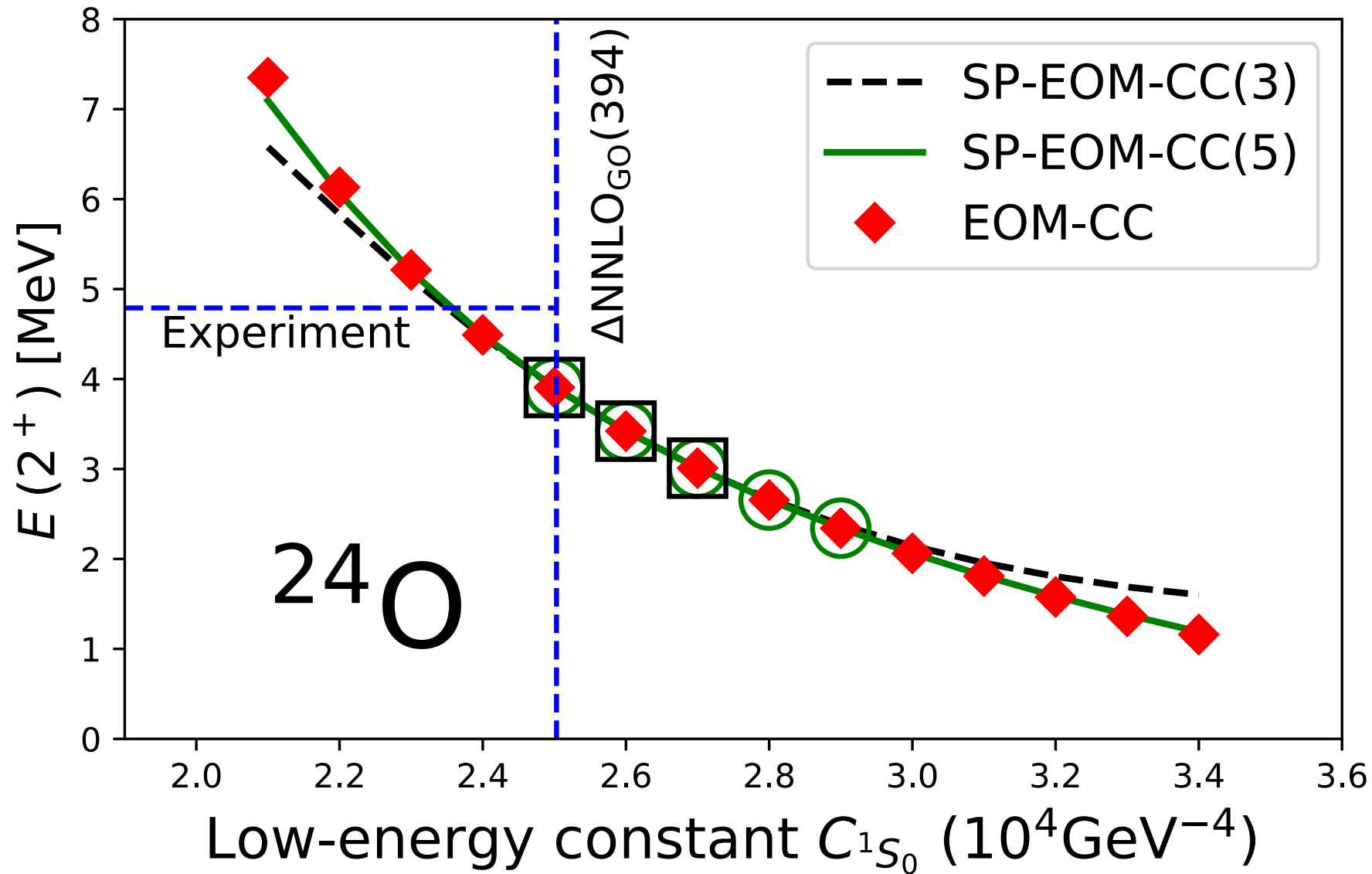
Sub-space projected coupled-cluster including triples excitations



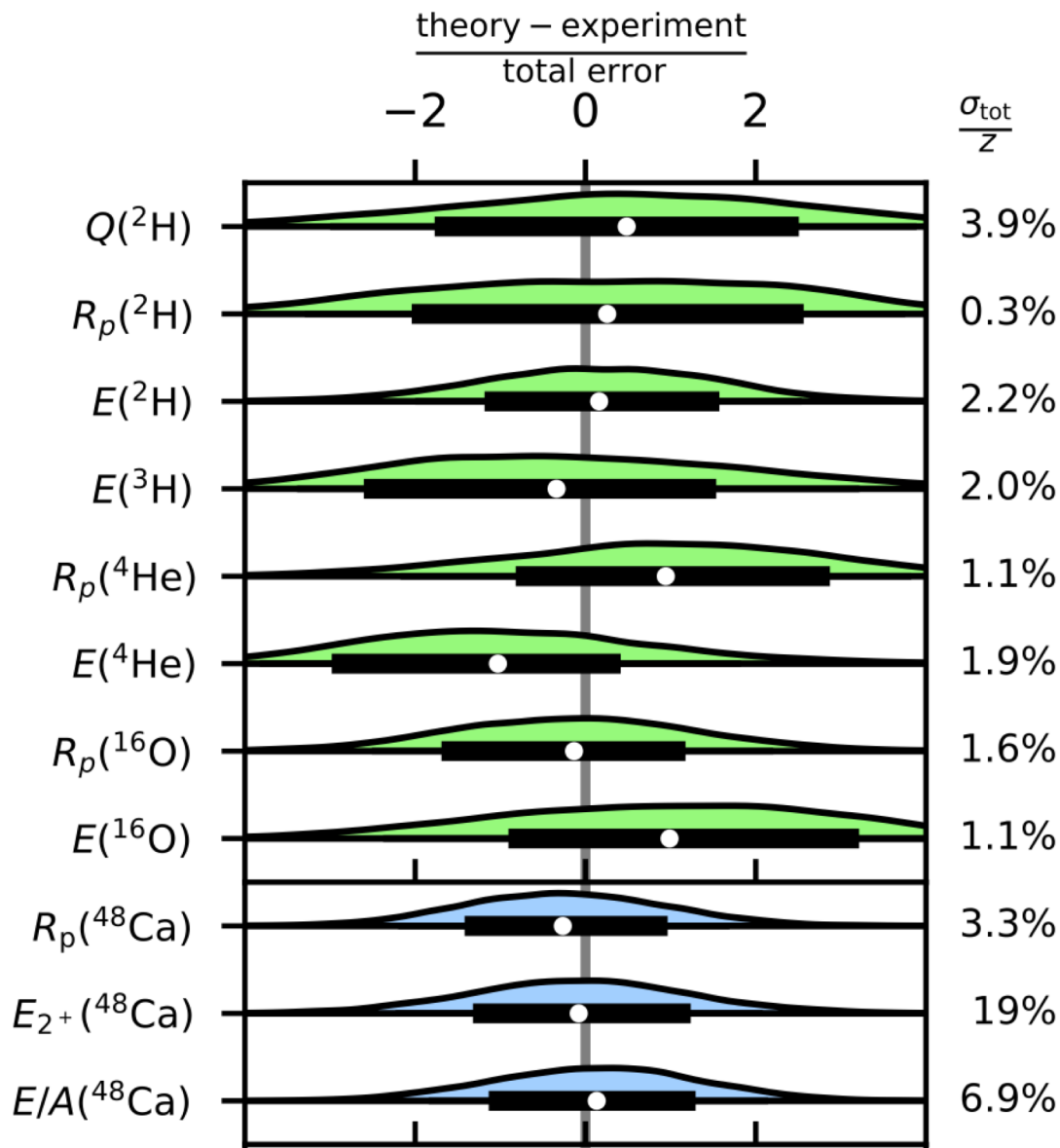
Sub-space projected coupled-cluster including triples excitations



Sub-space projected coupled-cluster for excited states



The neutron skin of ^{208}Pb



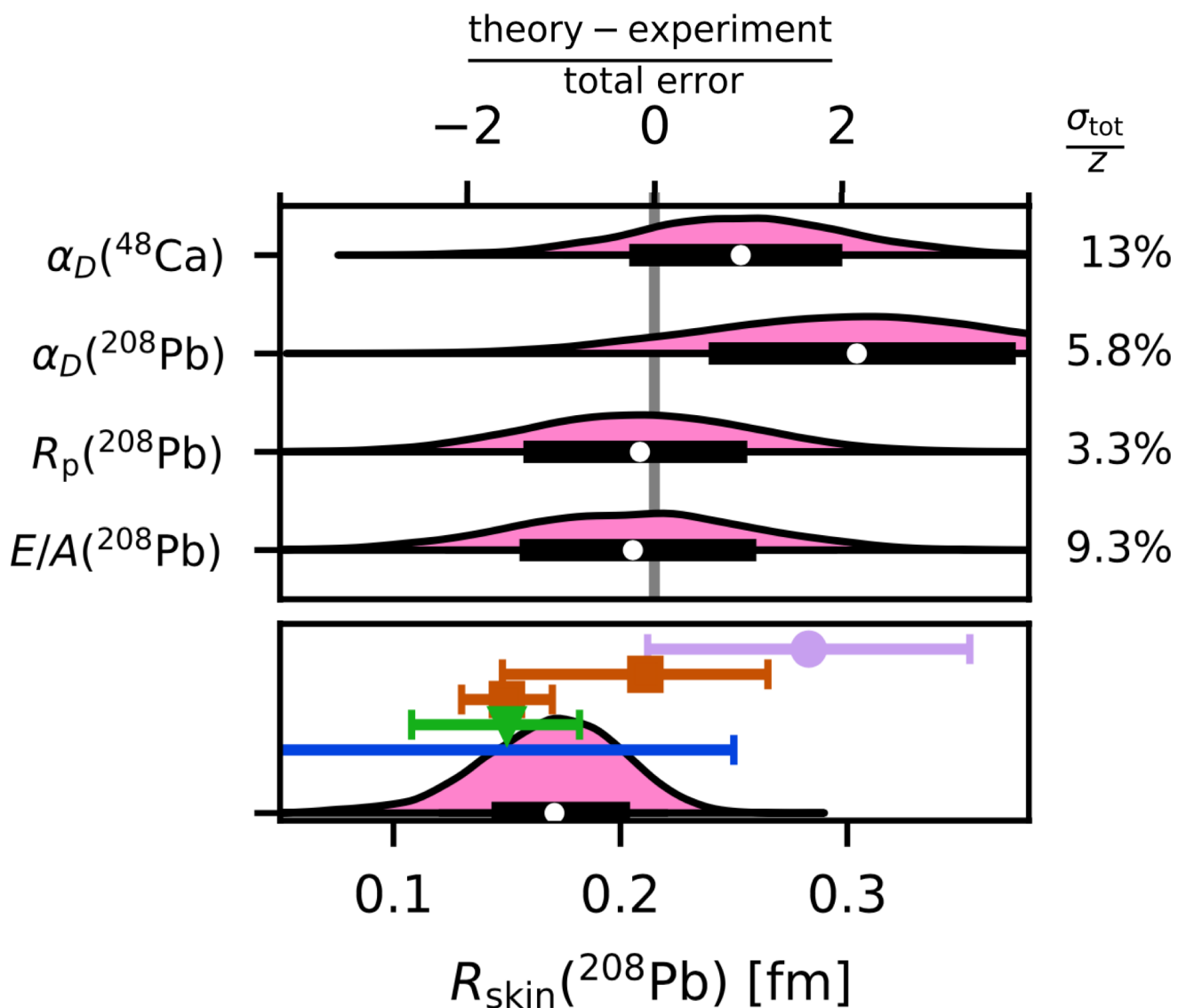
History matching

Calibration

- Emulators allows for billions of ab-initio simulations of selected nuclei
- Opens up new ways for making predictions and addressing uncertainties
- History matching – identify parameters of the model that give results consistent with data

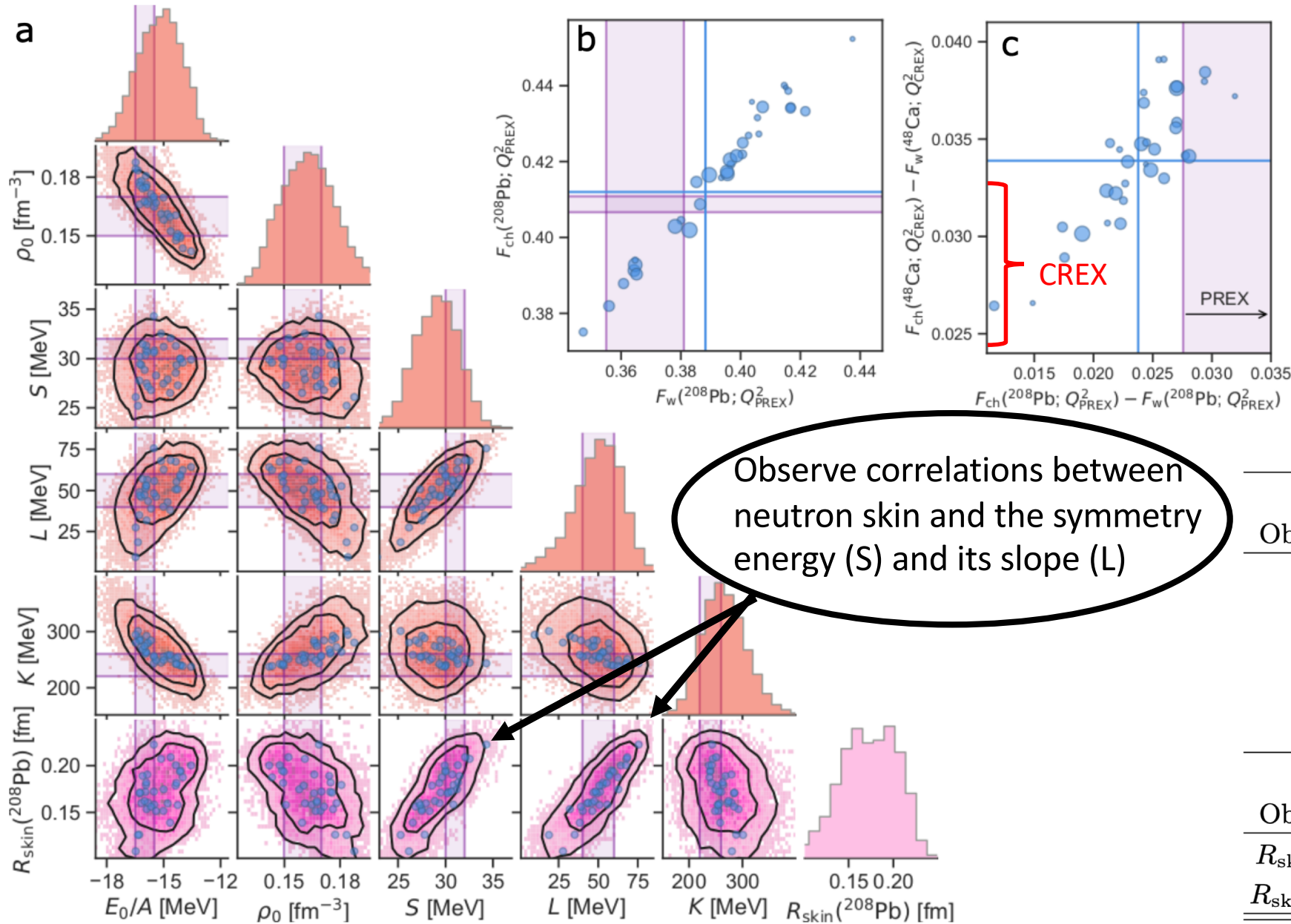
Explored 10^9 different parametrizations and found 34 non-implausible interactions
 Calibration on ^{48}Ca yields weighted samples for which we can use for quantified predictions of ^{208}Pb

The neutron skin of ^{208}Pb



- Posterior predictive distribution for the neutron skin in ^{208}Pb (experiments: electroweak (purple), hadronic (red), electromagnetic (green), and gravitational waves (blue) probes)
- $R_{\text{skin}}(^{208}\text{Pb}) = 0.14 - 0.20$ fm (68% credible interval) exhibits a mild tension with the value extracted from PREX-2

The neutron skin of ^{208}Pb

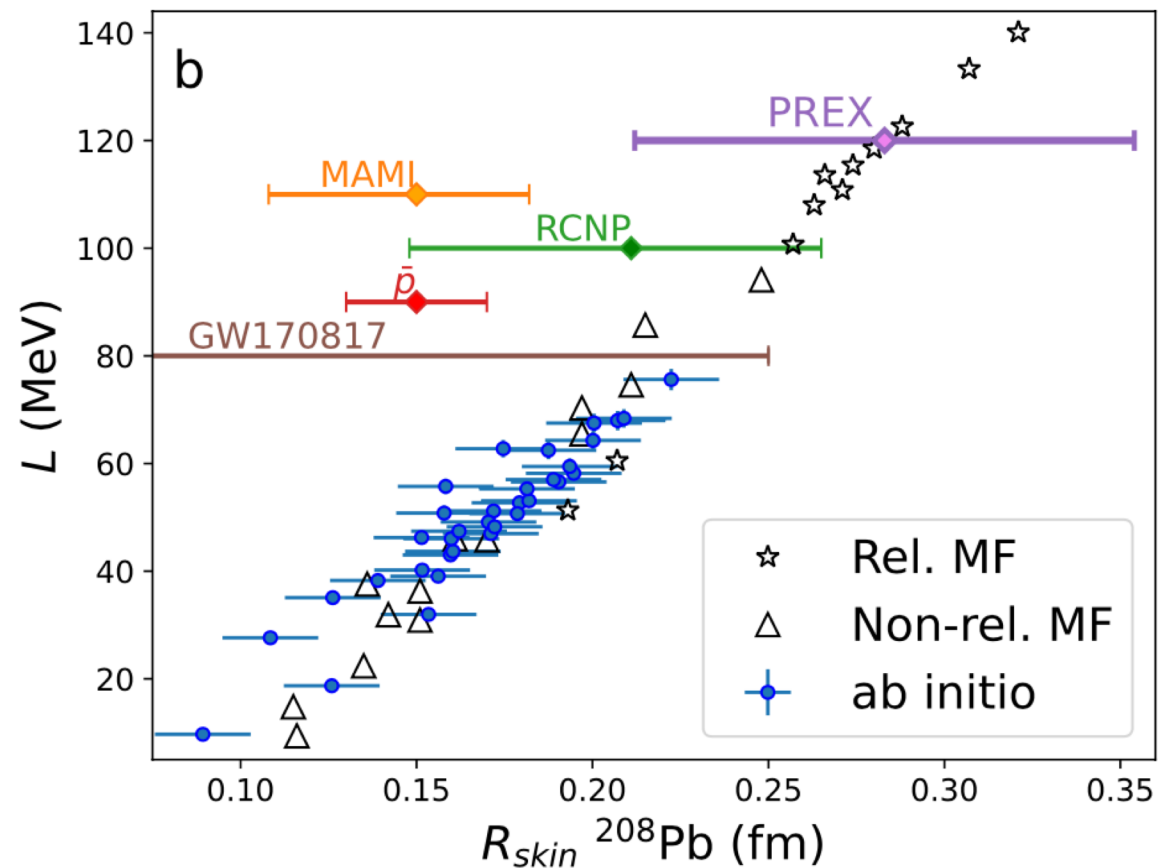
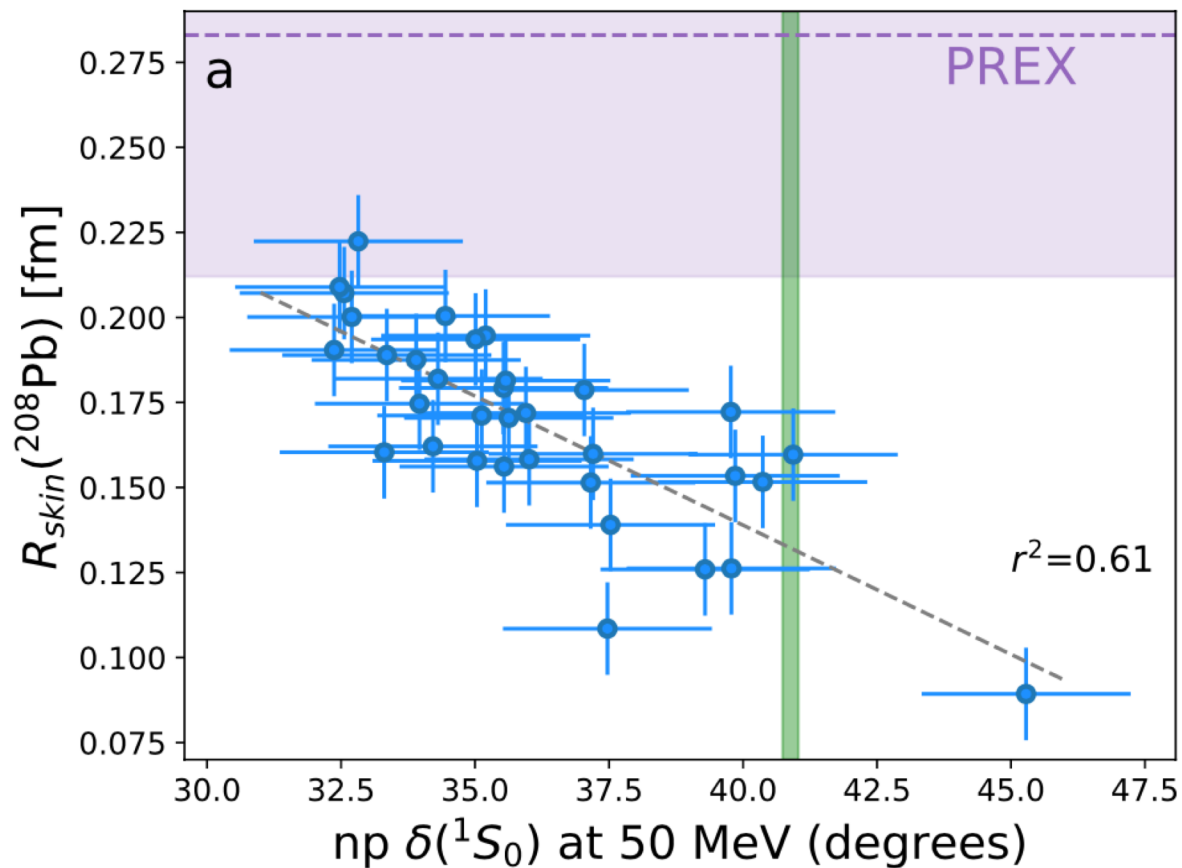


Summary of results:

Nuclear matter properties			
Observable	median	68% CR	90% CR
E_0/A	-15.2	[-16.3, -14.0]	[-17.2, -13.5]
ρ_0	0.163	[0.147, 0.175]	[0.140, 0.186]
S	29.1	[26.6, 31.3]	[25.1, 32.8]
L	50.3	[37.2, 68.1]	[22.6, 75.8]
K	264	[227, 297]	[210, 328]
Neutron skins			
Observable	median	68% CR	90% CR
$R_{\text{skin}}(^{48}\text{Ca})$	0.164	[0.141, 0.187]	[0.123, 0.199]
$R_{\text{skin}}(^{208}\text{Pb})$	0.171	[0.139, 0.200]	[0.120, 0.221]

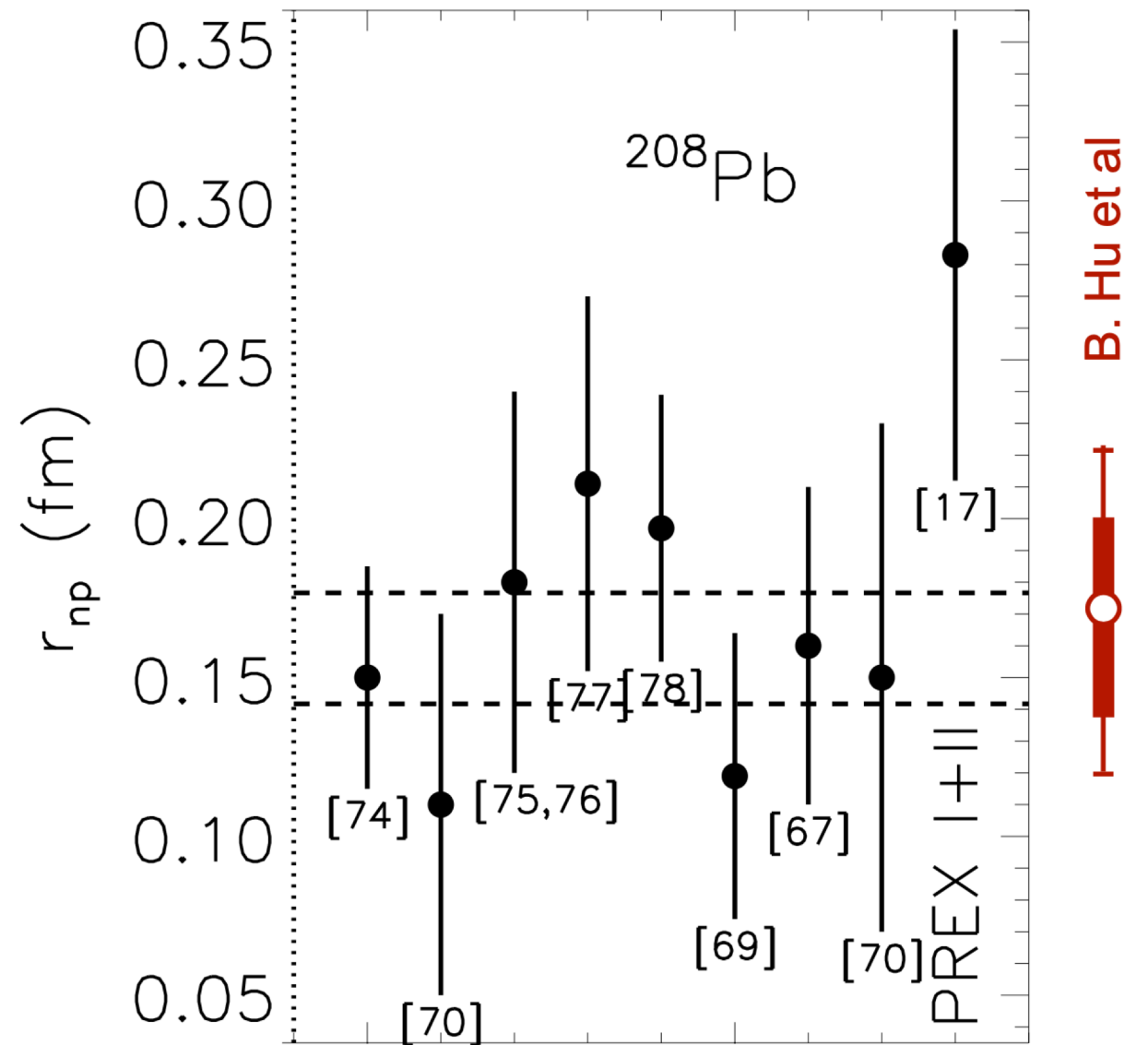
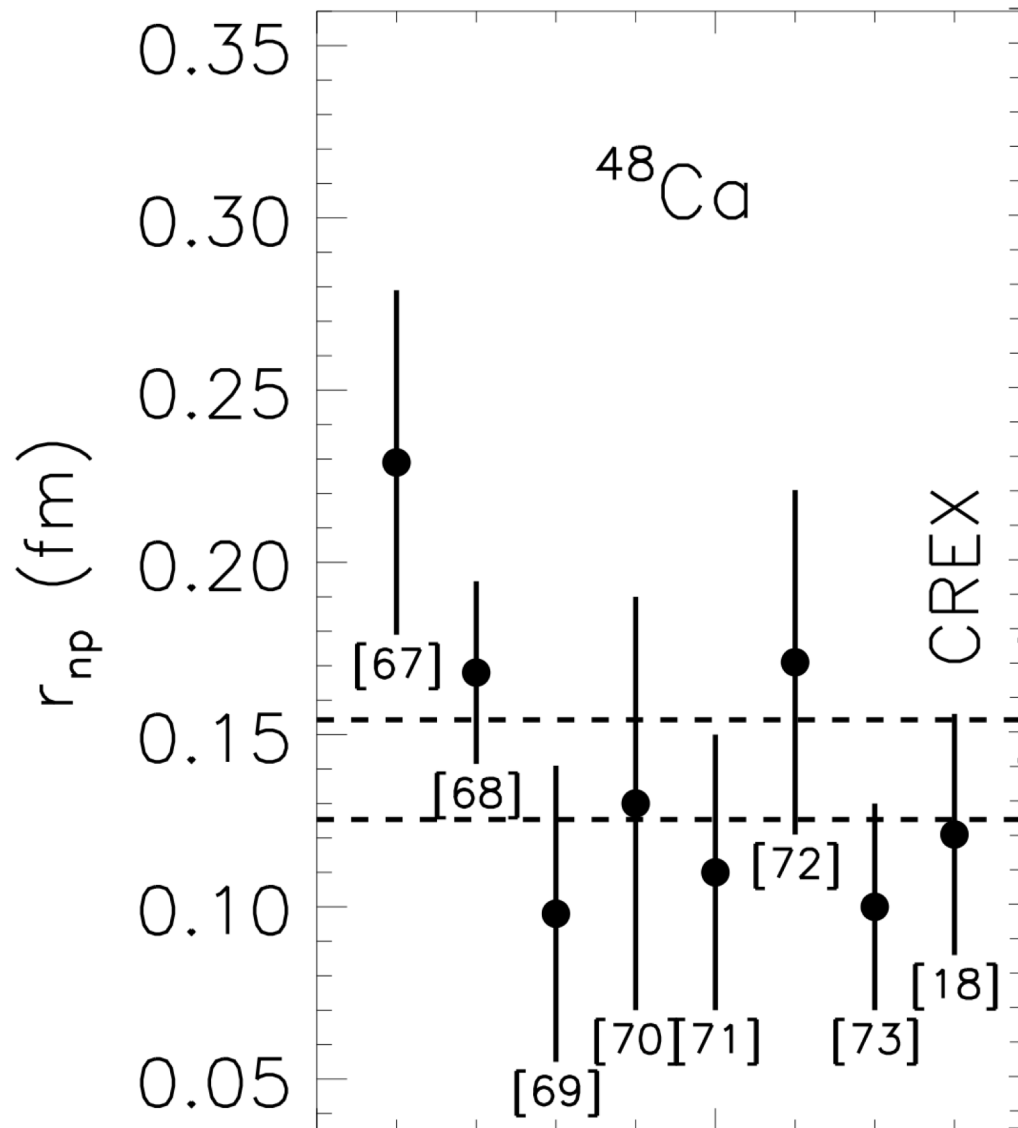
The neutron skin of ^{208}Pb

- Different models predict similar correlation between the neutron-skin and the slope of symmetry energy (L)
- The neutron skin of ^{208}Pb is (weakly) correlated with the 1S_0 scattering phase-shift at 50 MeV
- A realistic description of the 1S_0 scattering phase shift implies a neutron skin in tension with PREX-2



The neutron skin of ^{48}Ca and ^{208}Pb

Constraints on Nuclear Symmetry Energy Parameters J. Lattimer. Particles **6**, 30-56 (2023)

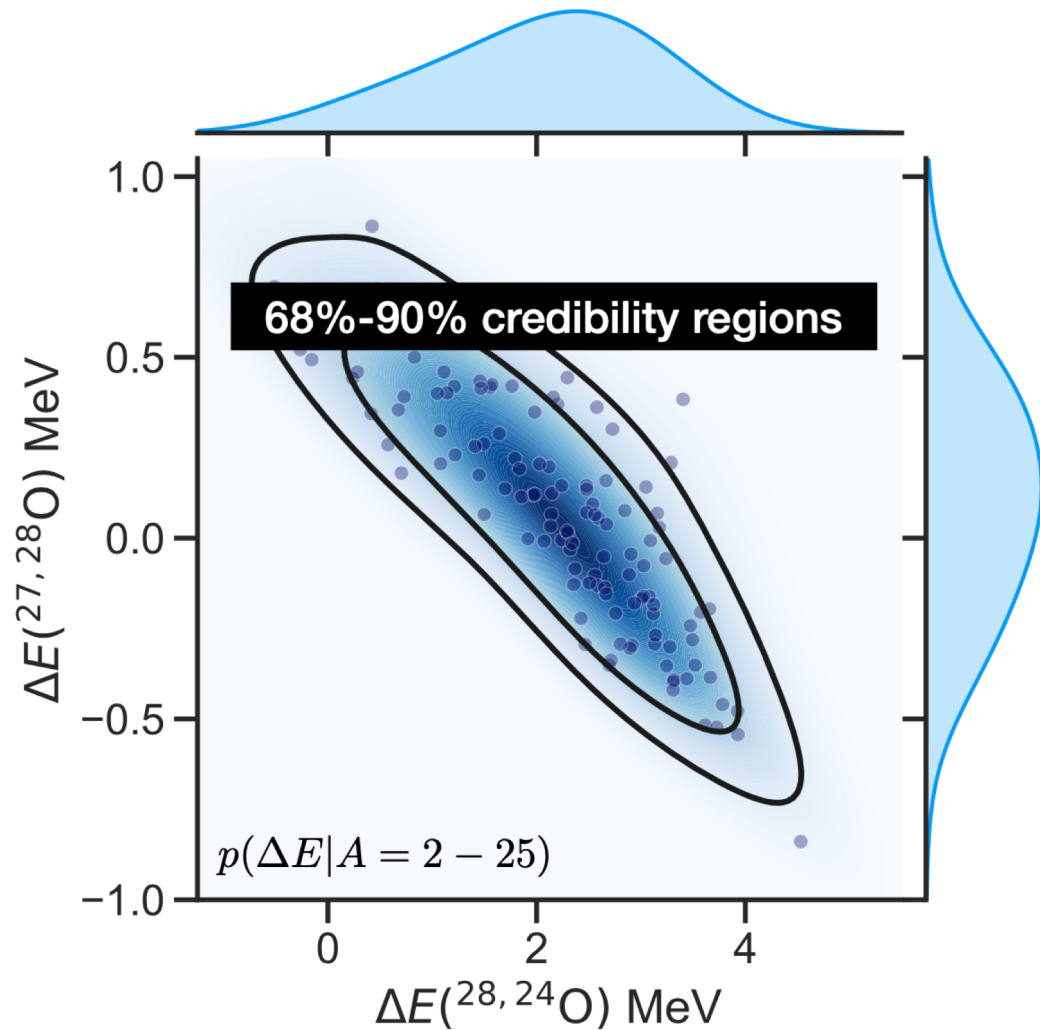


Does chiral Hamiltonians predict a bound ^{28}O ?

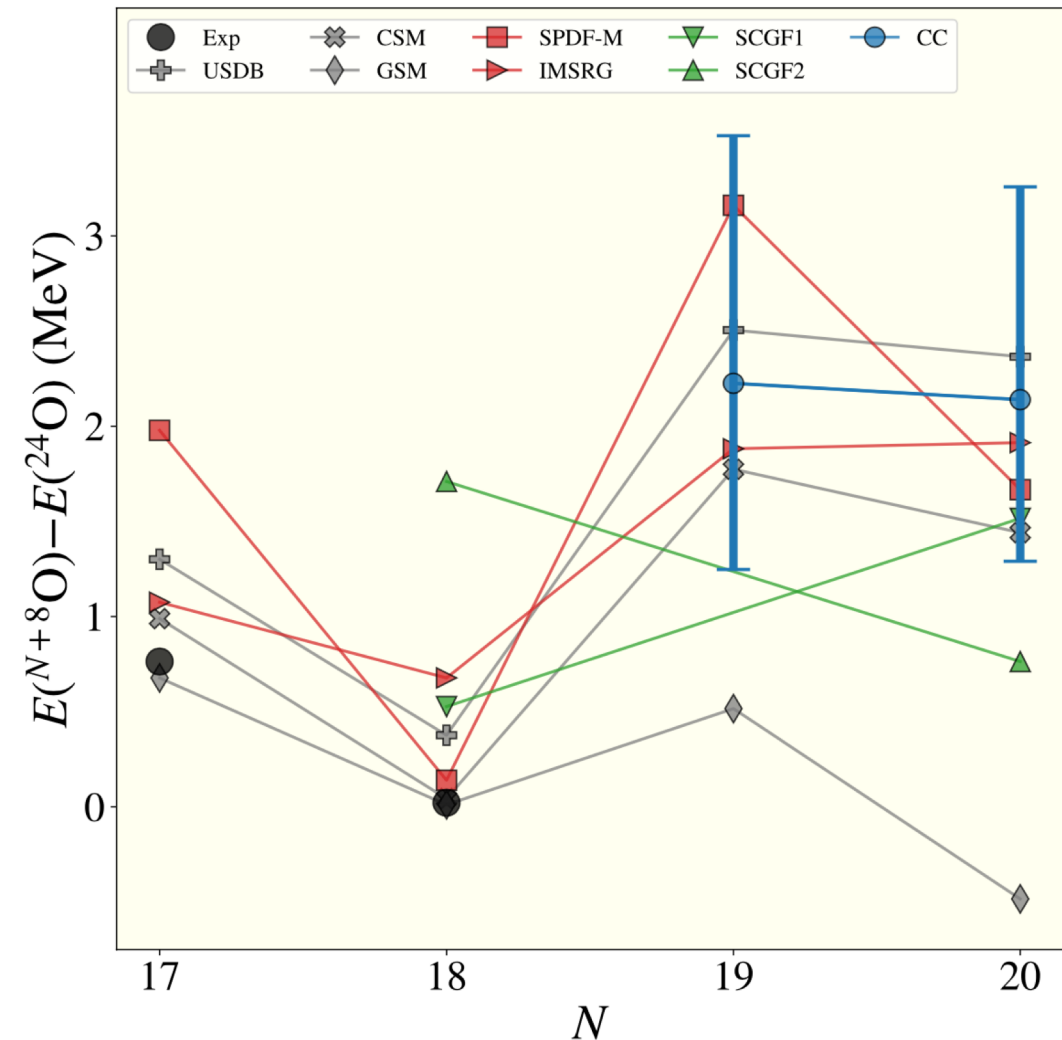
Ekström, Forssén, Hagen, Jiang, Papenbrock, Sun, Vernon

We claim with 98% certainty that ^{28}O is unbound

Used history matching and performed 10^8 predictions for ground- and excited states of nuclei up to ^{25}O



Prediction for ^{28}O shown as probability distribution where solid lines indicate the 68% and 90% probability density regions



Summary

- Towards mass-table computations based on Hamiltonian methods
 - Interactions with "good" saturation properties yield accurate description of BEs, radii and skins in light, medium-mass and heavy nuclei
 - shell closures predicted at $N = 8, 14$ in neon and magnesium and no signature of $N = 32$ shell closure in potassium
 - Universal trend of radii beyond $N = 28$ for even-even Ca-Zn isotopes
 - Predicted $N = 20$ shell closure is not supported by data in isotopes of neon and magnesium
 - Steep increase in radii beyond $N = 28$ in potassium challenges theory
- Prediction of small neutron skin in ^{48}Ca confirmed by CREX
- Coherent neutrino scattering on ^{40}Ar a stepping stone for neutrino response

Summary

- Developed emulators that allows us to sample $\sim 10^8$ different Hamiltonians in a short time for medium mass nuclei
 - A global sensitivity analysis revealed the role of various LECs in the binding energy and radius of ^{16}O
- Combining accurate emulators, novel statistical tools, and Bayesian inference allowed us to make accurate predictions for the neutron skin and related observables in ^{208}Pb
- Neutron skin of ^{208}Pb in mild tension with PREX-2
- Confirmed correlations (seen in mean-field approaches) between the neutron skin of ^{208}Pb and the symmetry energy and its slope in nuclear matter

Thank you for your attention!